Wolfgang Johann Fischer

A Novel Direct Method for Mechanical Testing of Individual Fibers and Fiber to Fiber Joints

DOCTORAL THESIS

Thesis Supervisors
Univ.-Prof. Dipl.-Ing. Dr.techn. Wolfgang Bauer
Ao.Univ.-Prof. Mag. Dr.rer.nat. Robert Schennach

Graz University of Technology
Institute for Paper, Pulp and Fiber Technology

Graz, 21.03.2013

Statutory Declaration

I declare that I have authored this thesis independently, that I have not used other than the declared sources / resources, and that I have explicitly marked all material which has been quoted either literally or by content from the used sources

Graz, 21.03.2013

Abstract

Paper is composed of individual fibers, which interact with each other, thus leading to the formation of a complex network. The property which is of great importance is the strength of this network. In order to get a better understanding of the strength of the paper network it is of utmost importance to understand the mechanical properties of the single fibers, fiber to fiber joints as well as their behavior during loading. Within the framework of this thesis a novel device for mechanical testing of individual fibers and fiber to fiber joints is developed. Besides the determination of the single fiber strength and the shear strength of single fiber crossings, this method also enables the determination of the bending stiffness of single fibers, the deformation during loading as well as the mode III strength of single fiber crossings. Furthermore, the bonding energy and the influence of biaxial loading on the breaking load of individual fiber to fiber joints can be examined. For a more precise description of the mechanisms taking place during the mechanical testing and to learn more about the impact of structural properties on the strength of fiber crossings, the formerly bonded area is investigated by means of the low-voltage scanning electron microscopy. Furthermore, the influence of different types of adhesives, used for fixation of the fibers, is investigated with this method. The combination of these tests will contribute to a better understanding of paper strength.

Keywords: fiber crossing, fiber to fiber joint, joint strength, shear strength, specific bonding strength, fiber strength, bending stiffness, bonding energy, mode III loading.

Kurzfassung

Papier besteht aus Einzelfasern welche miteinander interagieren und ein komplexes Netzwerk bilden. Eine der wesentlichsten Eigenschaften ist die Festigkeit dieses Netzwerkes. Um ein besseres Verständnis über die Gesamtfestigkeit des Fasernetzwerkes zu erlangen, ist es von grundlegender Bedeutung die mechanischen Eigenschaften der Einzelfasern, der Faser-Faser Bindungen sowie deren Verhalten unter Last zu untersuchen. Im Rahmen dieser Arbeit wurde ein neuartiges Messgerät zur Untersuchung von Einzelfasern sowie Faserbindungen entwickelt. Neben der Bestimmung der Einzelfaserfestigkeit und der Scherfestigkeit einzelner Bindungen, ermöglicht diese neuartige Methode auch die Bestimmung der Biegesteifigkeit von Einzelfasern, des Verformungsverhaltens unter Last sowie der Mode III Festigkeit von Faserkreuzungen. Des Weiteren besteht auch die Möglichkeit die Bindungsenergie, sowie den Einfluss einer biaxialen Belastung auf die Bruchkraft einzelner Bindungen zu untersuchen. Um die Vorgänge die während den Bruchversuchen ablaufen besser beschreiben zu können und um mehr über den Einfluss von strukturellen Eigenschaften auf die Bindungsfestigkeit zu lernen, wird die vormals gebunden Fläche mit der sogenannten "low-voltage" Rasterelektronenmikrokopie untersucht. Weiters wird die Auswirkung von verschiedenen Klebstoffen die zur Faserfixierung verwendet wurden, mit dieser Methode untersucht. Die Kombination dieser Tests trägt zu einem besseren Verständnis der Gesamtpapierfestigkeit bei.

Schlagwörter: Faserkreuzung, Faser-Faser Bindung, Bindekraft, Scherfestigkeit, spezifische Bindekraft, Faserfestigkeit, Biegesteifigkeit, Bindungsenergie, Mode III Belastung.

Acknowledgements

At this point I would like to thank Prof. Dr. Wolfgang Bauer for his support, helpful advices and the possibility to write this thesis at the Institute for Paper, Pulp and Fiber Technology. I also want to thank Prof. Dr. Robert Schennach for stimulating discussions and for giving me the opportunity to work in the CD-Laboratory for Surface Chemical and Physical Fundamentals of Paper Strength. Thanks to Ass.Prof. Dr. Ulrich Hirn for helping me with problems, for his encouragement and supervision.

I am thankful to Dr. Armin Zankel for his commitment and supporting the investigations of the formerly bonded area with scanning electron microscopy.

Thanks to Claudia Bäumel for her support with administrative tasks and nice conversations. I am also grateful to Barbara Hummer, Adelheid Bakhshi and Kerstin Roschitz for preparing the individual fibers and fiber to fiber joints. Christian Probst, Michael Dauer and Christian Natter for helping me with the construction of the micro bond tester. Special thanks to my friend and office college Christian Lorbach for the great working atmosphere. Albrecht Miletzky, Frederik Weber, Wolfgang Fuchs, Franz Schmied, Christian Ganser, Matthias Trimmel, Wolfgang Pacher and Karin Hofer for being great colleagues and friends. Thanks to all members of the CD-Laboratory as well as Mikael Magnusson for the great collaboration.

I would like to acknowledge Mondi Frantschach GmbH, Kelheim Fibres GmbH, Lenzing AG and Christian Doppler Research Association for funding this research project.

Finally, a big thank you to my family. My parents Johann and Franziska for their support and for making all of this possible. Gernot, Evelyn, Heidi, Alexander, Lea, Marco, Friedrich, Margit, Paul, Klaus and Nane for their help and encouragement. Last but not least I would like to thank my girlfriend Viktoria for her support and for listening to my problems. You have helped me through good and bad times.

Wolfgang J. Fischer
Graz, 21.03.2012.

Contents

List of Figures

List of Tables

Chapter 1

Introduction

1.1 Scope of the thesis

Paper strength mainly depends on the strength of single fibers and the strength of individual fiber to fiber joints (Page [1969], Torgnysdotter and Wågberg [2003]). For a more precise description of the strength of the paper network it is of utmost importance to investigate the mechanical properties of fibers and fiber crossings as well as their behavior during loading. This thesis is concerned with the determination of:

- the breaking load of single fibers (**single fiber tensile strength**)
- the force that is needed to break a single fiber to fiber joint (**breaking load**)
- the breaking load per unit bonded area (**specific bonding strength**)
- the energy needed to break individual fiber crossings (**bonding energy**)

Other topics of interest are the analysis of the fiber deformation during mechanical testing and the determination of the bending stiffness of single fibers which is of high importance in the formation of fiber to fiber joints (Forsström et al. [2005]). Furthermore, the influence of the three different modes of loading (mode I, II and III loading) on the strength of single fiber crossings is an important issue. For this a novel direct method for mechanical testing of single fibers and fiber to fiber joints is developed. The results of all of these tests will lead to a better understanding of fiber and joint failure mechanisms. These tests provide knowledge regarding fiber and joint parameters which can be used for network modeling (Kulachenko and Uesaka [2012], Magnusson [2013], Borodulina et al. [2012]). The models in turn contribute to a better understanding of paper fracture mechanics.

A combination of the results of all these tests will help to get a better understanding of the mechanical properties of paper as well as its behavior during mechanical

testing. Also the effect of fiber production, stock preparation and chemical additives on mechanical paper, fiber and joint strength can be studied.

1.2 CD-Laboratory for Paper Strength

This PhD thesis was carried out within the frame of the CD-Laboratory for Surface Chemical and Physical Fundamentals of Paper Strength which was funded in 2007. This research project is a collaboration between two university institutes from Graz University of Technology (Institute of Solid State Physics, Institute for Paper, Pulp and Fiber Technology), one from the Montanuniversität Leoben (Institute of Physics) as well as the industrial partners (Mondi Frantschach GmbH, Kelheim Fibres GmbH and Lenzing AG). Figure 1.1 gives an overview of the contributions of each group as well as the main object of this research project.

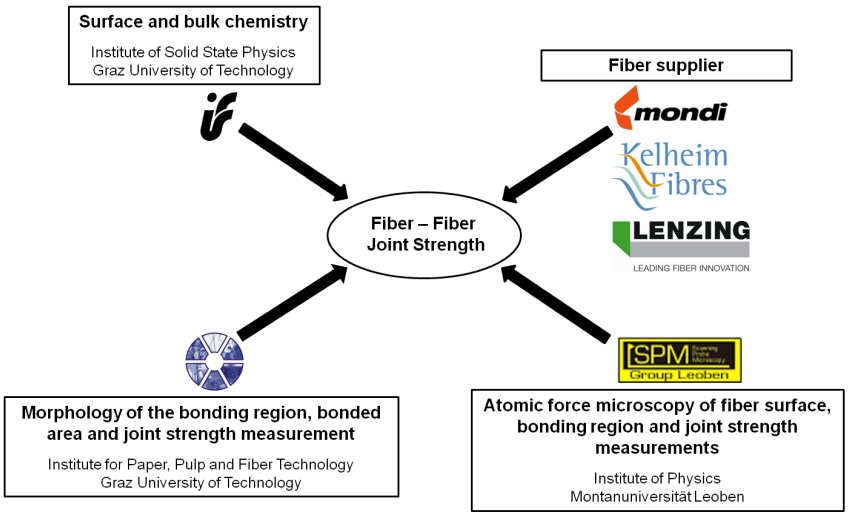

Figure 1.1 Working groups of the CD-laboratory for Surface Chemical and Physical Fundamentals of Paper Strength

The surface and bulk chemistry of the fibers is analyzed at the Institute of Solid State Physics using Attenuated Total Reflection Fourier Transform Infra Red Spectroscopy (ATR - FTIR). At the Institute of Physics in Leoben, the fiber surface as well as the bonding region is examined using Atomic Force Microscopy (AFM). Furthermore, the breaking load of individual fiber to fiber joints in z-direction is determined with an AFM based method. Research at the Institute for Paper, Pulp and Fiber Technology focuses on the investigation of the morphology of the bonding region and the determination of the size of the bonded area. Also the shear strength of single fiber crossings is measured. The industrial partners use and apply the knowledge developed in the CD-Laboratory to enhance the mechanical properties of their products.

The main goal of the CD-Laboratory for Surface Chemical and Physical Fundamentals of Paper Strength is to learn more about the properties of single fibers, fiber to fiber joints as well as the various bonding mechanisms in order to get a deeper understanding regarding the factors leading to the strength of the paper network.

1.3 Outline of this thesis

After this introduction chapter, the present thesis is divided into the following five chapters:

Chapter 2 *"Determination of fiber and joint properties"* gives an overview of the fundamental parts of a micro tensile tester as the concept of the device developed within the framework of this thesis is based on that for single fiber testing. An overview of different direct and indirect methods for measuring the strength of single fiber to fiber joints as well as the determination of the bending stiffness of single fibers is presented. Also the principles of the three possible modes of loading which are acting on the joint during testing are discussed.

In **Chapter 3** *"A novel micro bond tester for mechanical testing of single fibers and fiber to fiber joints"* the development as well as the most important parts of the micro bond tester are discussed in detail. It also covers an in-depth evaluation of the presented measurement system. Other topics of this chapter are the preparation of the individual fiber crossings, the test methods as well as the testing procedures for this novel testing device.

Chapter 4 *"Analysis of the bonding region"* describes the investigation of the formerly bonded area of fiber to fiber joints as well as the fiber surface by using the so-called low-voltage scanning electron microscopy. The influence of different types of adhesives is analyzed with this method and initial results of in-situ ultramicrotome investigations of a fiber crossing are presented.

In **Chapter 5** *"Results and Discussion"* the results of the different test methods are presented and compared with those of other studies. The different strength measurements are compared with each other and possible explanations for the difference are discussed. Furthermore, initial results of simulations demonstrate the influence of the different loading modes.

In **Chapter 6** *"Conclusions and Outlook"* the most important results obtained in this thesis are briefly discussed and an outlook on future work is given.

1.4 List of Publications

Papers

1. Magnusson, M.S., Fischer, W.J., Östlund, S. and Hirn, U. (2013). Interfibre Joint Strength under Peeling, Shearing and Tearing Types of Loading. In prepara-

tion for publication for the 15^{th} Fundamental Research Symposium, Cambridge, United Kingdom.

2. Fischer, W.J., Hirn, U., Bauer, W. and Schennach, R. (2012). Testing of individual fiber-fiber joints under biaxial load and simultaneous analysis of deformation. Nordic Pulp and Paper Research Journal 27(2):237-244

Contribution to conference proceedings

1. Fischer, W. J., Hirn, U., Bauer, W. and Schennach, R. (2012). Shear testing of individual fibre-fibre bonds. In CD-ROM Proceedings of the 6^{th} European Congress on Computational Methods in Applied Sciences and Engineering (ECCOMAS 2012), September 10-14, 2012, Vienna, Austria.

2. Ganser, C., Schmied, F., Fischer, W.J., Hirn, U., Schennach, R. and Teichert, C. (2012). Single fiber-fiber bond strength measurements using atomic force microscopy. In CD-ROM Proceedings of the 6^{th} European Congress on Computational Methods in Applied Sciences and Engineering (ECCOMAS 2012), September 10-14, 2012, Vienna, Austria.

3. Schmied, F., Ganser, C., Fischer, W.J., Hirn, U., Bauer, W., Schennach, R. and Teichert, C. (2012). Utilizing atomic force microscopy to characterize various single fiber-fiber bonds. In International Paper and Coating Chemistry Symposium, pages 141-143, June 10-14, 2012, Stockholm, Sweden.

4. Schmied, F., Ganser, C., Fischer, W.J., Hirn, U., Bauer, W.; Schennach, R. and Teichert, C. (2011). Insights into Single Fiber-Fiber Bonds Using Atomic Force Microscopy. In Progress in Paper Physics Seminar 2011 Conference Proceedings, pages 197-198, September 5-8, 2011, Graz, Austria.

5. Fischer, W.J., Hirn, U., Bauer, W. and Schennach, R. (2011). Konzept eines Messgerätes zur Bestimmung der Scherfestigkeit einzelner Faser-Faser Bindungen. In Minisymposium Verfahrenstechnik, pages 99-102, June 30 to July 01, 2011, Graz, Austria.

6. Schmied, F., Fischer, W.J., Hirn, U., Schennach, R. and Teichert, C. (2011). Mechanical properties of fiber–fiber bonds in paper studied by atomic force microscopy. In Verhandlungen, pages BP3.3-BP3.3, Frühjahrstagung der Deutschen Physikalischen Gesellschaft, March 13-18, 2011, Dresden, Germany.

7. Schmied, F., Fischer, W.J., Hirn, U., Bauer, W., Schennach, R. and Teichert, C. (2011). Static and dynamic load of single fiber-fiber bonds using atomic force microscopy. In Zukunft.Forum Papier, Österreichische Papierfachtagung, June 8-9, 2011, Graz, Austria.

Oral presentations

1. Fischer, W.J., Hirn, U., Bauer, W. and Schennach, R. (2012). Shear testing of individual fiber-fiber joints under biaxial load and simultaneous analysis of deformation. In International Paper Physics Conference, June 10-14, 2012, Stockholm, Sweden.

2. Kappel, L., Schmied, F., Hirn, U., Fischer, W.J. and Schennach, R. (2010). An Interdisciplinary View on the Strength of a Fiber-Fiber Bond in Paper. In Seminar on Fiber Testing, October 13, 2010, KTH Stockholm, Sweden.

Posters

1. Fischer, W.J., Kappel, L., Hirn, U., Bauer, W. and Schennach, R. (2010). Polarized Light Microscopy for Fiber-Fiber Bond Area Measurement Revisited. In COST Action FP 0802 Experimental And Computational Microcharacterization Techniques in Wood Mechanics, October 05-08, 2010, Hamburg, Germany.

Chapter 2

Determination of fiber and joint properties

Paper consists of single fibers, which interact with each other, leading to the formation of a complex network. These fibers consist of cellulose, hemicellulose and lignin. **Cellulose** is a linear polymer glucan with a uniform chain structure (Fengel and Wegener [2003]). The degree of polymerization ranges from 7000 to 15000. **Hemicellulose**, also called polyose, is a heteropolysaccharide and has a degree of polymerization ranging from 100 to 200 (Alén [2000]). The main differences compared to cellulose is that it is made up of several sugar moieties (pentoses, hexoses, heuronic acid, deoxy-hexoses) which are mostly branched (Sixta [2006]). Another difference is its alkaline solubility (Alén [2000]). **Lignin** is an amorphus substance which can be found in the middle lamella and in the secondary walls of a fiber, it is a complex macromolecule based on phenylpropane and other units (Fengel and Wegener [2003]).

Another characteristic of wood fibers is that they are built-up of different walls (see figure 2.1) which in turn are composed of microfibrils. These are the primary wall P,

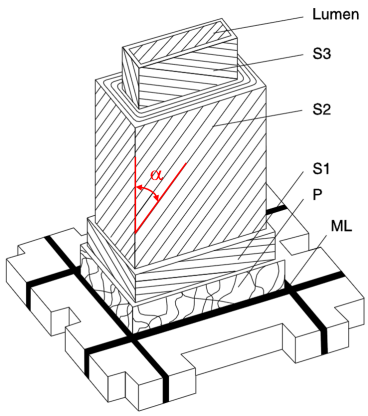

Figure 2.1 Structure of a fiber cell wall, middle lamella - ML, primary wall - P, secondary wall 1 - S1, secondary wall 2 - S2, secondary wall 3 - S3 (Sirviö [2008])

the secondary wall S1, S2 and S3. The middle lamella ML between the primary walls is holding the fibers together (Clark, J. d'A. [1985]). The S2 wall which is the thickest one (see table 2.1) has the biggest influence on the mechanical properties of single fibers. But not only the thickness of this layer is of great importance for the strength of single fibers, also the fibril angle α of the S2 wall (see figure 2.1) significantly influences the tensile behavior of the fibers (Page et al. [1972]). The deviation of the fibril angle from the fiber axis in the S2 wall is much lower than that of the P, S1 and S3 (see table 2.1). The lower the fibril angle in the S2 wall, the higher the strength of individual fibers. From table 2.1 it is also apparent that the thickness as well as the

fiber wall		mean fibril angle [°]	fiber wall thickness [μm]
primary wall P			0.05 to 0.1
secondary wall S1		50 to 70	0.1 to 0.3
secondary wall S2		5 to 30	1.0 to 8.0
	latewood	5 to 10	3.0 to 8.0
	earlywood	20 to 30	1.0 to 4.0
secondary wall S3		60 to 90	< 0.1

Table 2.1 Microfibril angles of the different fiber walls (Alén [2000])

microfibril angle depends on whether the fiber is an early- or latewood fiber.

As mentioned above, paper is made of wood fibers and these fibers interact with each other, leading to the formation of a complex network. The strength of paper mainly depends on two factors. These factors are the strength of a single fiber and the strength and number of fiber to fiber joints (Page [1969]; Schniewind et al. [1964]; McIntosh [1963]; Torgnysdotter and Wågberg [2003]). The formation of joints between individual fibers occurs due to five different bonding mechanisms (Lindström et al. [2005]). These mechanisms are shown in figure 2.2. **Mechanical interlocking**

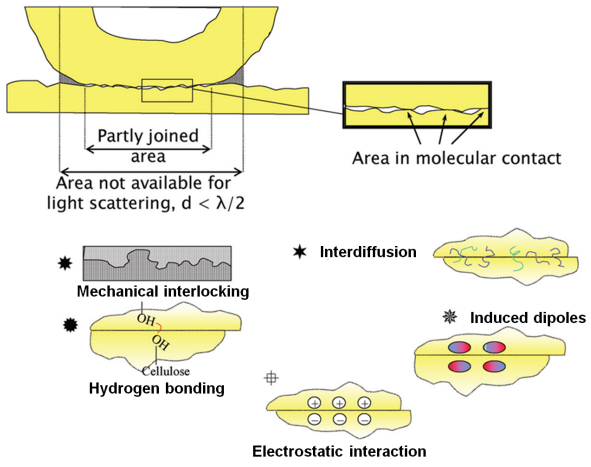

Figure 2.2 Bonding mechanisms (Lindström et al. [2005])

is caused by the roughness of the fiber surface as well as the entanglement of fibrils on the surface of the fibers. The migration of molecules from one fiber surface into another is referred to as **interdiffusion**. Another bonding mechanism is the formation of **hydrogen bonds** between the hydroxyl groups of cellulose and hemicellulose. Interactions between the negatively charged surface of a fiber and positively charged components on another fiber lead to electrostatic bonding (**electrostatic interaction**). Van der Waals interactions (**induced dipoles**) can be divided into three types (Askeland et al. [2011])

- London forces
  Fluctuations in the electron distribution cause weak dipoles which in turn induce transient dipoles in neighboring molecules and thus attraction.
- Debye forces
  Interaction between the permanent dipole of a molecule and the induced dipole of a neighboring molecule.
- Keesom forces
  Interaction between molecules that both have permanent dipoles.

Investigating the properties of individual fiber-fiber joints as well the properties of single fibers leads to a better understanding of fiber and joint failure mechanisms. In these tests, information about the material parameters are obtained. Such parameters are for example the E-modulus, the breaking load of single fibers and fiber crossings, the breaking energy of fibers and joints, the size and the shape of the fiber cross section, the stresses acting on the cross section of single fibers, the fiber elongation, the bending stiffness of single fibers, the area moment of inertia as well as the specific bonding strength (SBS). All of these material properties can be used to model and simulate the behavior of single joints as well as paper networks. This in turn will contribute to a better understanding of paper fracture mechanics.

2.1 Mechanical testing of single fibers

Single fiber testing is tedious and time consuming. This is due to the fibers small size which complicates manipulation. Several concepts and methods have been developed for determining the tensile strength of individual pulp fibers. They can be divided into the following three groups (Wathén [2006]):

- **micro tensile tester** (main topic of this section)
- **single fiber fragmentation test (SFFT)**
  In the single fiber fragmentation test the probability of a fiber breakage at a certain fiber length and degree of strain is given. Before the fibers can be tested,

they are embedded (parallel to loading direction) in vinyl ester (see figure 2.3a). After the matrix cured, the sample is fixed in a tensile tester (see figure 2.3b and 2.3c). Straining is carried out gradually in order to enable calculation of the number of fiber breaks per unit of length as a function of strain (Andersson et al. [2002]). A problem of this method is the introduction of stresses at the

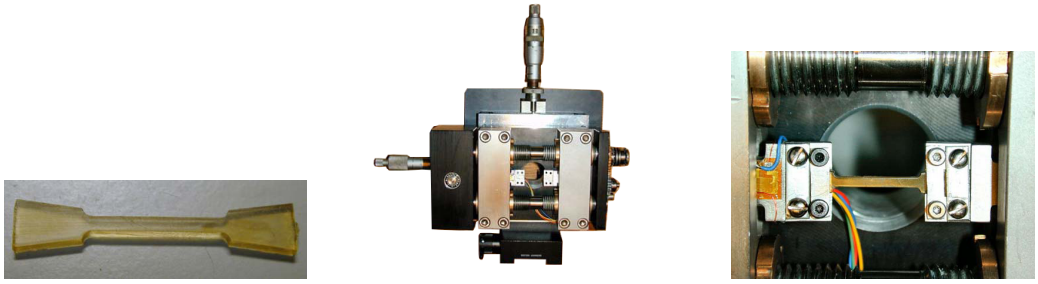

(a) specimen SFFT **(b)** testing device **(c)** specimen mounted in testing device

Figure 2.3 Specimen and testing device used in the single fiber fragmentation test (Feih et al. [2004])

interface between the fiber and the vinyl ester. Theses stresses lead to premature failure of the fibers. Furthermore, the fiber and the embedding agent have a different modulus of elasticity and due to this fact it is difficult to find out what is measured (contribution of fibers not known).

- **zero span tensile strength**
  The procedure of the zero span tensile test (ZSTT) is similar to the one of a common tensile test. The main difference of this kind of test is that the distance between the edges of the jaws, in which the paper sheet is fixed, is zero. This fact offers the possibility to clamp single fibers and thus to introduce the load into these fibers (Boucai [1971]). The principle of the zero span tensile test is shown in figure 2.4. Due to the complex loading situation of the zero span

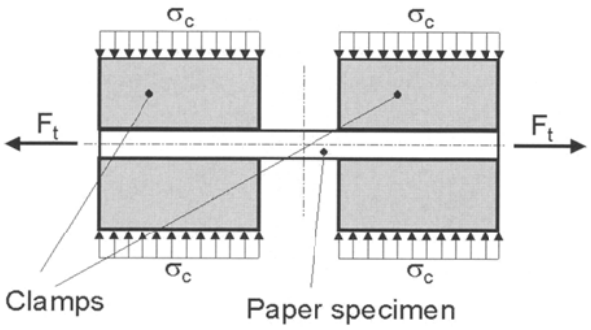

Figure 2.4 Principle of zero span tensile testing (Hägglund et al. [2004])

tensile test, which is the result of the three-dimensional stress distribution in the paper sample, it is impossible to extract the pure fiber strength. Another problem is that curled fibers, containing crimps and kinks, do not contribute to force transmission until these fibers are straightened (Seth [2001]) which in turn reduces the zero span strength.

This thesis focuses only on the so-called micro tensile testers. Until the present day various types of these kind of testers have been developed. Some of these instruments can be ordered directly from manufacturers. In some cases they are modified versions of devices which are used for conventional tensile tests. Conn and Batchelor [1999], Yu et al. [2011a], Page et al. [1972] and Hu et al. [2010] for example used an Instron tensile tester in order to determine the breaking load of different types of fibers. Other scientist developed their own testing devices. Figure 2.5 shows examples of modified as well as custom-built tensile testers.

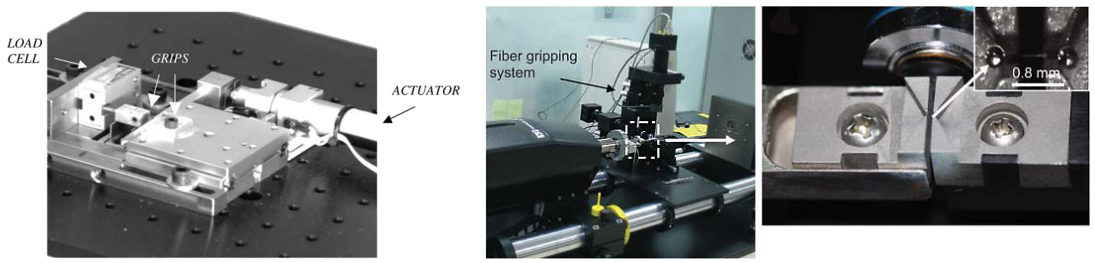

(a) custom-built tensile tester (Kompella and Lambros [2002])

(b) modified Instron tester (Yu et al. [2011b])

Figure 2.5 Examples of devices used for mechanical testing of single fibers

All these devices no matter whether they are standard, modified or custom-built instruments, consist of the same fundamental parts. These parts are a system for fixing the individual fibers, an equipment for force transmission and a force measurement system.

2.1.1 Fiber fixation

Before testing, the cellulose fibers have to be fixed on specially designed holders. The design of this part is of great importance. A possible consequence of a poor design is the misalignment of the samples which leads to stress concentrations within the fibers and therefore to premature failure of the samples (i.e. before testing). Basically this means that without a well planned design a correct measurement is not possible.

The fixation of the fibers must be carried out carefully. The individual fibers need to be fixed on a sample holder or in a specially designed clamping system without damaging them. Induced defects lead to premature failure of the fibers and

therefore to wrong measurement results. Conventional methods commonly used for fiber fixation are:

- mechanical clamping
- fixation with glue
- ball and socket system

Mechanical clamping

In conventional tensile tests, the samples are clamped in jaws. A logical conclusion would be to adopt this procedure to single fiber testing. An example of such a mechanical clamping device used for determining the breaking load of single fibers is shown in figure 2.6. The main problems when using mechanical clamps are the following

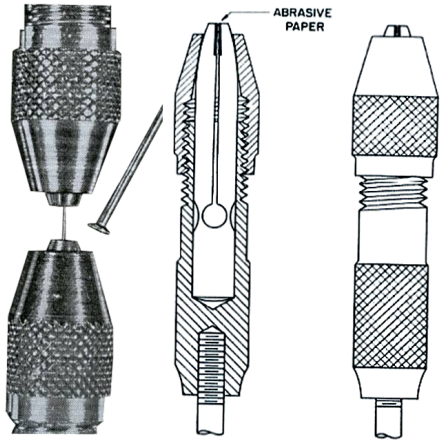

Figure 2.6 Mechanical clamping of a single fiber used by Jayne [1959]

- fragile nature of fibers
  Often, more than 50% of the fibers break in the region of clamping. The reason for this is the compression of the cell wall within the clamped region of the fibers (Groom et al. [2002]). This means that clamping induces additional defects.
- small sample dimension
  For fixing the fibers within the jaws, they must have a certain length (Hardacker [1962]). If they are too short it is not possible to grip both fiber ends.
- slippage of fibers during loading (Groom et al. [2002])
  In order to avoid slipping of the fibers, sufficient friction in the region of clamping is needed.

An advantage of this methods is that if the fibers have a certain length they can be fixed quickly. The advantages and disadvantages of mechanical clamping are summarized in table 2.2.

advantages	disadvantages
- fast fiber fixation - no dead time (no hardening of glue)	- introduction of defects in clamping region - slipping of fibers if load is applied - certain length of fiber required

Table 2.2 Pros and cons of mechanical clamping

Fixation with glue

Another possible method for fiber fixation is to use glue. In many cases the fibers are glued onto a special designed sample holder by using cyanoacrylate glue (Burgert et al. [2003], Kompella and Lambros [2002]), epoxy resin (Conn and Batchelor [1999], Page et al. [1972], Adusumalli et al. [2006]) or Duco cement which is a nitrocellulose solution (Leopold and McIntosh [1961], Van Den Akker et al. [1958]). For this kind of fiber fixation the properties of the sample holder are of utmost importance. Figure 2.7 shows examples of such sample holders. The sample holders are either made of paper

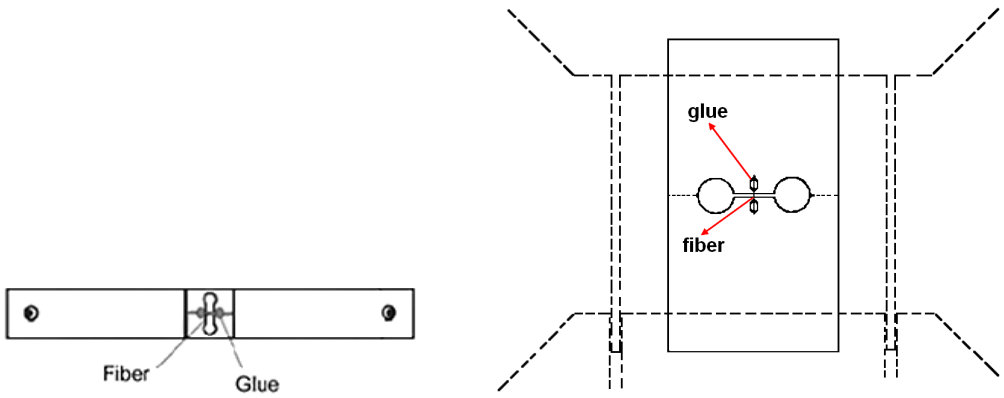

(a) Burgert et al. [2003] **(b)** Van Den Akker et al. [1958]

Figure 2.7 Sample holder used for single fiber testing

or plastic. The main problem in using paper is that if the bridges, which are keeping together the individual parts of the sample holder, are cut through, vibration could be induced. Due to this fact, additional defects are generated which may already lead to premature failure of the fiber before it can be tested. If plastic is used as carrier material for the individual fibers this problem can be avoided and reduced. The reason is that the bridges are melted by a hot wire and this procedure diminishes the negative influence of vibrations.

An advantage of this method is that no additional fiber defects are introduced in the fixation area (no clamping of fibers). Furthermore, slipping of the fibers can be avoided if a glue which provides sufficient adhesion is used. However, a possible penetration of the glue into the fiber cell wall will lead to wrong results. For this method the individual fibers are selected using tweezers which is very time consuming and tedious. A problem when using tweezers is that additional fiber defects can be introduced. These defects may lead to premature failure of the fiber (reduced tensile strength). Curing of the glue is another factor that takes a certain amount of time (depending on glue). The advantages and disadvantages of this fixation method are summarized in table 2.3.

advantages	**disadvantages**
- by selecting a suitable glue sufficient adhesion generated **-** no additional defects in the area of fixation (no clamping)	**-** tedious and time consuming **-** possible penetration of glue into cell wall (falsification of results) **-** additional defects in fibers due to handling with tweezers

Table 2.3 Pros and cons of gluing

Ball and socket system

The so called ball and socket system is one of the most widely accepted fixation methods for single fiber testing. In this method a drop of epoxy resin is applied to both ends of the fiber. During drying of the resin, the balls are formed (Peters [2010], Groom et al. [2002], Yu et al. [2011a,b], Mott et al. [1995]). This is shown in figure 2.8a. After the spheres are complectly cured, the balls are fixed in the so-called socket (see figure 2.8b). Within the system, the balls are able to rotate freely. Due to this fact the fibers can align themselves. This means that stress concentrations which are the result of fiber misalignments, can be avoided. Disadvantages of this method are that the fibers can be pulled out of the ball, the long waiting time due to curing of the resin, as well as the introduction of additional defects (with tweezers). Table 2.4 gives an overview of the advantages as well as the disadvantages of this method.

advantages	**disadvantages**
- no stress concentrations due to self alignment (no premature failure)	**-** possible indication of defects when applying resin (with tweezers) **-** fibers can be pulled out of "ball" **-** time consuming

Table 2.4 Pros and cons of the ball and socket system

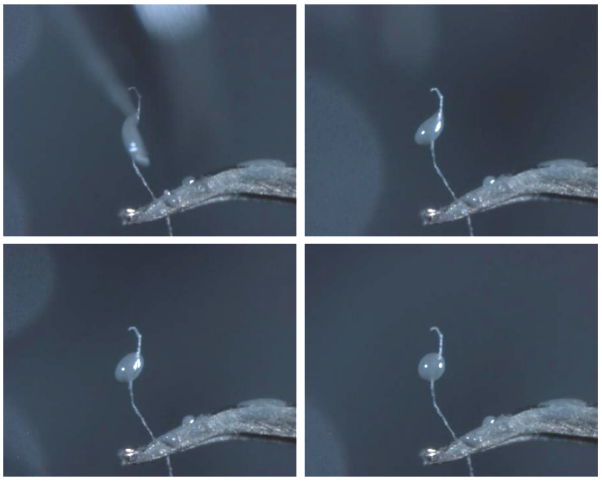

(a) fitting of resin and forming of ball (Peters [2010])

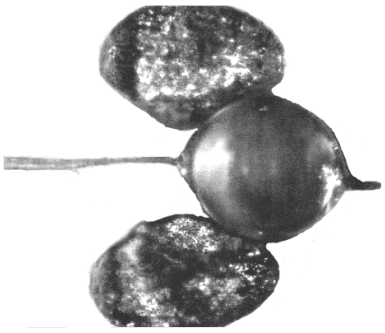

(b) ball and socket fixation of fiber (Groom et al. [2002])

Figure 2.8 Ball and socket system

2.1.2 Application of force

For the determination of the mechanical properties of single fibers it is necessary to apply an external force which will finally lead to failure. Drives with high positioning accuracy are used, as for example linear tables (Burgert et al. [2003], Kompella and Lambros [2002], a modified Mössbauer drive (Conn and Batchelor [1999]) as well as a piezo-electric actuator (Dunford and Wild [2002]). An important feature is that the tests should be carried out at low speed (in the range of a few $\mu m/\mathrm{s}$). At higher speed the application of force happens so quickly that the determination of the breaking load is almost impossible. The production of the drives also requires highest accuracy. A jerky approach or tilting of the linear tables due to dimensional variations of a few micrometers introduce additional defects into the fibers and this in turn will lead to premature failure of the tested sample.

2.1.3 Force measurement

The forces required to break a single fiber are measured by using load cells with a very high resolution (Yu et al. [2011a], Eder et al. [2008], Adusumalli et al. [2006], Mott et al. [1995]). In order to achieve the best results, the force sensors should be able to measure forces ranging from a few Millinewtons up to several Newton. The explanation is that the failure load of cellulose fibers is located somewhere in that force range. There are different types of force sensors (Ghosh [2009]) such as strain gauge load cells, piezoelectric load cells, inductive and reluctance based load cells, magnetoelastic load cells and others. The strain gauge force sensor, used in this study (see section 3.2.3), is the most common one. Load cells are often composed of

a spring and a sensor element (Elwenspoek and Wiegerink [2001]). Application of load to force sensor leads to a deformation of the spring element. The deformation is detected by the sensor element (strain gauge) and converted into an electrical signal (see figure 2.9). In some cases the sensor element (strain gauge) is at the same time the

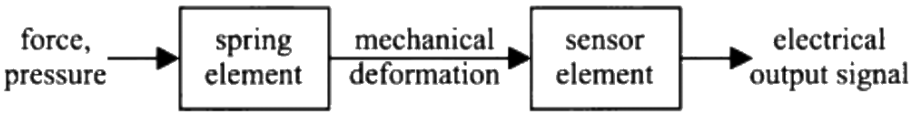

Figure 2.9 Measurement principle of a force sensor (Elwenspoek and Wiegerink [2001])

spring element. The deformation of the strain gauge changes its resistance (resistance of the strain gauge is a function of applied load) and thus the electrical output signal of the sensor (Fraden [2011]).

The handling of these sensors is difficult. This is due to the fact that the maximum forces which may be applied to the load cells are very low and in case of overloading the sensors are irreversibly damaged. Furthermore the sensors are very sensitive to bending of the active bolt. Long lasting bending will lead to wrong measurement results and even to damage of the load cells. There are three possible defects of strain gauge force sensors. These are:

- **overloading of the sensor**
  In case of overloading the strain gauges are deformed plastically. This means that the signal is shifted (offset shifted i.e. higher signal although no load is applied), the slope (linear relationship between senor signal [V] and applied load [g]) remains the same. A measurement is possible if the new offset is taken into account.

- **come off of strain gauge**
  If a strain gauge is coming off inside the force sensor, very high signals are generated. This is due to curling of the strain gauges which means that they are constantly under tension.

- **damage due to voltage surge**
  A voltage surge could cause burning of the strain gauges and for that reason the determination of the breaking loads is no longer possible.

2.1.4 Summary

The most important parts of a micro tensile testing device are the fiber fixation, an equipment for force application as well as a force measurement system. The most important one is the fiber fixing system. Conventional fixation methods are:

- **mechanical clamping**
  Clamping of the fibers offers a quick method for fixing single cellulose fibers.

The first big problem is that additional defects are introduced (in clamping regions) and the second one is that the fiber could be pulled out of the clamps (slipping out of fibers) if load is applied.

- **fiber fixation with adhesive**
  A significant disadvantage of this method is that it is tedious and time consuming (hardening of adhesive). By selecting a suitable glue sufficient adhesion is generated and slipping of the fiber can be avoided. A problem is that the glue could penetrate into the cell wall of the fiber and this in turn could lead to a falsification of the measurement results.

- **ball and socket system**
  Due to the self alignment of the fiber, stress concentration and thus premature failure can be avoided. Problems of this method are that the fiber can be pulled out of the ball and it is also time consuming (hardening of epoxy resin).

The pros and cons of these fiber fixation systems are summarized in table 2.5.

method	initiation of defects	expenditure of time	fixation of fibers	stress concentrations in fiber
mechanical clamping	- -	+ +	- -	- -
fixation with glue	-	- -	+	-
"ball and socket"	-	- -	+	+ +

Table 2.5 Pros and cons of the different fixation systems

Application of force

The devices used for force application could also introduce additional defects due to tilting of the linear tables or a jerky approach. Thus the design of such devices already requires highest accuracy.

Force measurement

For measuring the breaking loads of single fibers high precision load cells are used. Due to the fact that these fibers break at very low forces, the sensors must have a high resolution (in the range of a few Newton).

2.2 Joint strength

Until today numerous efforts have been undertaken to determine joint strength (in the context of this thesis the breaking load in mN) and specific bonding strength (here the breaking force divided by the area of the fiber-fiber joint) of fibers, a review is given by Uesaka [1984]. They can be divided in two different approaches. Direct methods are measuring the strength of individual fiber joints on specifically prepared fiber crossings. Indirect methods use results obtained from sheet testing. These results are

used for calculating the strength of fiber to fiber joints.
The following section gives an overview of such methods. Also the strength and weaknesses of these methods are discussed in more detail.

2.2.1 Loading modes acting on the joint

In fracture mechanics there are three different types of loading modes to which a crack may be subjected (Perez [2004]). These are the following:

- **mode I loading (opening mode)**
  In mode I the load is applied normal to the crack surface.
- **mode II loading (in plane shear mode, sliding mode)**
  In mode II the load is applied parallel to the crack surface and normal to the crack front.
- **mode III loading (out of plane shear mode, tearing mode)**
  In mode III the load is applied parallel to the crack surface and also parallel to the crack front.

Figure 2.10 shows the principle of the three loading modes in fracture mechanics. An important remark is that each loading mode results in a different strength. Due

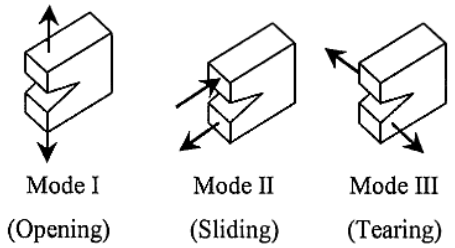

Figure 2.10 Modes of loading acting on a crack (Perez [2004])

to this fact it is important to know whether mode I, II or III is acting on the crack. The principle of these loading modes can also be applied for mechanical testing of single fiber to fiber joints. Also the strength of single fiber crossings is significantly influenced by the actual mode of loading (see section 5.4 and section 5.5). In this subsection the principle of the loading modes which are acting on a joint are discussed in more detail.

Mode I loading of joint

In mode I loading of a fiber-fiber joint, the force is acting perpendicular to the bonded fiber surface. The principle of this loading situation is shown in figure 2.11a. A method for measuring the mode I strength of a fiber to fiber joint was developed by

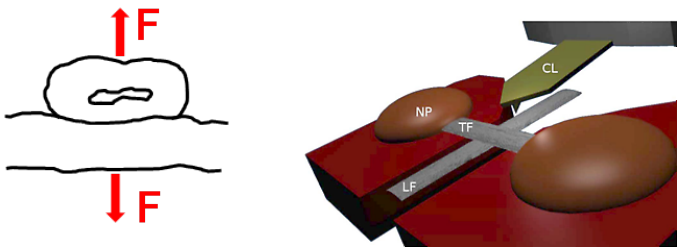

(a) **(b)** Schmied [2011]

Figure 2.11 Mode I loading of a fiber-fiber joint

Schmied [2011]. The principle of this method is shown in figure 2.11b. In this work a fiber-fiber joint is fixed on a self-made sample holder. The so-called top fiber (TF) is fixed with nail polish (NP) and the other one (lower fiber LF) is free. After fixation of the fiber crossing, the sample holder is placed in an atomic force microscope (AFM). The tip of a cantilever is positioned as close as possible to the joint (see figure 2.11b). In the next step, the cantilever is used for force transmission. The lower fiber is loaded with the tip until the joint breaks (fiber pressed away from joint). From the deflection of the cantilever beam Schmied is able to determine the mode I breaking load of the joint. A precise description of this method is given in Schmied et al. [2012].

Mode II loading of joint

Mode II loading of a fiber crossing is a conventional shear test. In this case one of the fibers, the longitudinal fiber, is pulled away from the cross fiber (see figure 2.12 left). The cross fiber is the one glued with both ends to a sample holder. Figure 2.12 right shows the principle of mode II loading. So, in this case the force is acting parallel to the bonded fiber surface. An important remark is that, in this case, mode II is

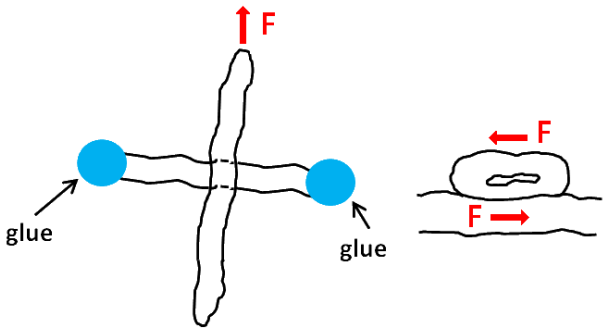

Figure 2.12 Mode II loading of a fiber-fiber joint

predominating but there is also mode I loading due to twisting of the cross fiber.

Mode III loading of joint

A joint configuration that is close to pure out of plane shear testing is shown in figure 2.13. If the longitudinal fiber is pulled away from the joint a counter force is created. The interplay between these forces leads to torsional loading of the joint. So, there is a moment that is acting on the joint. This situation is close to mode III loading of the fiber to fiber joint. Mode III loading is also generated if the crossing angle of

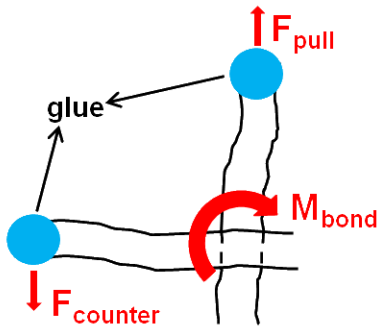

Figure 2.13 Mode III loading of a fiber-fiber joint

the joint shown in figure 2.12 differs from 90°. The greater the deviation from 90°, the greater the moment that is acting on the joint, leading to a more pronounced mode III loading. This means that in a conventional shear test, there is a mixture of mode I, II and mode III loading (see mode II loading of joint). In case of mode III testing (see figure 2.13) there is also mode II loading due to transmission of the force F through the contact zone.

Summing up, it can be said that there is always a mixture of the different loading modes. In order to get representative results, the interplay between them must be taken into account. The results presented later on (see section 5) show that there is a big influence of the loading mode on the strength of single fiber crossings. The question that is left is, if the mode III model can be applied for networks. This can be explained by the fact that paper is only loaded in z-direction (mode I loading of paper web) as well as in tension (mode II loading of paper web) during manufacturing, finishing and testing.

2.2.2 Direct methods

Several different setups for direct testing have been developed. Most of these methods use glue to fix the fiber joints on sample holders. After curing of the glue the joints are broken and the breaking force is recorded. Some methods also record elongation during testing.

Button [1979] investigated the strength of fiber-fiber joints by using single lap joints made of cellophane. He made macro and micro lap joints. The joints were tested

my means of an Instron testing machine and the so-called Fiber Load Elongation Recorder (FLER). Furthermore he investigated the effect of structural and material parameters on bonding strength. He studied the effect of bond length, fiber width, fiber thickness, axial Young's modulus, conformability, and interfacial cracks. He found that the bond length and several other structural parameters of the bond and the fibers have a significant influence on the strength of a fiber-fiber joint. Due to the lap joint configuration torsional loading (see mode III loading section 2.2.1) of the joint is avoided. In this way Button managed to obtain a rather well defined loading situation which is beneficial for studying parameters affecting specific bond strength. Button presented initial results of lap joints made of loblolly pine holocellulose. The

Figure 2.14 Single lap joint configuration used by Button [1979]

forces needed to break single joints range from 28.3 to 142.8 mN for summerwood and from 28.3 to 78 mN for springwood.

Stratton and Colson [1990] determined the strength of loblolly pine fiber crossings. Furthermore the influence of polymeric strength aids on bonding strength (A/C polyamidpolyamine epichlorohydrin, D/C polydiallyldimethyl ammonium chloride) was investigated. For the tests joints with a crossing angle of 90° were prepared. Thus the influence of varying crossing angle could be excluded. In order to determine the breaking load they glued the ends of bonded fibers on a Mylar mount using Epon 907 or hot melt (see figure 2.15). In this way the bonding region was free to rotate out of

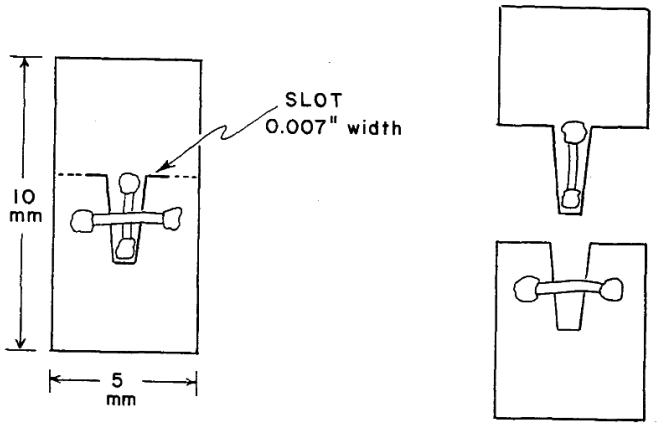

Figure 2.15 Mylar mount used by Stratton and Colson

the plane. The Mylar mount was installed in the clamps of the FLER2 and the load at failure was recorded. They also examined the effect of springwood vs. summerwood

and refining on the strength of fiber crossings. An overview of the results of this study is given in table 2.6.

fiber type	strength chemical	mean breaking load [mN]	bonded area [μm^2]	bond strength [N/mm^2]
springwood	-	4.61 ± 4.71	2410 ± 840	2.1 ± 2.1
summerwood	-	8.53 ± 5.49	1500 ± 540	6.4 ± 4.1
570ml CSF	-	7.16 ± 6.38	2070 ± 720	3.5 ± 2.8
345ml CSF	-	6.67 ± 4.71	2290 ± 1070	3.7 ± 4.4
springwood	A/C	11.18 ± 4.71	3000 ± 770	3.9 ± 1.7
570ml CSF	A/C	14.13 ± 11.97	2130 ± 800	7.5 ± 6.7
570ml CSF	D/C	14.81 ± 9.03	2040 ± 740	9.3 ± 5.7

Table 2.6 Result of Stratton and Colson [1990](± values = σ)

Schniewind et al. [1964] investigated the shear strength of summerwood, springwood and summerwood-springwood joints of douglas fir holocellulose, bleached kraft pulp (dried) as well as Tappi reference pulp (sulfite pulp, dried). These specimens were fixed on paper tabs. One of the fibers was placed across a slot (1 to 1.5 mm wide) and both ends of this fiber were pressed into masking tape. The other fiber protruded the tab. Afterwards the paper tab was fixed in the upper grip of a table model Instron tensile tester, while the protruding fiber was clamped with the lower grip and pulled away from the joint (testing speed 2.54 mm/min). Clamping of the fibers seems problematic, because it might introduce defects to the clamped fiber. A benefit of this study is that the effects of varying moisture contents as well as reproducibility were investigated. The results are summarized in table 2.7.

		bond strength	σ	breaking load		
	joint type	[MPa]	[MPa]	mean [mN]	max [mN]	n
holocellulose	sum-sum	3.74	3.87	7.65	23.54	16
	spr-spr	1.93	2.68	10.20	38.85	14
	sum-spr	2.83	2.61	10.79	38.96	21
dried kraft	sum-sum	0.77	1.03	1.37	2.75	10
pulp	spr-spr	0.37	0.25	1.08	1.77	4
	sum-spr	0.98	1.52	2.26	11.77	12
dried sulfite	sum-sum	0.32	0.17	0.78	1.37	4
pulp	spr-spr	0.21	...	0.59	0.59	1

Table 2.7 Results obtained by Schniewind et al. [1964]

Magnusson and Östlund [2011] are fixing joints with glue to a steel specimen holder. Here as well one fiber is placed across a small gap. Both ends of this fiber and one end of the other fiber are fixed (see figure 2.16). The crossings are tested using an Instron ElectroPulse E1000 electrodynamic tensile testing machine. In their work

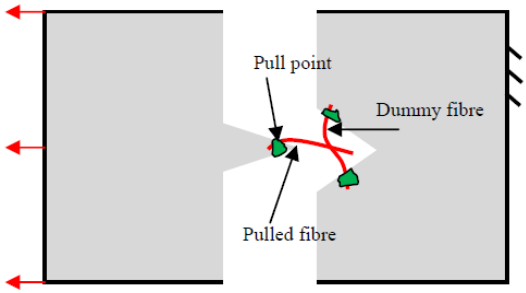

Figure 2.16 Sample holder used by Magnusson and Östlund [2011]

they also investigated the loading situation in the joint using a finite element method. They evaluate the amount of normal and shear loading which is an important step towards determining the local stresses which are leading to bond failure. For their model they assumed the fibers to be hollow, rectangular, non straight and elastic.

A different approach for fixing individual fibers is used by Saketi and Kallio [2011a]. For bond testing the fibers are fixed using microgrippers. Both ends of one fiber are clamped with the grippers (see figure 2.17a) and one end of the other fiber is glued onto a load cell (see figure 2.17b). For future applications it is planned to grip the fiber with a third gripper. Then the load cell and the attached fiber is moved

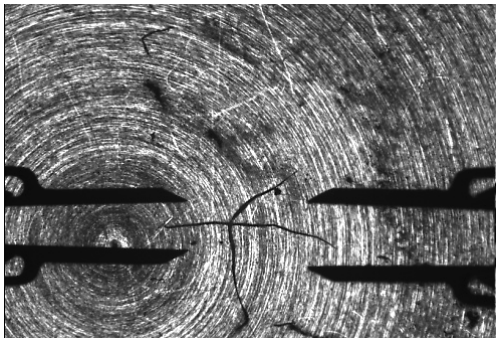

(a) gripping of cross fiber (Saketi and Kallio [2011a])

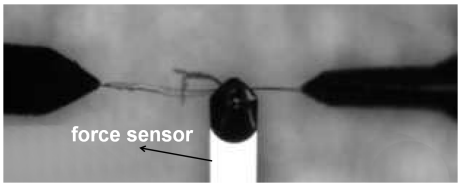

(b) gluing of longitudinal (Saketi and Kallio [2011b]) to force sensor (bottom)

Figure 2.17 Joint strength measurement using microgrippers

away from the joint (downwards in figure 2.17b). The advantage of this method is that the bonds are fixed with microgrippers. So no additional sample holder or manipulation of the bonds is needed. A problem is that after testing the glue has to be removed from the sensor with the help of acetone. In order to see that the sensor is not influenced by the chemical, it has to be calibrated after cleaning. When using microgrippers for determining the strength of individual fiber crossings there is always a possibility that the ends of the fiber are slipping out of the grippers during testing.

In their tests they obtained a mean breaking load of about 4.98 $\pm$ 4.55 mN and a specific bonding strength of 8.07 $\pm$ 8.6 MPa for untreated softwood pulp.

Mayhood et al. [1962] investigated unbeaten/beaten, unbleached/bleached, sulfite (spruce only) and kraft (spruce and pine) pulps. For their tests they modified a chain weight balance. First of all a new base, which fitted inside the balance cabinet as a separate unit, was installed. The sample pan was replaced by a specimen holder. In order to increase the loading capacity they build-in a heavier chain. To provide a constant loading rate of about 0.4 g/min, the chaino mechanism was linked to a 1 r.p.m. motor gear reducer. Furthermore the glass panels were removed and replaced by plastic film flaps to provide ready access and to reduce negative influences of air currents. The specimen holder consists of a moving mount, a stationary mount and an aligning device. The fiber-fiber joints are fixed across a slot of a knife-edge by using strain-gage cement. The positioning of the fiber crossing is shown in figure 2.18. The

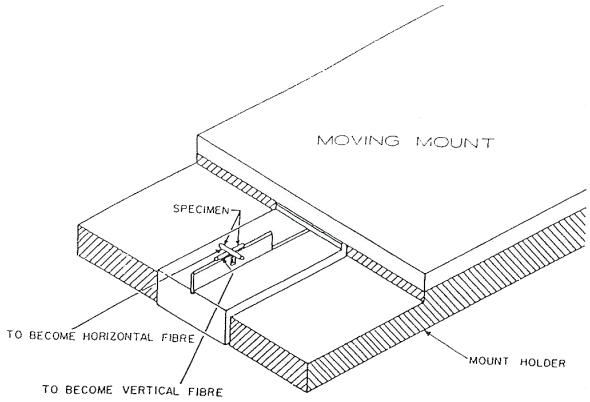

Figure 2.18 Joint fixation used by Mayhood et al. [1962]

optical bonded area was determined by using the method according to Page [1960]. The results of their investigations for unbeaten, unbleached sulfite (spruce) and kraft (mixture of spruce and pine) pulp are shown in table 2.8. A problem of this study is

pulp type	load [mN]	$A_{contact}$ [μm^2]	force per area [MPa]	$\overline{T}$ [°C]	$\overline{R.H.}$ [%]	n
sulfite pulp [a]	3.875	1344	2.86 $\pm$ 1.18	24.6 $\pm$ 2.7	41.9 $\pm$ 18.7	13
kraft pulp [a]	6.102	2097	2.94 $\pm$ 1.34	19.9 $\pm$ 1.9	49.9 $\pm$ 7.0	11
kraft pulp [b]	5.749	2069	2.83 $\pm$ 1.34	24.3 $\pm$ 1.6	58.4 $\pm$ 5.2	15
kraft pulp [c]	5.356	1564	3.54 $\pm$ 1.47	23.3 $\pm$ 1.0	56.6 $\pm$ 4.9	14

[a] unbeaten, unbleached
[b] mildly beaten, unbleached
[c] well beaten, bleached

Table 2.8 Result of the investigation of Mayhood et al. [1962]

that the tests are not carried out under controlled conditions (see table 2.8).

Mohlin [1974] developed a method for measuring the strength of bonds between a cellophane strip and a cellulose fiber. This means that in this case a cellophane-fiber crossing was referred to as a bond. In order to determine the strength of these bonds, the cellophane strip was glued with epoxy resin on a metal plate and the free fiber end was glued on a second one (see figure 2.19). The two plates were connected via

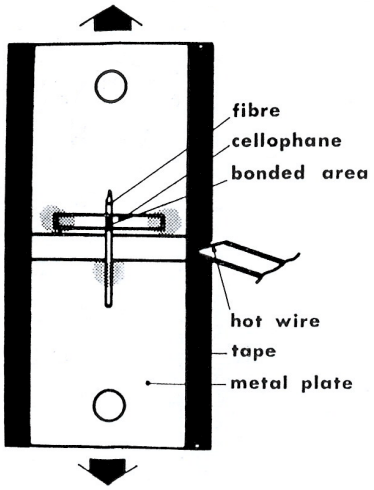

Figure 2.19 Test setup according to Mohlin [1974]

a tape which was cut by means of a hot wire. After cutting the tape, the bonds were broken with an Alwetron stress-strain instrument (0.1 mm/min) at 20° C and 65% relative humidity. In order to determine the area of contact, photo micrographs of the joints were taken and the area was planimetrically measured. The same measurement procedure was also used to determine the strength of sulfite pulp fiber to fiber joints (9 crossings tested). From these tests a mean joint strength of about 5.98 MPa was obtained.

McIntosh [1963] investigated the breaking load of joints between a fiber and a shive as well as between single fibers of loblolly pine kraft pulp. For the test he used a modified analytical balance which has been developed to determine breaking force of individual fibers (Leopold and McIntosh [1961]). In order to determine the tensile strength, a fiber was positioned between the ends of two paper tabs. These tabs were fixed in a modified spring clamp and the fiber ends were glued to the tabs by using Duco cement. The whole assembly was mounted in the testing device by means of two jeweler's chains. These chains were connected to the paper tabs via hooks which were inserted into holes on the tabs. One of the chains was fixed to one end of the balance arm and the second one to the balance platform. After fixation the clamp was released and the joint was ready for testing. In order to measure the breaking load a beaker (counterbalanced) was placed on the other arm of the balance and water was added until the fiber broke. The same device and measurement principle was used for joint testing. For mounting the sample in the tester, the ends of the shive were

glued to a cellophane piece which in turn was glued onto one of the paper tabs. In this configuration, the free fiber end extended beyond the edge of the cellophane and the contact area was imaged by using polarized light microscopy. After imaging the free fiber end was fixed to the second paper tab. During the whole fixation procedure the assembly was held in the spring clamp. When the glue was hardened, the paper tabs with the joint were mounted to one end of the balance arm. The beaker on the other arm was again filled up with water at a rate of 0.5 ml/s until the joint broke. A comparison between fiber-shive and fiber-fiber strength obtained in this study is given in table 2.9.

		breaking load [mN]	contact area [μm^2]	bond strength [MPa]
summerwood	fiber to shive	97.12	16140	5.79
	fiber to fiber	15.70	2620	6.18
springwood	fiber to shive	43.16	26550	1.77
	fiber to fiber	9.81	5310	2.06

Table 2.9 Results obtained in the study of McIntosh [1963] for loblolly pine

Russell et al. [1964] investigated the influence of two different types of wet strength resins (melamine formaldehyde "Parez 607", polyamide "Kymene 557") on the stress strain properties of single fibers, the wet and dry shear strength of fiber crossings as well as on the degree of bonding. For their tests they used unbeaten and unbleached, bisulfate softwood pulp. The breaking load of fiber to fiber joints was measured with a device already used by Mayhood et al. [1962]. In order to calculate the force per unit area, the optical bonded area was determined according to the method of Page [1960]. The results of this study are shown in table 2.10.

	untreated		Parez 607		Kymene 557	
joint properties	dry	wet	dry	wet	dry	wet
breaking load [mN]	5.49	0.63	5.10	1.77	5.00	2.06
contact area [μm^2]	2260	2300	2440	2140	2040	2170
fore per area [MPa]	2.51	0.28	2.34	0.84	2.44	1.02

Table 2.10 Result of Russell et al. [1964]

The results obtained in the different studies show that there is a strong scatter in the measured values. Natural fiber defects as well as defects due to handling reduce the force needed to break a single fiber crossing. Some of the joints are more damaged than others and this explains the high σ values. The strength values obtained by Button [1979] are considerably higher than those of the other studies. This can be explained by the lap joint configuration that was used by Button. Due to this configuration torsional loading of the joint can be avoided. This indicates that the strength of individual fiber to fiber joints is significantly influenced by the crossing

angle (see section 2.2.1). The results obtained by Mayhood et al. [1962] indicate that the strength of single fiber crossings is also influenced by the relative humidity. The joints prepared from beaten fibers have a lower breaking load than joints made of unbeaten fibers. The reason for the reduced breaking load is the higher relative humidity during testing (see table 2.8).

A comparison between fiber crossings prepared from sulfite and kraft pulp (Mayhood et al. [1962], Schniewind et al. [1964]) shows that the strength of joints made of kraft pulp is higher than the one of sulfite pulp (see table 2.7 and table 2.8). The explanation for this is the reprecipitation of hemicellulose (increase the strength of fiber crossings) on the fibers in the kraft cooking process.

Direct methods discussed in this thesis focused only on the strength of softwood fiber crossings. The strength of joints made of hardwood has never been tested. In case of hardwood the problem is the fixation of the short fibers. Due to the short fiber length it is not possible to glue the joint to a sample holder (Stratton and Colson [1990], Schniewind et al. [1964], Magnusson and Östlund [2011], Mayhood et al. [1962], Mohlin [1974], McIntosh [1963], Russell et al. [1964]) or to grip them with microgrippers (Saketi and Kallio [2011a]). This indicates that the fibers must have a certain length.

Furthermore, there is a difference in the strength of summerwood to summerwood and springwood to springwood joints (Button [1979], Stratton and Colson [1990], Schniewind et al. [1964], McIntosh [1963]). According to Stratton and Colson [1990], the stress distributions which lead to failure of the joint are influenced by the fiber wall thickness. Another explanation is that springwood fibers have more naturally occurring defects which reduce the strength of fiber crossings (Button [1979]). Button also indicated that the difference between springwood and summerwood joints is due to the difference in the fibril angles and the fiber wall thickness.

2.3 Indirect methods

Indirect methods are based on results obtained from measurements on paper sheets. Joshi et al. [2011] investigated the effect of drying and low consistency refining on bond strength. For their tests they prepared handsheets from unbleached, never dried radiata pine pulp (60% yield) and a northern bleached softwood kraft pulp which was a mixture of white spruce, lodgepole pine and balsam fir. The fibers in the handsheets were weakened using HCl acid vapor until the strength of the fibers equals joint strength. After tensile testing, the samples were dyed with acridine orange, impregnated with immersion oil and investigated by using a confocal microscope. The images were used to calculate the fraction of broken fibers and this in turn was used to determine the so-called critical exposure time (lowest time of acid exposure at which all fibers that were bonded on both sides of the fracture line seemed to be broken).

The next step was to determine the zero span strength (Pulmac troubleshooter), the fiber width $\mathbf{D}_w$ (using Image Pro 5 software) and the cross sectional area $\mathbf{X}_f$. These values were used to calculate the the fiber-fiber shear bond strength σ_b. According to Joshi et al. [2011], σ_b is calculated as follows:

$$F_b = \sigma_f^c \cdot X_f \tag{2.1}$$

σ_f^c ..... fiber strength at critical point
F_b ..... force needed to break a fiber to fiber joint

$$\sigma_f^c = \frac{8}{3} \cdot Z_c \cdot \rho \tag{2.2}$$

Z_c ..... zero-span strength at critical point
ρ ..... fiber wall density

Substitution of equation 2.2 into equation 2.1 results in

$$F_b = \frac{8}{3} \cdot Z_c \cdot X_f \cdot \rho \tag{2.3}$$

$$\sigma_b = \frac{F_b}{A_b} \; and \; A_b = \frac{D_w^2}{\overline{cos\ \theta}} \tag{2.4}$$

A_b ..... bonded area of a joint (rhombus with height D_w)
θ ..... crossing angle
$\overline{cos\ \theta}$ ..... average of cos θ values

Equation 2.3 together with 2.4 results in

$$\sigma_b = \frac{8 \cdot Z_c \cdot \rho \cdot X_f \cdot \overline{cos\ \theta}}{3 \cdot D_w^2} \tag{2.5}$$

The results of these investigations are shown in table 2.11. Their results for specific bond strength are considerably higher than those obtained in other studies, although the size of the contact area seems to be overestimated (rhombic). If A_b is corrected, the strength values would even be higher ($\sigma_b = F_b/A_b$ i.e. $A_b \downarrow$ and $\sigma_b \uparrow$). This indicates that there is a problem in the calculation of the bonding strength. Furthermore, the assumption that $\mathbf{F}_{break\ fiber}$ is equal to $\mathbf{F}_{break\ bond}$ has not been verified. It is not known if there is an influence of the acid vapor exposure on the strength of fiber crossings. Besides the fibers, the joints could also be weakened by the acid. This remains to be clarified.

Pulp	Drying history before sheet manufacture	Refining treatment	Critical acid gas exposure time (min)	Calculated fiber–fiber shear bond strength (MPa)
Unbleached 60% yield radiata pine softwood	Never-dried	12 min in Valley beater, separation of shives and fines	115	25.0 ± 3.3
	Sheet formed, air-dried then reslushed		110	19.7 ± 2.8
	Sheet formed, oven-dried then reslushed		105	16.1 ± 2.4
NIST reference material 8495: bleached northern softwood kraft	Supplied as dry lap sheet from manufacturer	Unrefined	410	13.9 ± 1
		5 min refining in Valley beater after reslushing dried sheets	195	21.8 ± 1
		40 min refining in Valley beater after reslushing dried sheets	126	37.0 ± 1.1

Table 2.11 Result of Joshi et al. [2011]

Nordman et al. [1952, 1958] defined the ratio between the work consumed during a loading and unloading cycle of a strip of paper and the increase of the light scattering coefficient as a relative measure of bonding strength. The increase in the light scattering coefficient can be explained by the increase of the surface area and this in turn is due to loading and unloading of the paper strip which leads to breaking of bonds. Figure 2.20 illustrates the principle of the device and the testing procedure used in this study. They plotted the scattering coefficient over the irreversible work per gram

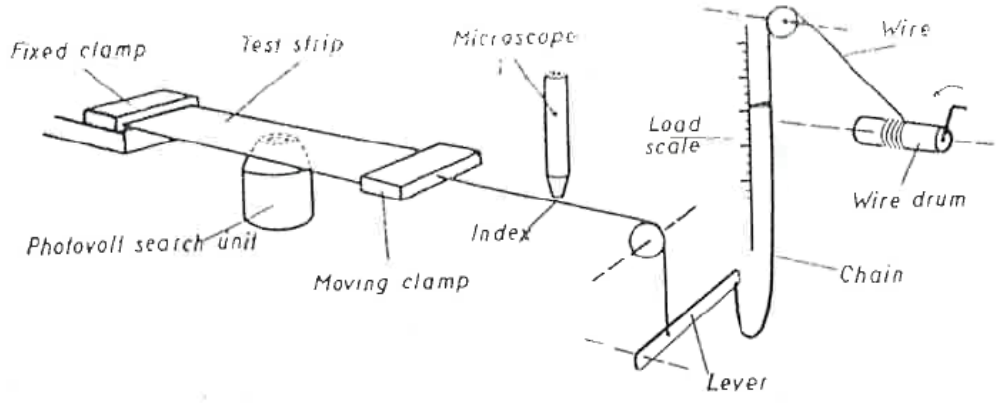

Figure 2.20 Testing setup used by Nordman et al. [1952, 1958]

of paper for several paper strips of the same sample. The result of these tests was a diagram in which a straight line was obtained and the cotangent of the angle of inclination of this line was the bonding strength value (see figure 2.21). Nordman et al. claim that the result is the energy needed to break fiber to fiber joints and to increase the internal surface within a strip of paper. Furthermore they assume that no other

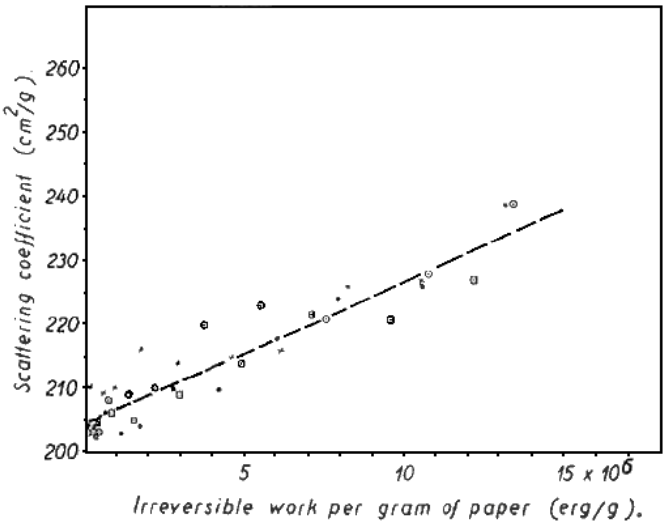

Figure 2.21 Diagram for the determination of the Nordman bond strength (Nordman et al. [1952])

energy consuming processes occur during the loading and unloading cycles. It has however been argued that Nordman bonding strength includes energy consumption due to structural changes in the sheet during tensile straining, rather than the interface strength of the fiber-fiber joint (Uesaka [1984]). Nordman obtained a bonding strength value of $4 \cdot 10^{-5}$ kJ/cm^2 for unbleached sulphate pulp and $2 \cdot 10^{-5}$ kJ/cm^2 for bleached aspen pulp.

Stone [1963] performed tests that were similar to those of Nordman et al. [1952, 1958]. In this study five pulps with different xylan contents were investigated (see table 2.12). Handsheets were prepared and from the sheets, strips with a width of 32 mm were cut out. In the next step the strips were strained to failure by using an Instron tester. The strain at failure was noted and the machine was set in a way that the crosshead moved back to the starting position if 90% of this value was reached (loading / unloading cycle). The area of the hysteresis loop (energy adsorbed by the strip) in the stress strain curve was measured with an integrator which was attached to the Instron tester. In order to calculate the energy adsorbed per gram of paper, the 10 cm long strip (involved in the energy adsorption) between the clamps was cut out and weighed. The internal surface area of the paper strips were determined optically with the Zeiss Elrepho (scattering coefficient determined before and after straining) and with BET nitrogen adsorption method. After testing, the specific energy E_b which is the irreversible energy per gram consumed in straining the sample divided by the change in specific surface area, was calculated. Table 2.12 shows the results of these tests. A drawback of this study is that different types of pulps were investigated (see table 2.12). The problem is that the pulps differ in their behavior during mechanical testing. On this account it is not possible to compare the influence of the different

	xylan content [%]	E_b (N_2 adsorption) [kJ/cm^2]	E_b (light scattering) [kJ/cm^2]
alkali extracted spruce sulfite	1.8	$8.0 \cdot 10^{-7}$	$3.2 \cdot 10^{-5}$
hollow filament rayon	2.6	$1.4 \cdot 10^{-6}$	$5.1 \cdot 10^{-5}$
bleached spruce kraft	7.6	$2.0 \cdot 10^{-6}$	$6.0 \cdot 10^{-5}$
bleached esparto soda	19.7	$2.2 \cdot 10^{-6}$	$7.8 \cdot 10^{-5}$
bleached hardwood kraft	24.2	$1.4 \cdot 10^{-6}$	$6.9 \cdot 10^{-5}$

Table 2.12 Results obtained by Stone [1963]

xylan contents on the energy needed to break the paper strip. A better approach would be to use only one pulp with different xylan contents.

Jones [1972] used different techniques in order to characterize the strength of unbleached kraft pulps. Such techniques are the zero-span tensile strength of sheets as well as the tensile strength of individual fibers which was measured with a modified Instron tensile tester. The surface area was determined by using BET nitrogen adsorption. In this study also the light scattering coefficient was measured (Elrepho reflectometer). The results of these measurements were used to calculate the relative bonded area (RBA). Fiber dimensions such as the coarseness (equal to Aρ) were determined according to TAPPI method T234 cm-02, the fiber length by projecting the fibers onto a grid and the fiber width was measured by using a microscope eyepiece micrometer. In order to determine the fiber perimeter, the width was multiplied by a factor of 2.2. The load elongation properties of sheets were determined by using a table model Instron tester. All of these results were used to calculate the bond strength of spruce pulp (beaten to different CSF) by using the Page equation (see equation 2.6 and 2.7 (Page [1969])).

$$\frac{1}{T} = \frac{9}{8Z} + \frac{12A\rho g}{bPL(RBA)} \tag{2.6}$$

T ..... tensile strength of paper strip [cm]
Z ..... zero-span tensile strength [cm]
A ..... fiber cross sectional area [cm^2]
ρ ..... fiber density [g/cm^3]
g ..... acceleration due to gravity [cm/s^2]
b ..... specific bonding strength (force per unit area) [dynes/cm^2]
P ..... fiber perimeter [cm]
L ..... fiber length [cm]
RBA ..... relative bonded area [-]

Later on the equation was used for 50% and 60% yield pulps. In the last case the total surface area was not determined. The bond strength values obtained in this study are shown in table 2.13.

type of pulp	fiber-fiber bond strength [MPa]
slash pine (50% yield)	7.1
slash pine (60% yield)	9.3
spruce	8.7

Table 2.13 Bond strength values as calculated by Jones [1972]

In the work of Gurnagul et al. [2001] the question regarding the contribution of the shear bond strength of single fiber crossings to the decrease in sheet strength upon drying and reslushing was re-examined. In this study a never dried, beaten and unbeaten, unbleached black spruce kraft pulp with a yield of 47.2% was used. They only used the R14 (long fiber) fraction in order to exclude the impact of fines. Sheets prepared from this pulp were dried fully restrained and referred to as never dried. After determining the physical properties, the sheets were reslushed, new ones were prepared and referred to as once dried. For measuring the zero span index Z they used a Pulmac apparatus, the light scattering coefficients S was measured with a Zeiss Elrepho photometer, the fiber curl with a fiber quality analyzer and the fiber length L and coarseness c with a Kajaani FS-200. All tests were carried out at 23°C and 50% relative humidity. In the next step the bonding strength was determined using the following equations.

$$\frac{1}{T} = \frac{9}{8Z} + \frac{12c}{bPL(RBA)} \tag{2.7}$$

$$k = \frac{12c}{PL} \tag{2.8}$$

$$RBA = \frac{S_0 - S}{S_0} \tag{2.9}$$

Equation 2.7 together with equation 2.8 results in

$$\begin{aligned} \frac{1}{T} - \frac{9}{8Z} &= \frac{k}{b(RBA)} \\ \left[\frac{1}{T} - \frac{9}{8Z}\right]^{-1} &= \frac{b(RBA)}{k} \end{aligned} \tag{2.10}$$

Substitution of equation 2.9 into equation 2.10 results in

$$\left[\frac{1}{T} - \frac{9}{8Z}\right]^{-1} = \frac{b\frac{(S_0 - S)}{S_0}}{k} = \frac{b(S_0 - S)}{kS_0} \tag{2.11}$$

$$\left[\frac{1}{T} - \frac{9}{8Z}\right]^{-1} = \frac{b}{k} - \left(\frac{b}{kS_0}\right) S \tag{2.12}$$

Finally they plotted the left part of equation 2.12 (Page bonding strength index) versus the light scattering coefficient (see figure 2.22).

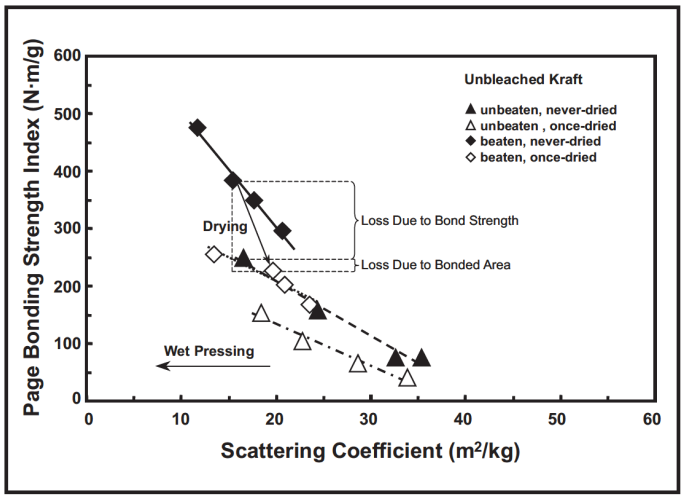

Figure 2.22 Results obtained by Gurnagul et al. [2001]

The right part of equation 2.12 is a straight line equation. According to Gurnagul et al. [2001], the intercept b/k is proportional to the shear bond strength. The results obtained in this study are shown in table 2.14.

	b/k [Nm/g]	standard error [Nm/g]
unbeaten, never dried	399	9.22
unbeaten, once dried	278	11.2
beaten, never dried	698	25.4
beaten, once dried	373	38.2

Table 2.14 Results obtained by Gurnagul et al. [2001]

Indirect methods which are based on the Page equation are difficult to interpret because they are often hard to understand. In some cases (e.g. Gurnagul et al. [2001]) it is almost impossible to compare the results with those of other studies. Another important remark is that it is difficult to predict the strength of a fiber to fiber joint by using the Page equation. Several different measurement methods (see Jones [1972]) are needed and the uncertainty in the measurements is also a significant problem. Each measurement error influences the results of the Page equation. Another problem is the uncertainty of the Page equation itself.

2.4 Fiber bending stiffness

The bending stiffness E · I [Nm^2] which is also called flexural rigidity is the product of the modulus of elasticity ***E*** and the area moment of inertia ***I*** (Fenner and Reddy [2012], Lossada [1998]). The flexibility of single fibers which is the inverse of the bending stiffness, characterizes the deformation ability of fibers due to loading by a bending moment. Another factor that describes the deformation behavior is the deformability due to shear loading which is called conformability. These fiber properties are of great importance for the formation of joints between fibers (Leopold and McIntosh [1961], Paavilainen [1993], Forsström et al. [2005]). Thus, it can be said that the lower the bending stiffness, the more joints can be formed and the stronger the paper.

A fiber property which has a major impact on the bending stiffness is the fibril angle of the S2 layer. As this layer is the thickest one it mainly controls the mechanical properties of the fiber (see introduction of 2). It is well known that the modulus of elasticity is changing from fiber to fiber due to different fibril angles (Page et al. [1977]) in the S2 layer. The development of the E-modulus over the fibril angle is shown in figure 2.23. From this figure it is apparent that the larger the fibril angle, the smaller

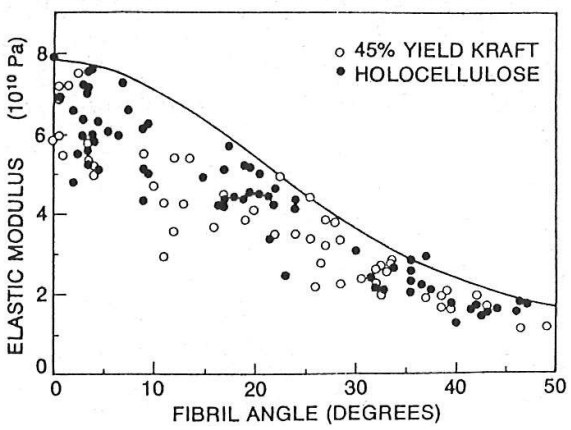

Figure 2.23 Development of the E-modulus over fibril angle (Page et al. [1977])

the modulus of elasticity and the smaller the bending stiffness of individual fibers. The moment of inertia is influenced by the shape of the cross sectional area (oval, circle etc.), the fiber wall thickness (springwood or summerwood fiber), changes in degree of fiber collapse, weak spots along fiber as well as by permanent fiber deformations (Robertson et al. [1961]). All these factors lead to different moments of inertia and this in turn has a direct influence on the bending stiffness as it is the E-modulus multiplied by the moment of inertia I. In figure 2.24 different cross sectional areas are illustrated. The cross section B,C,D and E have the same area and cross section A has a smaller one. The main difference between them is that they all vary in shape (except cross section A and B). A comparison of A and B (same shape but different areas) shows

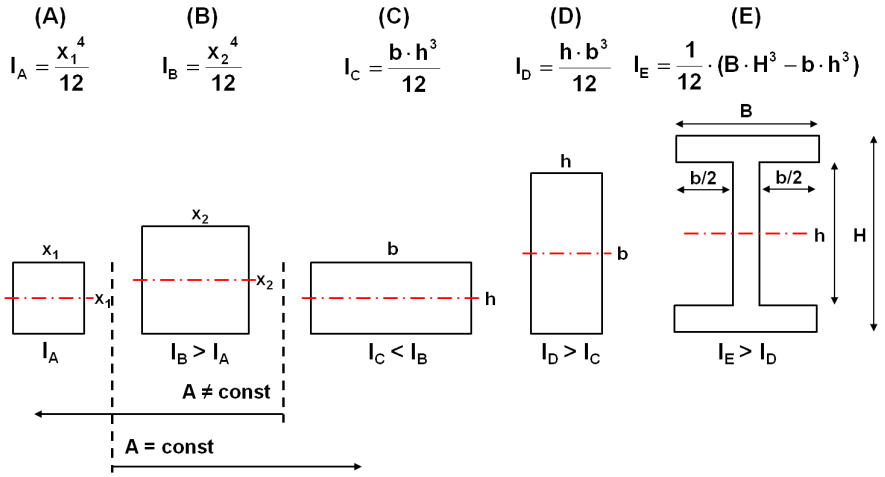

Figure 2.24 Influence of the size as well as the shape of the cross sectional area on the second moment of area (Schnell et al. [1995])

that in this case the area moment of inertia is significantly influenced by the size of the area. If the cross sections have the same area (cross sections B, C, D, E in figure 2.24), the shape is the important factor that controls I. Furthermore it is apparent that the farther away the mass is located from the centerline, the stiffer the system is (compare cross section E with the cross sections A, B, C and D in figure 2.24).

Schniewind et al. [1966] investigated the bending stiffness of dry and wet pulp fibers (first dry then wet). In order to determine the flexural rigidity the single fibers are fixed in a clamp. For their tests they assume the fiber to be a cantilever beam. The bending force is applied near the free end of the fiber by means of a quartz helix spring. Figure 2.25 shows the principle of this method. To determine the load ***P*** that is

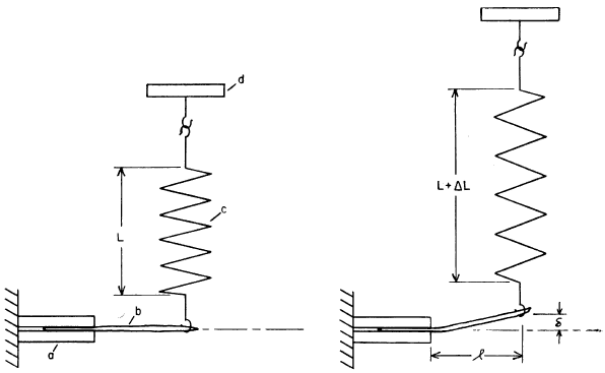

$$E \cdot I = \frac{P \cdot l^3}{3 \cdot \delta} \qquad (2.13)$$

P ..... load
l ..... span length
δ ..... deflection

Figure 2.25 Bending stiffness measurement according to Schniewind et al. [1966]

needed to bend the fiber, the spring extension ΔL is measured. The deflection δ as well as the span l (free length of fiber) are measured with a microscope and the bending

stiffness is calculated with equation 2.13. These investigations were made with white fir kraft pulp. The results of this study are shown in table 2.15. From the results shown

	dry state	wet state
unbeaten earlywood	$2.90 \cdot 10^{-11}$ Nm^2	$9.32 \cdot 10^{-12}$ Nm^2
unbeaten latewood	$1.45 \cdot 10^{-10}$ Nm^2	$2.60 \cdot 10^{-11}$ Nm^2

Table 2.15 Results of bending stiffness measurements obtained by Schniewind et al. [1966]

in table 2.15 it is apparent that the wet bending stiffness is only somewhat lower than the dry stiffness. As a result of swelling, the fiber becomes softer but at the same time the cross sectional area increases. Due to the larger area the area moment of inertia is also increased and this in turn explains the small difference between the wet and dry bending stiffness (due to swelling E $\downarrow$ and I $\uparrow$). The difference between earlywood and latewood fibers can be explained by the larger cross sectional area of latewood fibers (if $A_{cross\ section}$ increases $\rightarrow$ I and E increase $\rightarrow$ E $\cdot$ I increases).

The method used in the study of Schniewind et al. [1966] is based on that of Seborg and Simmonds [1941] who developed a device with which it is possible to determine the bending stiffness of single fibers in water as well as in air. In their tests, the fiber was also supported as a cantilever. A quartz spring was used for load application which had a sensitivity of 5 cm elongation per [mg] of load. In this case a cathetometer was used to measure the extension of the spring (readable to 0.005 cm). The spring elongation in centimeter was converted to a force in milligram which was the final test value i.e. the bending stiffness.

Saketi and Kallio [2011b] investigated the flexibility of single softwood (bleached pine kraft pulp) and bleached hardwood fibers. Furthermore, they tested pine pulp fibers that were peeled in such a way that only the S2 and S3 layers remained in the fiber wall. Prior to testing, the fibers were soaked in deionized water for about 5 min. Both fiber ends were fixed by using the microrobotic method discussed in section 2.2.2. For bending the fiber the load cell was pressed against the center of the clamped fiber. The deflection was obtained by reading out the position sensor of the XY-table. The force and the fiber length were measured and by using these data, the flexibility and the bending stiffness were calculated. Figure 2.26 shows the principle of this method. They also determined the bending stiffness of fibers after applying

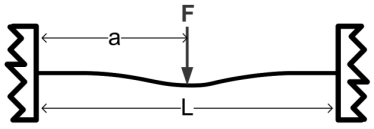

Figure 2.26 Principle of the bending stiffness measurement used by Saketi and Kallio [2011b]

$$E \cdot I = -\frac{F \cdot L^3}{192 \cdot y_{max}} \quad (2.14)$$

F ..... load
L ..... length of beam
y_{max} ..... maximum deflection

axial tension to them. The results of their investigations are shown in table 2.16

	bending stiffness [Nm^2]	flexibility [$N^{-1}m^{-2}$]
softwood ZAT	$1.2 \cdot 10^{-10} \pm 4.2 \cdot 10^{-11}$	$9.37 \cdot 10^{9} \pm 4.2 \cdot 10^{9}$
softwood UAT	$3.0 \cdot 10^{-10} \pm 1.0 \cdot 10^{-10}$	$3.73 \cdot 10^{9} \pm 1.37 \cdot 10^{9}$
hardwood	$7.7 \cdot 10^{-12} \pm 4.4 \cdot 10^{-12}$	$2.05 \cdot 10^{11} \pm 1.70 \cdot 10^{11}$
softwood S2-S3	$2.9 \cdot 10^{-10} \pm 2.4 \cdot 10^{-10}$	$7.63 \cdot 10^{9} \pm 6.93 \cdot 10^{9}$

Table 2.16 Bending stiffness values obtained from Saketi and Kallio [2011b] (ZAT = zero axial tension, UAT = under axial tension)

Navaranjan et al. [2007] examined the longitudinal flexibility F of single fibers by using an Atomic Force Microscope (AFM). A wet fiber (one end glued) was positioned over a gap with the length L. So, the setup used in this study is similar to a beam that is fixed on one end and the other end is freely supported (see figure 2.27a). The load was applied at the center of the fiber via a glass bead which was attached to the cantilever. This is shown in figure 2.27b. The reason why a glass bead was used in this study is that a conventional tip is sharp and therefore penetrates into the fiber. With the data (load P, gap width L and δ deflection) obtained from the tests they calculated the flexibility of the fibers using equation 2.15. The results obtained by Navaranjan

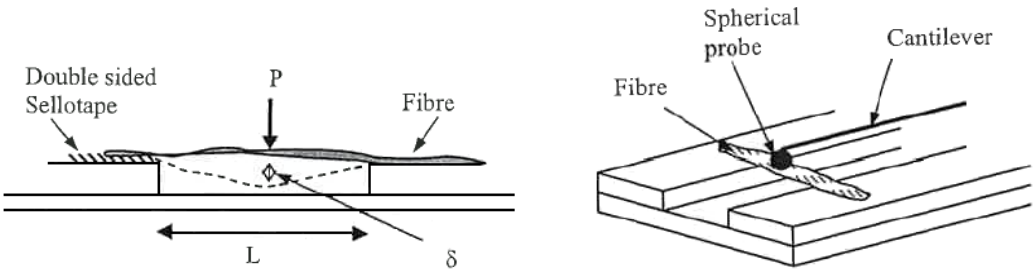

Figure 2.27 Bending stiffness measurement of kraft pulp according to Navaranjan et al. [2007]

et al. [2007] are shown in table 2.17.

	flexibility [$N^{-1}m^{-2}$]	σ [$N^{-1}m^{-2}$]
latewood	$0.73 \cdot 10^{11}$	$0.59 \cdot 10^{11}$
earlywood	$5.49 \cdot 10^{11}$	$3.81 \cdot 10^{11}$

Table 2.17 Results of the flexibility measurements obtained by Navaranjan et al. [2007]

$$\frac{1}{E \cdot I} = F = \frac{768 \cdot \delta}{7 \cdot P \cdot L^3} \quad (2.15)$$

2.5 Summary joint strength and bending stiffness

Joint strength measurement

Direct methods are plausible because they are observing individual fiber to fiber joints during loading. But there are some problems associated with these tests. First the individual joints are very fragile and difficult to handle. This means that they can easily be damaged. Furthermore, the results are difficult to interpret. The direct result - joint strength (breaking force) - is of minor interest because it is so heavily influenced by the morphology of the fibers (e.g. fiber wall thickness, crossing angle) involved and the structure of the tested joint as pointed out by Button [1979] and Uesaka [1984]. Also the type of cooking (sulfite or kraft cooking process, e.g. Schniewind et al. [1964]), the type of fiber (summerwood or springwood fiber, e.g. Stratton and Colson [1990]) as well as the relative humidity (e.g. Mayhood et al. [1962]) influence the strength of individual fiber to fiber joints. The true parameter of interest, specific bond strength - bonding force per unit area of the bond - is hard to obtain from those tests.

By using indirect methods all sheet structure related strength properties like sheet density, fiber interlocking, z-directional entanglement are not taken into account. It is difficult to determine the effects of these parameters on the results. Furthermore the influence of the different modes of loading is not addressed at all. Several measurement methods are needed (e.g. Russell et al. [1964]) and the uncertainty in the measurements is also a significant problem because each error influences the result of the bond strength calculation (e.g. Joshi et al. [2011]). Also the uncertainty of the equations used in these studies is a problem. The big advantage of these methods is that they are much less time consuming and laborious because variability of the results is much lower than for direct methods.

In conclusion there is no method yet to determine the actual specific bonding strength, i.e. the bonding force per unit area, of fiber-fiber joints. The reason is that the structure of the tested joints is not considered in the analysis.

Bending stiffness measurement

The bending stiffness of individual pulp fibers is of great importance for the formation of fiber to fiber joints and this in turn has a direct impact on the strength of the paper network. Fiber properties which significantly influence the bending stiffness are the microfibril angle, the fiber cross sectional properties (shape, wall thickness etc.) as well as weak spots and permanent fiber deformations. Until today, studies carried out in this subject area mainly focused on the determination of the wet fiber flexibility as it plays an important role during the sheet forming process. There is less literature about the determination of the dry bending stiffness available. A method with which it is possible to determine the bending stiffness in a completely dry and wet state

would be preferable (eg. Schniewind et al. [1966]). Using a method which offers this possibility, enables a direct comparison between the dry and wet bending stiffness of individual fibers. From the study of Schniewind et al. [1966] it is apparent that the wet stiffness is almost the same as the dry stiffness (see table 2.15). The reason for this is the increased cross sectional area of the fibers due to swelling.

Chapter 3

A novel micro bond tester for mechanical testing of single fibers and fiber-fiber joints

In order to measure the load for breaking a single fiber joint directly, different devices have been developed. The devices used in previous studies (discussed in chapter 2) only allow uniaxial loading of the joints. They only provide information regarding the deformation over the travel distance in one direction. In the course of this thesis a novel direct method for mechanical testing of single fibers and joints has been developed. With this device not only the strength of single fiber crossings can be measured, but also bonding energy, load geometry, deformation during testing and bending stiffness of single fibers can be determined. The measurement principles of the different methods are shown in figure 3.1 and figure 3.2. Figure 3.1a illustrates the

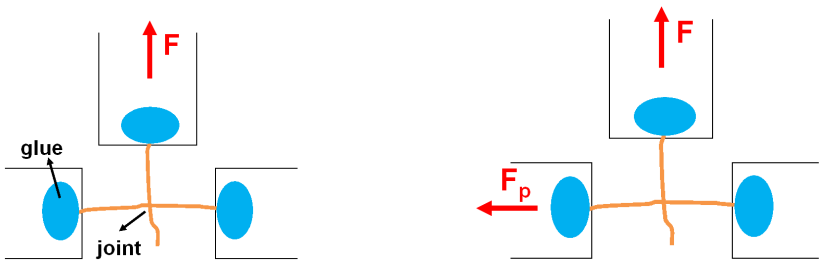

(a) shear strength and bonding energy measurement

(b) shear strength test with preloading of cross fiber

Figure 3.1 Measurement principles

principle of a conventional shear strength test. Here, the longitudinal fiber (one fiber end glued to sample holder) is loaded until the joint breaks. The same principle is used for measuring the bonding energy. In this case, the longitudinal fiber is loaded

up to a certain force below the breaking force and then the force is released back to zero again. Several loading and unloading cycles with increasing load are carried out until the fiber to fiber joint breaks. In order to investigate the influence of biaxial loading on the strength of single fiber crossings, the cross fiber (both fiber ends glued to sample holder) is preloaded before the longitudinal fiber is pulled away from the joint. The principle of this kind of test is shown in figure 3.1b. The principle used

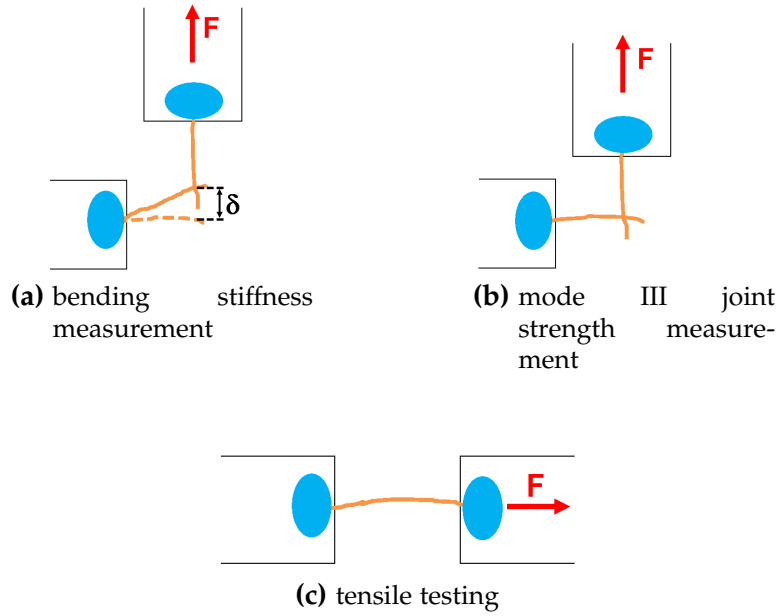

(a) bending stiffness measurement

(b) mode III joint strength measurement

(c) tensile testing

Figure 3.2 Measurement principles

to determine the bending stiffness of a single fiber as well as the mode III strength of a fiber joint is shown in figure 3.2a and b. For these tests only one end of the cross fiber is glued to the sample holder. Again the longitudinal fiber is pulled upwards until the joint breaks. The force needed to break the crossing is referred to as mode III strength. Furthermore, the deflection δ directly before breaking is measured and used to calculate the bending stiffness. The principle of single fiber testing is shown in figure 3.2c. Here, a single fiber is loaded until it breaks.

3.1 Development of a micro bond tester

The concept of the micro bond tester is based on a single fiber tester (Burgert et al. [2003], Kompella and Lambros [2002]). A description of the principle and design of such devices is given in section 2.1. One of the main differences of the novel device compared to other bond testers is that it is possible to preload the cross fiber of the joint. The term cross fiber is related to the fiber with both ends glued on the sample holder. This feature allows the investigation of the behavior of a single joint if both

fibers are loaded and also the influence of preloading on the strength of an individual fiber-fiber joint. This situation resembles more closely the actual loading state of a fiber to fiber joint in a paper network under stress. Figure 3.3 shows a picture of the micro bond tester with its most important components. The linear tables are used for force transmission. One of them is used to preload the cross fiber and the other one is used to break the joint. With the load cells the force needed to break the joint as well as the preloading force is measured. The whole setup is placed under a microscope

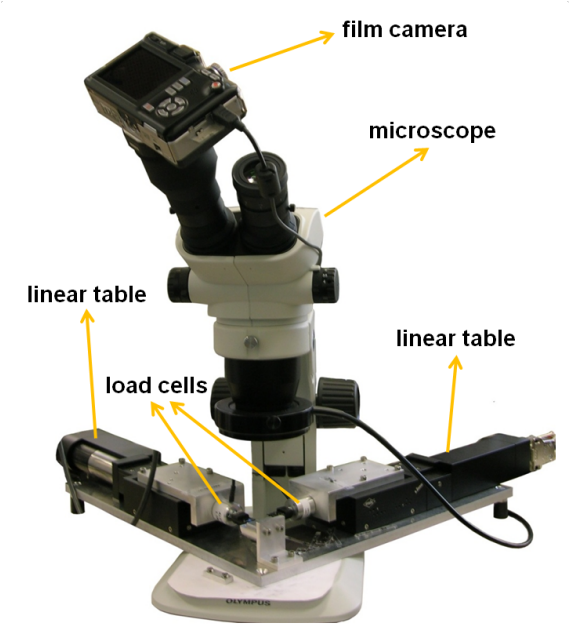

Figure 3.3 General view of the micro bond tester

which is equipped with a film camera. Thus it is possible to record and subsequently analyze the loading situation and the deformation of the fibers during loading.

3.2 Measurement system

3.2.1 Sample holder

One of the most important parts of the tester is the sample holder. This unit serves as carrier for the individual fiber joints (see section 3.5.1). The first version of this part was made of paper. The problem of using paper is that cutting the bridges leads to premature failure of the bond. An explanation for this is that paper is not rigid enough. For that reason the paper was replaced by plastic.

The first design of the sample holder is shown in figure 3.4a. For simple and fast production it was decided to cut out the sample holder using an automated laser. The main problem using this sample holder is that during the fixation of the fiber-fiber joint, glue could also be applied into the slots which are located around the nose of

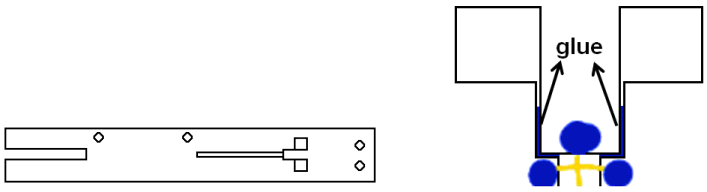

(a) general view **(b)** glue in slots

Figure 3.4 First version of the sample holder

the upper part of the sample holder (see figure 3.4b). This could have a negative effect on the test because after melting of the bridges (see section testing procedure 3.4 step two) the parts are still connected via the glue. For that reason this part was redesigned (see figure 3.5). The modified version of the one piece holder looks similar

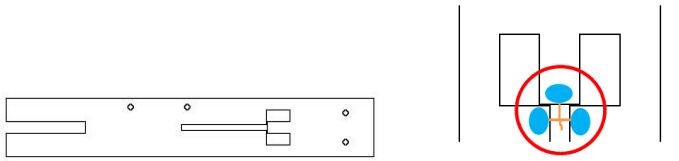

(a) general view **(b)** close up of holder

Figure 3.5 Modified version of the sample holder

to the original version. The difference between the old and new version is that the part for fixing the fiber crossings is partly changed. Due to this modification the chance of applying glue into the remaining slots could be minimized. Additional tests with a two piece sample holder have been made. By using this kind of holder, the bridges keeping together the upper and lower parts do not need to be melted (see figure 3.6). The risk of introducing vibrations during melting is minimized and there fore premature failure of the fiber-fiber joint can be avoided. The problem with the two piece holder is that the longitudinal fiber can only be fixed after the lower part is mounted in the tester. Before testing one has to wait until the glue on the upper part is cured. Another possible layout of a two piece sample holder is shown in

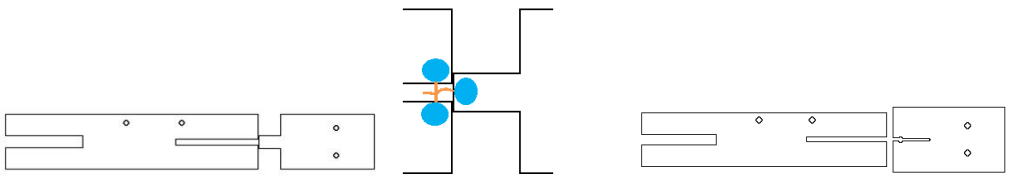

(a) **(b)** micro gripper version

Figure 3.6 Possible designs of a two piece sample holder

figure 3.6b. In this case the upper part of the holder is designed as a so-called micro gripper. After applying glue into the mouth of the micro gripper (see figure 3.7a), the fiber is positioned inside the slot and the clamping force is applied by using a special designed clamping arrangement (see figure 3.7b). First trials with this kind of two

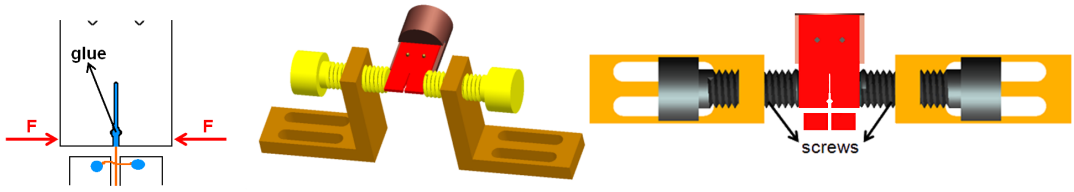

(a) fiber fixation **(b)** clamping arrangement

Figure 3.7 Fiber fixation by using the micro gripper sample holder

piece sample holder showed that it is difficult to apply glue into mouth of the micro gripper. Another problem is that the fiber could not be positioned inside the glue.

Due to the problems which arise when using two piece sample holders (longer waiting time, application of glue etc.), it has been decided to use the modified version of the one piece sample holder which is shown in figure 3.5a.

3.2.2 Mounting of sample holder

The mounting of the sample holder within the bond tester consists of three parts. These parts are:

- two small mounting supports
- dowel pins
- big support

Small mounting supports and dowel pins

The two small supports are used to sustain the sample holder and also serve as link between the linear tables and the sample holder. After assembly of all parts, the small supports are brought into the correct position. This is required to ensure an exact positioning of the holder within the tester. If they are not correctly aligned, the dowel pins and the holes on the sample holder do not fit into each other (see figure 3.8). Thus the fiber joint could be damaged during the fixation of the holder. The dowel pins are used to transmit the force generated by the linear tables to the fiber - fiber joints.

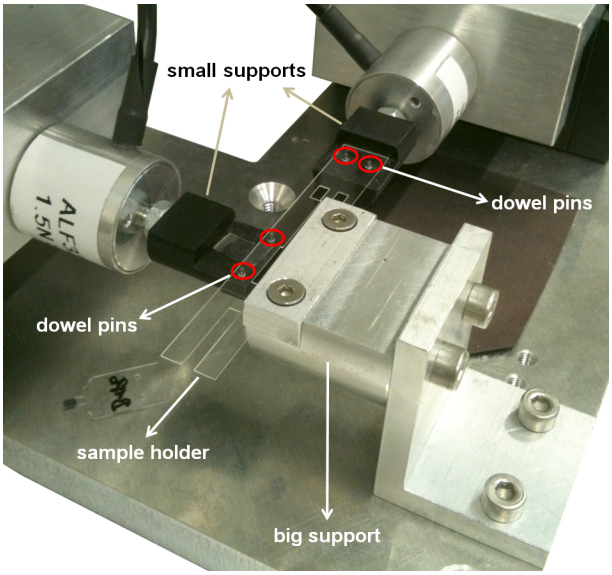

Figure 3.8 Positioning of sample holder

Big support

One part of the sample holder is clamped in the big support (see figure 3.8). This is needed for fixation of the sample holder and in order to allow preloading of the cross fiber.

3.2.3 Load cells

The tester is equipped with two strain gauge based load cells from ALTHEN GmbH Mess- und Sensortechnik (see figure 3.3) with a maximum force of 1.5 N (load cell type ALF329). These load cells have a resolution of 0.5 mN. The load cell signal is amplified by using an SG-IP-24E-420 amplifier from ALTHEN GmbH Mess- und Sensortechnik. In order to ensure a precise and noise free voltage supply of the force sensor as well as the amplifiers a laboratory power supply is used.

The load cells are very sensitive to bending. This has to be considered in the design of the small mounting supports which are directly mounted to the active pin (see figure 3.9). For that reason, these small supports have to be very light to prevent ini-

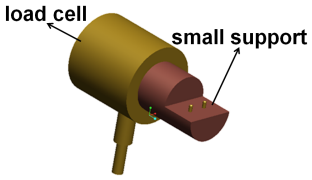

Figure 3.9 Load cell equipped with a small support

tiation of bending forces. Bending leads to false measurements and/or to irreparable damage of the load cells.

Force calibration of the load cells

For the calibration of the force senor, the load cell is mounted on a support and the active pin of the sensor is directed towards the ground (see figure 3.10). After the sen-

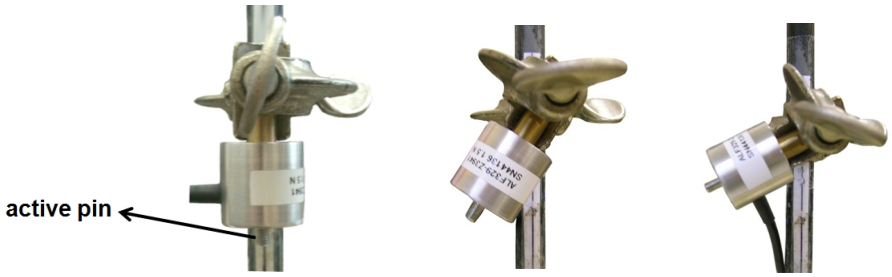

(a) standard procedure **(b)** 30° **(c)** 60°

Figure 3.10 Force calibration of the load cells

sor is mounted, the active pin is loaded with different weights and the corresponding signal is detected. The result of this test is a straight line equation (see figure 3.11). This means that there is a linear relationship between the signal [V] and the load [g]. From the equation a slope is obtained which is used to convert the signal [V] into the corresponding force [mN]. In addition the load cells are calibrated at different angles

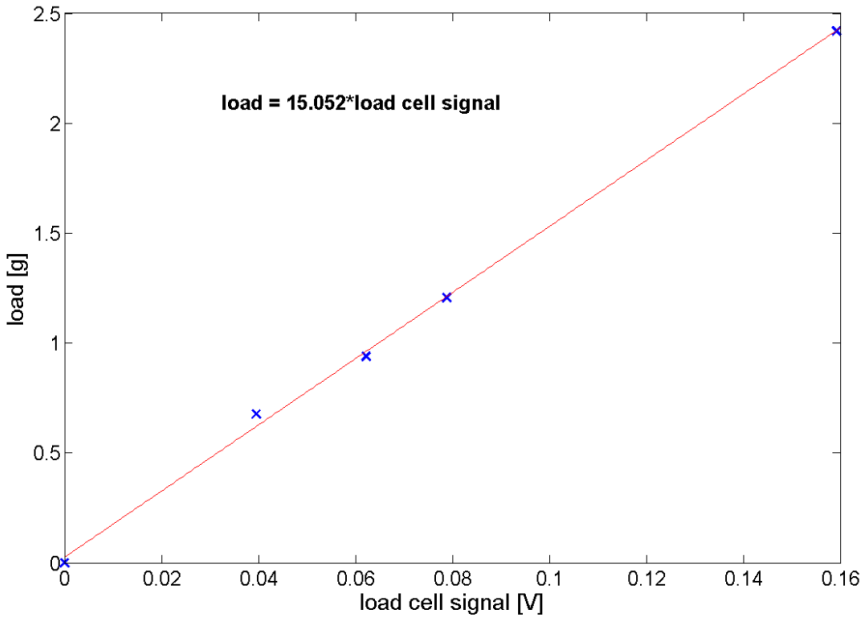

Figure 3.11 Relationship between signal and applied load

(see figure 3.10b and c). These test were performed in order to see whether there is an

influence of bending on the slope. Another reason was that the load cells are rotated by 90° for mounting at the tester (see figure 3.8). The results of these tests showed that there is nearly no influence of bending, as the slope is almost constant (mean deviation of about 3.6%). Therefore it was decided to use this calibration procedure for calibrating the force sensors.

3.2.4 Force transmission

Two high precision linear tables (LIMES 60-20-HiDS) from OWIS GmbH ensure biaxial loading of the fiber-fiber joints (see figure 3.3). One is used to preload the cross fiber and the other to break the fiber crossing. Figure 3.12 illustrates the principle of preloading and breaking of fiber-fiber joints. Both linear tables have a displacement

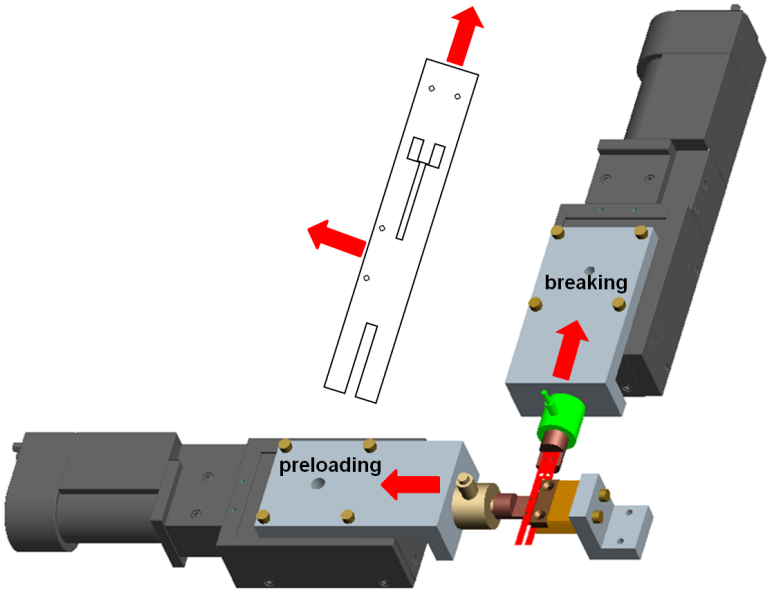

Figure 3.12 Principle of biaxial loading

range of 20 mm and velocity range from 1 to 125 $\mu m/s$.

3.2.5 Device control and data acquisition

The entire device and data acquisition is controlled by a PC. A custom software written in LabVIEW form National Instruments ensures synchronized table movement and force measurement and provides fully automated testing sequences. Several parameters such as the velocity, sampling rate, travel distance in [μm] or a certain load in [g] can be predefined in the software. After definition of all parameters the settings are sent to the linear tables by a control unit. The control unit also serves as power supply for the linear tables. Figure 3.13 shows the principle of the device control and figure 3.14 a close up of the software GUI.

Figure 3.13 Device control

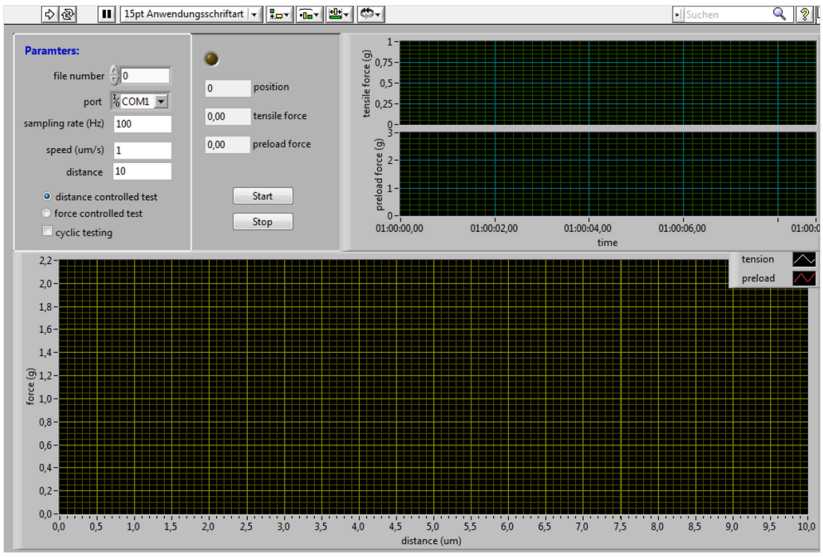

Figure 3.14 User interface of the control software

Data acquisition

Data acquisition is also processed by the software written in LabVIEW. If load is applied to the force sensors a signal is generated. The load cell signal is amplified by using an SG-IP-24E-420 amplifier from ALTHEN GmbH Mess- und Sensortechnik. After amplification the analog signal is converted to a digital signal by a DAQ-card (NI PCI-6221) from National Instruments Ges.m.b.H (Austria). The software then stores the signal in a txt-file. Figure 3.15 shows the principle of the data acquisition. In the final step of data acquisition the txt-file is analyzed with MatLab.

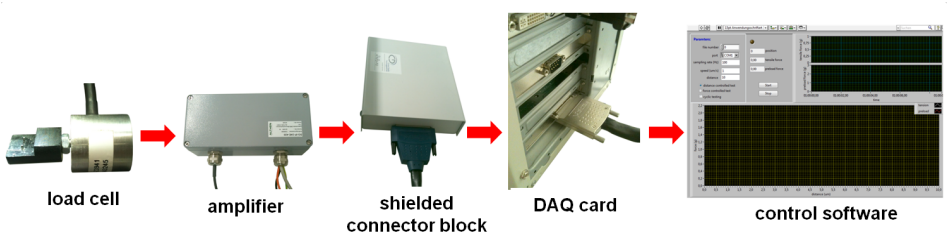

Figure 3.15 Data acquisition

3.3 Evaluation of the measurement system

Due to the fact that the load cells used in this study are operated at the lower limit of their measuring range and in order to ensure constant test conditions an evaluation of the measurement system was carried out. Initial trials using the micro bond tester have shown that there are three important aspects that need to be considered. These are:

- noise in load cell signal
- long-term and short-term drift
- influence of light source (microscope)

In the following these points will be discussed in more detail.

Noise in load cell signal
In order to reduce the noise problem two modifications of the system were made. The first one was to use shielded cables instead of unshielded ones and the second one was to use a filter. A low pass filter with a cutoff frequency of 10 Hz was directly integrated in the control software (LabVIEW program). Figure 3.16 shows the difference between a filtered and an unfiltered load cell signal. It is apparent that there are

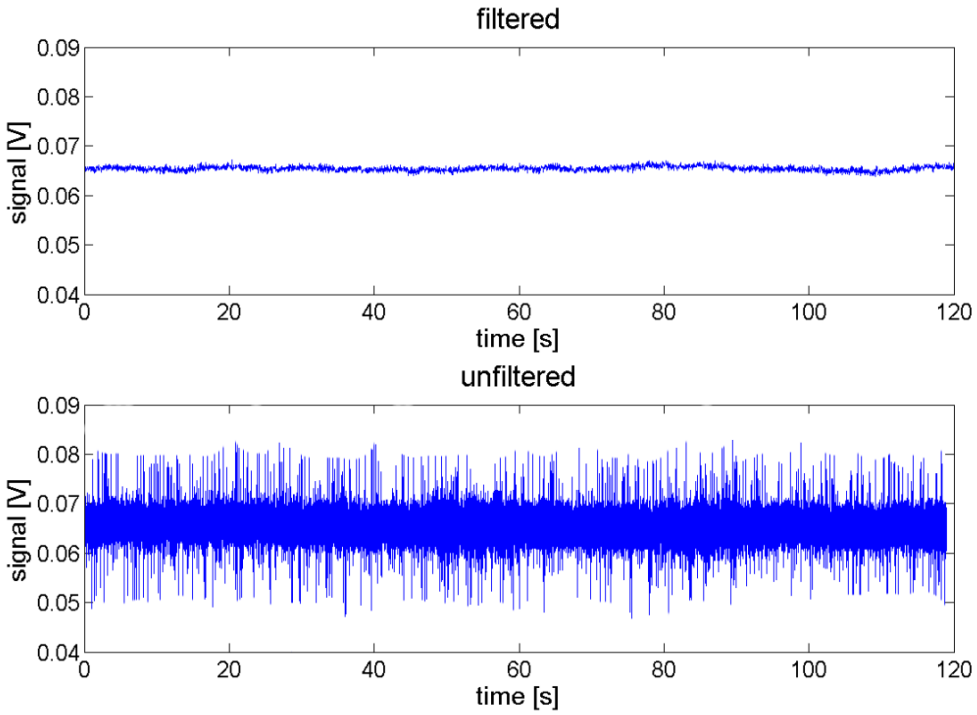

Figure 3.16 Filtered vs. unfiltered load cell signal

two big problems if the signal is not filtered. First, a wrong joint strength value is

obtained when the signal is not filtered because all potential sources of noise would be included in the signal (see figure 3.16 unfiltered). If the signal is not filtered the highest peak of the signal instead of the true breaking load is determined. Second, a representative visualization of the force-distance curve is impossible as the shape of the force-distance curve is difficult to reconstruct. Due to this fact it is almost impossible to detect the breaking load of a fiber to fiber joint as well as of individual fibers without filtering.

Figure 3.16 also shows that there is still some noise if the signal is filtered. Therefore the influence of the noise by calculating the so-called signal-to-noise ratio (SNR) was evaluated. The SNR can be described as the mean value of the measured signal divided by its standard deviation which is the noise of the signal (Smith [2003]).

$$SNR = \frac{\mu}{\sigma} = \frac{\text{mean load cell signal}}{\text{standard deviation load cell signal}} \tag{3.1}$$

In order to determine the noise in the signal, the data of a test with a measurement duration of 1 hour (data short-term drift, see figure 3.18) were divided into 30 intervals of 2 minutes. The reason for this classification is that one strength measurement takes about 2 minutes. For each interval the standard deviation σ (noise) was calculated and these values in turn were used to determine the mean value of σ for all intervals. The mean converted signal (μ) measured for the shear strength tests without preloading is about 0.6707 g, 0.2777 g with preloading, and 0.1078 g for the bending stiffness tests (see section 5). These mean strength signals as well as the obtained standard deviation of 0.00797 g were used to calculate the SNR values (see table 3.1) by using equation 3.1. From the SNR values it is apparent that the proportion of the noise is

	mode II F_{preload} = 0 mN	mode II F_{preload} = 20 mN	mode III
SNR	84.20	34.86	13.53

Table 3.1 SNR values of the different types of measurement

one to two orders of magnitude smaller than the measured signal. The proportion of the noise of the detected strength signal was also calculated. For mode II testing without preloading it is about 1.19%, with preloading 2.87% and for mode III testing (bending stiffness tests) it is about 7.39%. These relatively low proportions indicate that a possible influence of the noise can be neglected.

Long-term and short-term drift

During the determination of the breaking load of individual fiber to fiber joints a drift of the zero signal (signal without loading the sensor) of the load cell was observed. In order to study this effect, long-term measurements without loading the force sensor over 5, 7 and 23 hours with a cutoff frequency of 20 Hz were performed. The first two tests showed that there is still a decrease in the load cell signal. The measurement

performed for 23 hours showed that the long-term drift is stopped after about 10 hours. Based on these findings it has been decided to heat up the system for at least this time. In order to provide the same test conditions (same zero signal) for all measurements, the system is switched on at least 10 hours before testing. The result of the measurement performed for 23 hours is shown in figure 3.17.

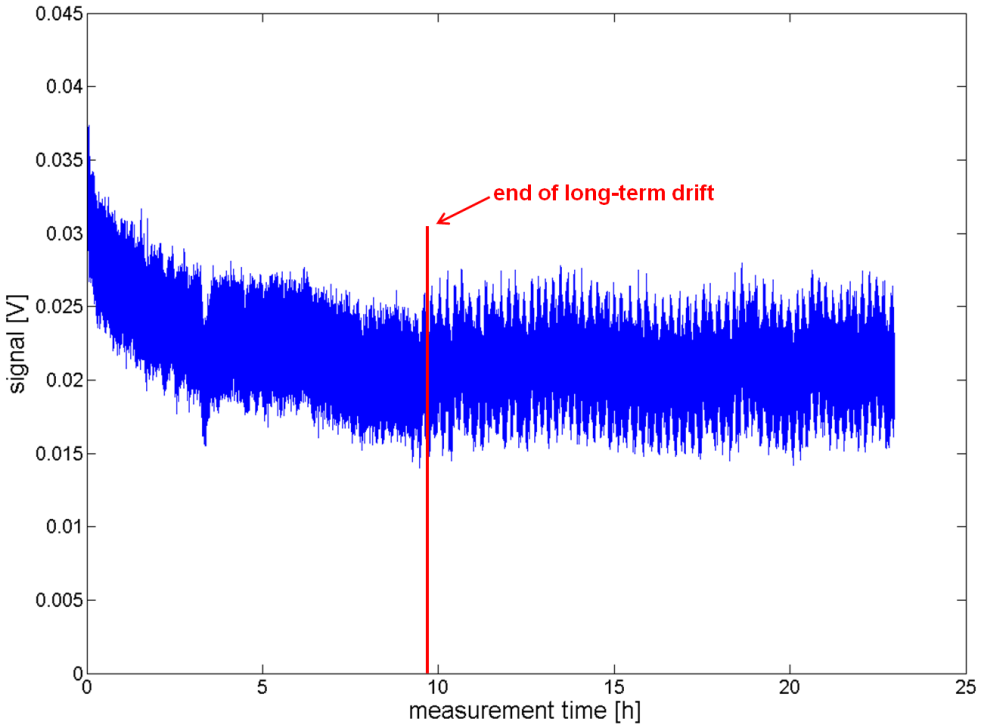

Figure 3.17 Long-term drift of the load cell signal (cutoff frequency 20 Hz)

Furthermore, this figure shows that there is also a short-term drift of the signal. In order to find out how strong this drift is, a test for a measurement time of one hour was performed (without load application). For this test we assume that the drift in the unloaded state is equal to the drift in the loaded state. Figure 3.18 shows the result of the short-term test. The evaluation of the data obtained in this investigation showed that the short-term drift is about $\pm$ 0.1623 mN per hour. Compared to the mean breaking loads (6.58 mN for conventional mode II testing, 2.72 mN for mode II testing with preloading the cross fiber and 1.057 mN for mode III testing) the drift is rather low. The value obtained in this test is about 2.5% of the one measured in a shear strength test without preloading the cross fiber, 5.97% of the one with preloading the cross fiber, and in case of mode III testing it is about 15.4%. Even if the proportion of the short-term drift is relatively high for mode III testing, its influence can be neglected in all of the above mentioned tests as well as for the determination of the bonding energy. Since the actual measurement duration for each test is much lower than one hour. A bond strength test (with and without preloading the cross

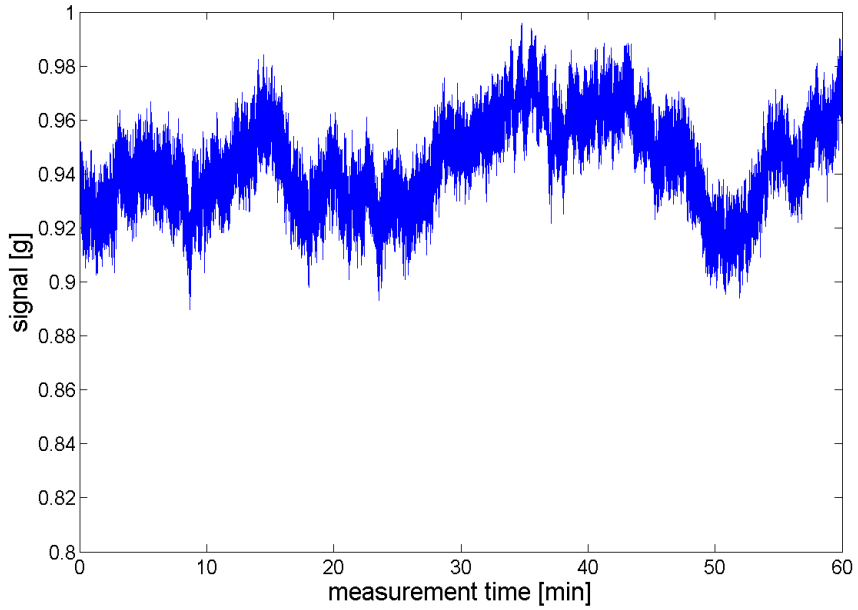

Figure 3.18 Short-term drift of the load cell signal (cutoff frequency 10 Hz)

fiber) takes about 2 minutes, the determination of the bonding energy 2.5 minutes, and a bending stiffness test 1 minute.

Summing up it can be said that a negative impact of the long-term drift can be avoided if the system is switched on about 10 hours before testing. A possible influence of the short-term drift can be neglected due to the fact that the measurement time for all tests is much lower than one hour.

Influence of light source

Further, there seems to be an influence of the illumination of the microscope. When the light is switched on, the signal of the load cell is increased and after some time (30 to 45 min) it decreases again but it is still slightly higher than without illumination. In order to ensure constant measurement conditions it has been decided to switch on the light about 1 hour before starting the measurements.

3.4 Sample preparation and joint fixation

All tests in this thesis were performed using a once-dried, unrefined, unbleached softwood kraft pulp, a mixture of spruce and pine. The fibers have a mean width of 32 μm (determined with 3D serial sectioning technique, see Lorbach et al. [2012]) and a mean length (length weighted average) of 2.13 mm (determined with Kajaani fiber lab). To prepare the individual fiber to fiber joints a suspension with a consistency of about 0.01% is produced (Kappel et al. [2009]). Small droplets of this suspension

are put on a teflon foil (see figure 3.19a). In the second step this teflon foil is covered

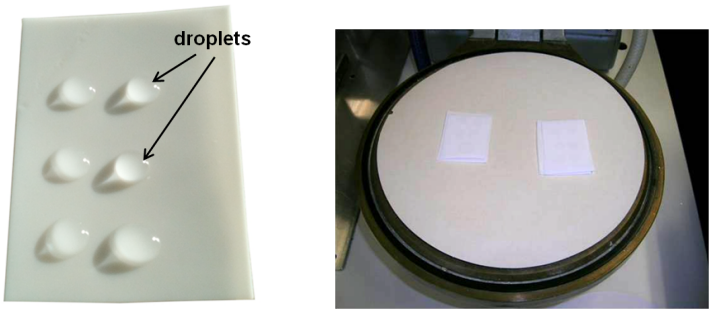

(a) suspension droplets on teflon foil

(b) teflon-paper sheet sandwich in sheet dryer

Figure 3.19 Preparation of single fibers and fiber to fiber joints

with a second one and afterwards the foils are placed between two paper sheets. In the third step the paper sheet-teflon foil sandwich is dried in a conventional Rapid-Köthen sheet dryer (see figure 3.19b) for about 45 min until the fibers have dried. After drying, the individual fibers and joints on the teflon foils (see figure 3.20), are

Figure 3.20 Fiber to fiber joint on teflon foil

selected by using a pair of tweezers and glued to the sample holder.

3.4.1 Joint fixation

As already discussed in section 2.1.1, three different types for fiber fixation can be used. For single fiber-fiber joint testing clamping as well as gluing of the fiber crossings are the standard methods. The ball and socket system is not a suitable method, since the balls would lead to breaking of the joint. Gripping of the fibers is also not taken into account because no one in the CD-laboratory has experience with this method. Furthermore, microgrippers are expensive and difficult to mount to a load cell. Another problem with microgrippers is the slipping of the fibers. Therefore,

the decision was taken to glue the individual fiber to fiber crossings onto a sample holder. Tests with different types of glues have been made. Nail polish was used for fiber fixation in the evaluation of the joint strength, the bending stiffness of single fibers as well as the bonding energy of a fiber crossing. The reason will be discussed in more detail in section 4. For determining the tensile strength of single fibers a two-component glue (UHU PLUS Sofortfest) is used, since the nail polish is too weak for single fiber testing. The fiber is pulled out of the nail polish already at a force much lower than the breaking load of the fiber.

3.5 Testing methods

The developed micro bond tester introduces two additional aspects to the conventional measurement of force and displacement. First the geometry and the deformation of the joint during testing is filmed and analyzed. Second biaxial loading of the fiber-fiber joint is possible, i.e. both fibers forming the joint can be loaded. The additional information about loading geometry, fiber deformation and behavior under biaxial load will help to clarify the specific loading situation of the tested joints and thus provide a step towards obtaining information about specific bonding strength.

With this method not only the strength of individual fiber joints can be measured. Also bonding energy, load geometry, deformation during testing and bending stiffness of single fibers can be determined. Furthermore it is possible to evaluate the effect of mode II and mode III shear load on fiber joints.

3.5.1 Mode II joint strength measurement

With the bond tester it is possible to examine the influence of biaxial load on joint strength. This means that the joint strength measurements can either be performed with or without preloading of the cross fiber. Figure 3.21 shows a fiber to fiber joint before (left) and after preloading (right) the cross fiber.

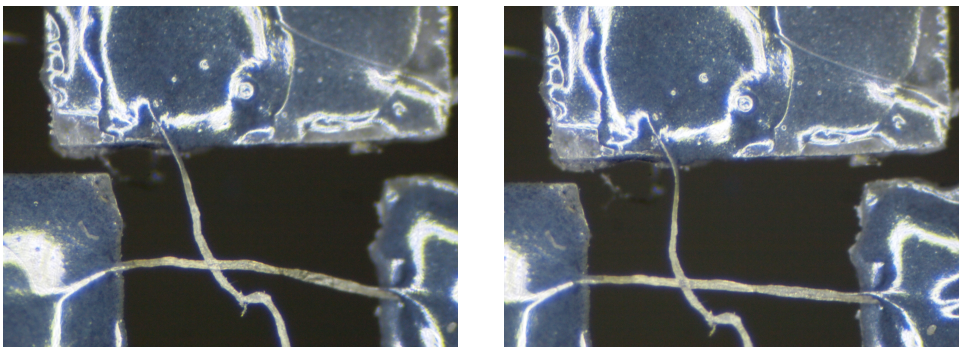

Figure 3.21 Fiber-fiber joint with preloaded cross fiber (right) and without preloaded cross fiber (left)

Testing procedure

Testing is done using a purpose-built sample holder. The testing procedure consists of three or four steps depending on whether the cross fiber is preloaded or not. The procedure is illustrated in figure 3.22.

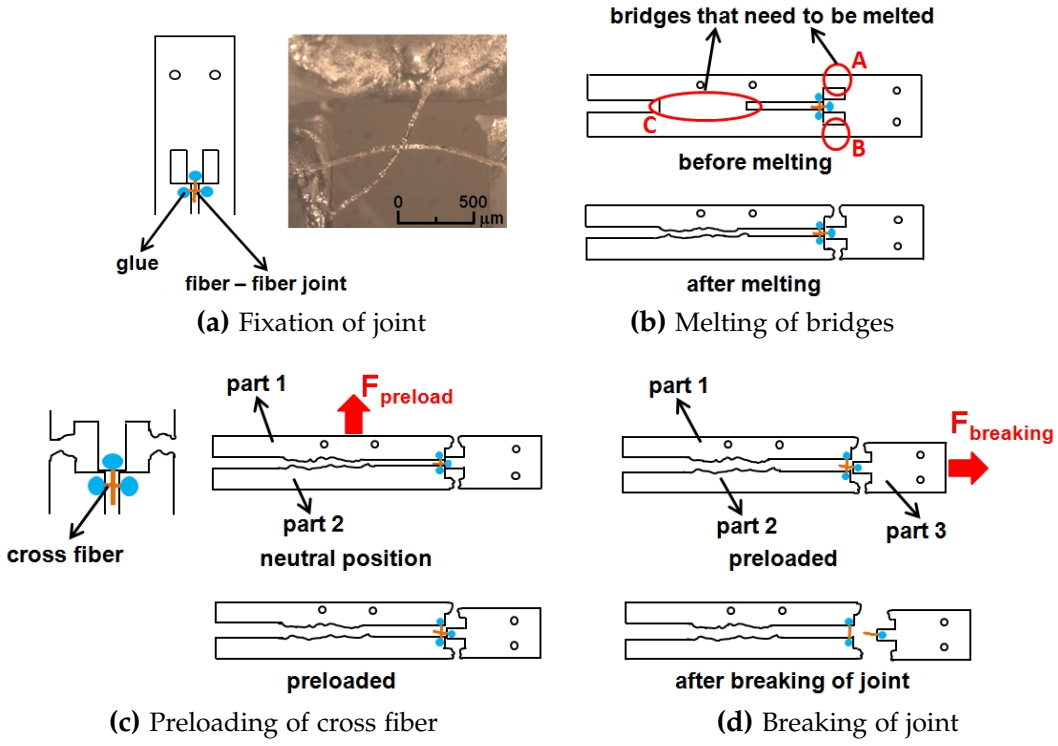

(a) Fixation of joint **(b)** Melting of bridges

(c) Preloading of cross fiber **(d)** Breaking of joint

Figure 3.22 Main steps of the testing procedure

Step one of the testing procedure

In the first step the individual fiber-fiber joints are glued to the sample holder using nail polish "essence colour & go" from cosnova GmbH (reason given in section 4). This step is shown in figure 3.22a. When the nail polish has hardened, the sample holder is mounted at the tester.

Step two of the testing procedure

In the second step the bridges holding together the upper and lower parts of the sample holder are melted by a soldering rod. Melting of the bridges is shown in figure 3.22b. In order to measure the strength of individual fiber crossings without preloading, which is a conventional shear bond strength test, only the upper bridges A and B need to be melted. After melting, the individual parts of the sample holder are only connected via the fiber - fiber joint.

Step three of the testing procedure (only for preloaded joints)

In the third step, the cross fiber is preloaded (figure 3.22c). The preload is achieved by pulling away part one of the sample holder from part two. The cross fiber is loaded with one of the linear tables until a defined preloading force of 20 mN is reached. Preloading of the cross fiber is carried out gradually. The load is increased stepwise until a static load of 20 mN remains stable for 60 seconds. This is necessary in order to compensate a drop in preloading force due to creep and plastic deformation in the fibers and ensures a fairly constant preload during joint strength measurement. Step three is only needed if the influence of biaxial load on joint strength is investigated.

Step four of the testing procedure

In step four, the joint is broken (figure 3.22d) by pulling away part three of the sample holder from part one and two.

3.5.2 Bonding energy measurement

Nordman et al. [1952] subjected a strip of paper to several loading and unloading cycles. The area between the ascending and descending curves of one cycle represents the irreversible work absorbed during this cycle. In this thesis a method for determining the energy needed to break a single fiber joint was developed.

Testing procedure bonding energy

Cyclic tests are made in order to determine the bonding energy of the fiber-fiber joint. The longitudinal fiber is loaded up to a certain force and released back to zero again (one cycle). Several loading and unloading cycles with increasing force are carried out until the fiber crossing breaks (see figure 3.23). For each individual cycle

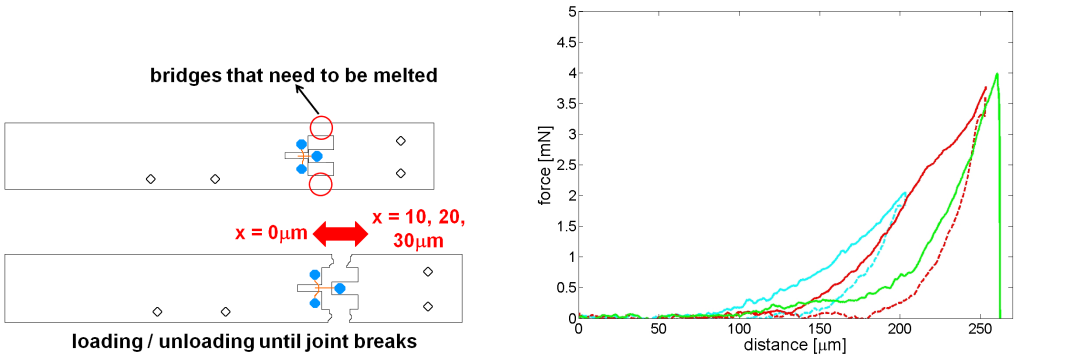

(a) principle of testing procedure

(b) hysteresis curves of loading / unloading cycles

Figure 3.23 Determination of bonding energy

the amount of the elastic energy can be determined. Elastic energy is the integral under the force-distance curve during unloading. It is the energy stored elastically in the fibers which is returned during the unloading part of the cycle. The dissipated energy, which is the total energy absorbed in one cycle, is the difference between the force distance integrals of the loading and unloading curves. This energy consists of bonding energy, the energy needed to break a single joint, and plastic energy, which is the energy consumed due to plastic deformations in the fibers. Viscous effects such as creep and stress relaxation are included in the plastic energy. Summing up the different energy fractions from each individual cycle gives the final value.

$$
\begin{aligned}
E_{total\ cycle_1} &= \int_0^{s_{max\ cycle_1}} F_{loading\ cycle_1} \cdot ds \\
E_{elastic\ cycle_1} &= \int_{s_{max\ cycle_1}}^{0} F_{unloading\ cycle_1} \cdot ds \\
E_{dissipated\ cycle_1} &= E_{total\ cycle_1} - E_{elastic\ cycle_1} = E_{bond\ cycle_1} + E_{plastic\ cycle_1} \\
E_{dissipated\ total} &= \sum_{k=1}^{N} E_{dissipated\ cycle_N}
\end{aligned}
\tag{3.2}
$$

For bonding energy measurements the sample holder was slightly modified to ensure that it is as stiff as possible, reducing its deformation during testing and thus its energy uptake. Figure 3.24 shows the modified version of the sample holder. Due

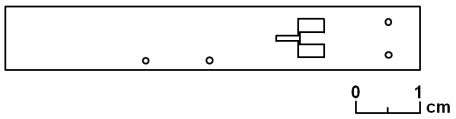

Figure 3.24 Sample holder used for bonding energy measurements

to the small slot there is no deformation of the sample holder during testing and only the energy of the fiber crossing is detected.

3.5.3 Determination of fiber bending stiffness

Another fiber property which is of great importance for the strength of the paper network is the bending stiffness of single fibers. With this bond tester it is also possible to determine the dry bending stiffness of individual fibers.

Testing procedure bending stiffness

For these investigations the longitudinal fiber is glued to the sample holder as usual, but in this case only one end of the cross fiber is fixed, the other one is free (see

figure 3.25a). The cross fiber is deflected (see figure 3.25b) by pulling the longitudinal fiber away. We see the cross fiber as an elastic cantilever beam (see figure 3.26) fixed

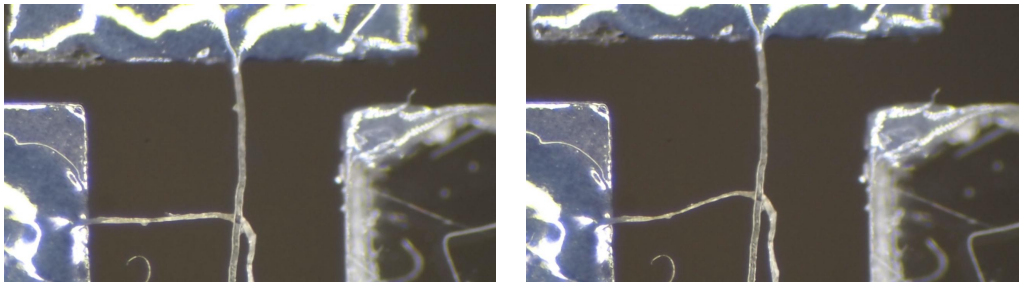

(a) fiber-fiber joint at starting position

(b) fiber-fiber joint with maximum bending of the horizontal fiber

Figure 3.25 Measurement of fiber bending stiffness

on one side. An important remark is that the longitudinal fiber has to be straight. If the fiber is twisted, all possible side effects (e.g. the straightening force) are also measured and these in turn influence the results of the measurement.

From the camera images the deflection as well as the length of the fiber can be measured and by using the equation for the deflection curve of a cantilever beam from standard mechanics textbooks, it is possible to determine the bending stiffness E·I $[Nm^2]$ of a single fiber (see equation 3.3). Here l is the free fiber length, w the

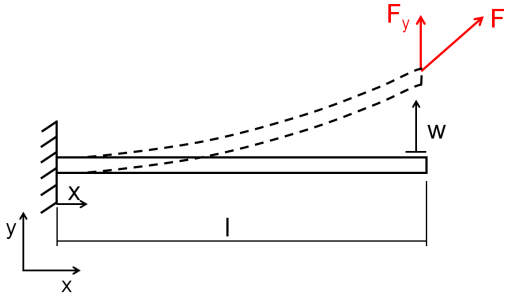

$$E \cdot I = \frac{F_y \cdot l^3}{6 \cdot w} \cdot (3 \cdot \frac{x^2}{l^2} - \frac{x^3}{l^3}) \qquad (3.3)$$

Figure 3.26 Principle of a cantilever beam

deflection at the measurement point on the fiber, Fy [N] is the force component in y-direction, E $[N/m^2]$ is the modulus of elasticity and I $[m^4]$ is the moment of inertia of the fiber cross section. The bending stiffness can be calculated at different positions x_1, x_2, x_i along the fiber (x is the x-coordinate of the measurement point). At the end of the beam where x is equal to l ($w = w_{max}$) the bending stiffness is calculated according to equation 3.4.

$$E \cdot I = \frac{F_y \cdot l^3}{6 \cdot w} \qquad (3.4)$$

The method used in this thesis is based on the same principle as used by Schniewind et al. [1966].

3.5.4 Mode III joint strength

During determination of the bending stiffness it became apparent that the joint configuration used in these test is close to a pure shear test with mode III loading, compare figure 3.27. When the longitudinal fiber is pulled upwards a counter force is created. The interplay between the loading force and the counter force leads to torsional loading of the joint with a moment acting on the joint. This situation is close to mode III loading of the fiber to fiber joint (see section 2.2.1).

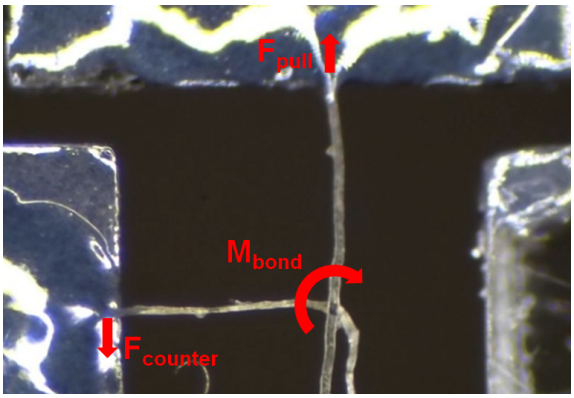

Figure 3.27 Principle of mode III loading of a fiber-fiber joint

Testing procedure - mode III strength

The testing procedure for these kind of tests is similar to the one used for the determination of the bending stiffness of a single fiber.

3.5.5 Tensile strength of single fibers

Besides the strength of fiber to fiber joints, the strength of single fibers is the second factor that influences paper strength. With the device presented in this thesis it is also possible to determine the tensile strength of single fibers. Again a new sample holder which fits the requirements of this kind of test was designed (see figure 3.28). Two version of the holder are produced. One with a span of 1 mm and another one

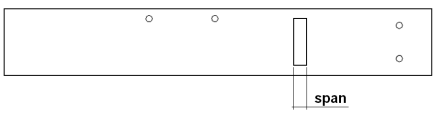

Figure 3.28 Sample holder used for single fiber tensile tests

with a span of 2 mm. Using different test spans offer the possibility to get a rough indication regarding the negative influence of natural as well as induced fiber defects on the breaking load of single fibers. The larger the free fiber length, the higher is the probability of fiber defects in this area and the higher the probability of a premature failure.

Testing procedure - tensile testing

After the single fibers are fixed to the sample holder with the two-component glue (see section 3.4.1), the bridges A and B are melted using a soldering rod. In the next step, the fiber is loaded (loading rate 2 $\mu m/s$) with the linear table until it breaks. This is done by pulling away part 2 from part 1 (see figure 3.29). Again the whole

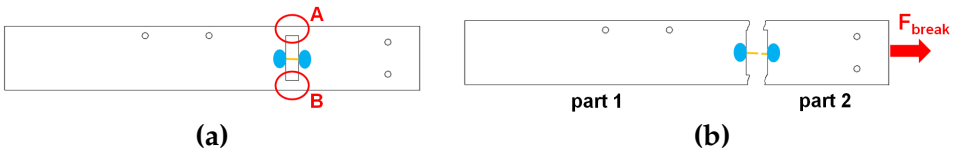

Figure 3.29 Step of the testing procedure used to determine the tensile strength of single fibers

testing procedure is filmed and subsequently analyzed. From the images the exact initial length l_0 and the length at failure l_1 are determined (see figure 3.30) and by using equation 3.5 it is possible to calculate the fiber elongation.

$$\varepsilon = \frac{\Delta l}{l_0} = \frac{l_1 - l_0}{l_0} \tag{3.5}$$

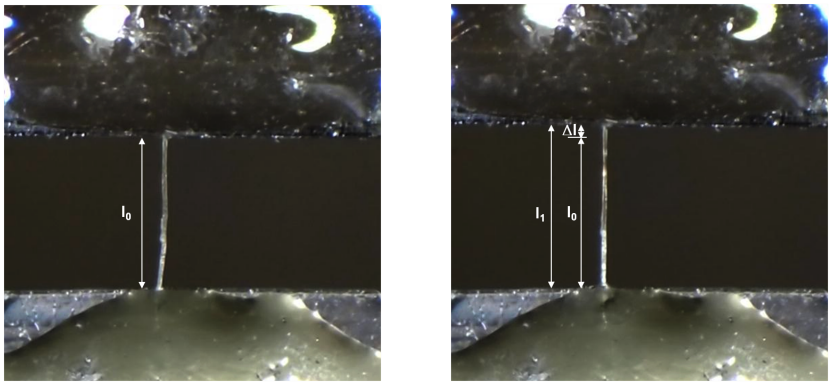

(a) fiber before tensile testing **(b)** fiber after tensile test

Figure 3.30 Tensile testing of a single fiber

An important remark is that the data (F_{break}, E, ε, σ) of fibers that break at one edge

should be excluded. The reason for this is that there are stress concentrations in the edges of the fibers due to curing of the glue as well as misalignment of the fibers (angle between fiber and sample holder not exactly 90°). These stress concentrations lead to a reduction of the breaking load, the stress acting on the cross sectional area as well as the elongation and this in turn leads to wrong E-modulus values. Therefore, only the data of fibers that break in the free span should be included.

Chapter 4

Analysis of the bonding region

The size of the area between two bonded cellulose fibers is of essential importance for the strength of paper. The contact zone in turn is influenced by the morphology of the fibers. In order to get a better understanding of the mechanisms taking place during mechanical testing as well as to learn more about the impact of structural properties on the strength of single fiber crossings, investigations of the contact zone before and after breaking of single joints are needed.

Several researchers have examined the bonded or formerly bonded area (FBA) using different techniques. One method for investigating the FBA of a single fiber crossing is scanning electron microscopy (Stratton and Colson [1990]). After the joint was broken with the Fiber Load Elongation Recorder, the fibers were coated with gold palladium and placed in the SEM. The result obtained by Stratton and Colson [1990] showed that the FBA as well as the area of the failure was clearly visible. In another study (Kang et al. [2004]) an atomic force microscope (AFM), a confocal laser scanning microscope (CLSM) and a scanning electron microscope (SEM) was used to examine single fiber - fiber joints loaded to failure by means of an Alwetron TH1 tensile tester from L & W. For investigating the FBA in the SEM the fibers were coated with platinum. The findings of this study showed that beating increased the number of fibrils and also led to a smoother fiber surface (roughness of unbonded fiber regions is stronger influenced than roughness of the formerly bonded area). Jayme and Hunger [2003] investigated paper and pulp in a SEM by using a so-called *direct replica method*. The sample was coated with metal and the resulting film was shadowed with carbon. Afterwards, the film consisting of metal and carbon was supported using polystyrene and in order to create the replica the cellulose was destroyed. The SEM images clearly showed the difference between the primary wall and the secondary walls S1, S2 and S3. Jayme and Hunger [2003] also found out that drying leads to special roughnesses on the surface of the fiber and these may impede the bonding

process. Furthermore, they said that microfibrils are the reason for bonding in the contact zone.

Another topic of interest is the investigation of the surface of different types of fibers by means of scanning electron microscopy (Li et al. [2010], Zhao et al. [2007], Molin and Daniel [2004], Okamoto and Meshitsuka [2012]). In each of these studies the fibers were coated for example with carbon, Au/Pt, gold or Pt/Pd.

In this thesis the formerly bonded area as well as the surface of cellulose fibres was investigated by using a high resolution scanning electron microscope. These tests allow an insight into the morphology of the contact zone after mechanical testing and those of the fiber surface. Furthermore, the impact of the different types of loading (conventional shear strength test or cyclic testing) as well as the mode of loading (mode I, mode II or mode III) on the fracture behavior of single fiber crossings can be analyzed. Also information of possible mechanical interlocking and perhaps even regarding the area in molecular contact is obtained. The results of the SEM investigations will also contribute to learn more about the type of material failure in the bonding region.

The main difference compared to previous studies is that the fibres were not coated. Also joints which were embedded in resin (for microtome cutting) were analyzed by means of an in-situ ultramicrotome which is located in an ESEM. This was carried out in order to see whether the resin penetrates into the bonding region, see section 4.2.

4.1 Low-voltage SEM investigations

Traditional scanning electron microscopy is operated at electron energy values ranging from 5 to 30 (50) keV (Reimer [1993]) whereas low-voltage SEM investigations are carried below 5 keV (0.5 to 3 keV, Liu [2000]). One of the big advantages of this mode is that polymers, biological as well as insulating samples can be investigated without coating them with metal (Reimer [1993]). At low energy values the electron beam interacts much stronger with the material than at higher values. The penetration depth of the electrons into the sample decreases with decreasing incident energy. SEM's operated in an energy range from 10 to 30 keV give information about the bulk of the sample whereas LVSEM is limited to the surface and on this account it is much more sensitive to the topography (illustrated in figure 4.1). Problems caused by charging of the specimen as well as beam damage (faster than at high energies but limited in physical extend) can be minimized by careful adjustment of the scanning electron microscope in low voltage mode without affecting the quality of the images (Joy [1996]).

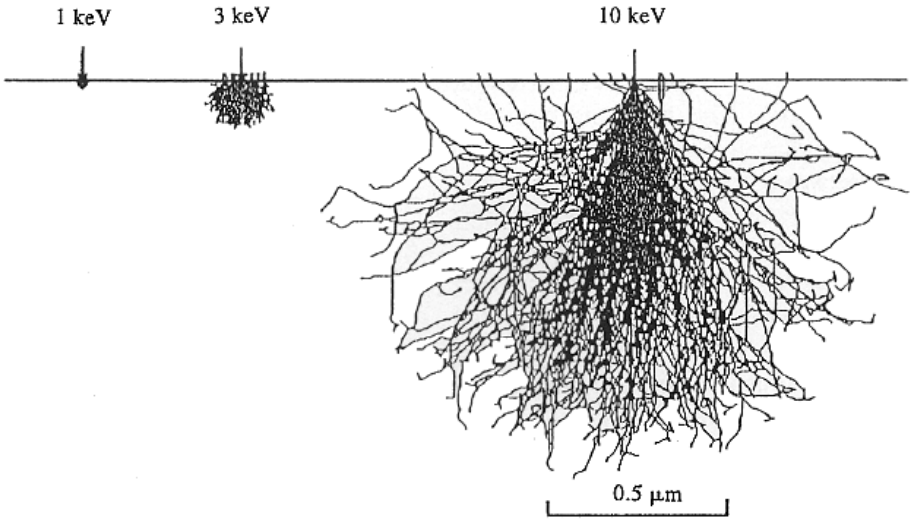

Figure 4.1 Monte Carlo simulation of the beam interaction at different beam energies (Joy [1996])

4.2 High resolution imaging of fibers and the FBA

After the fiber to fiber joints have been tested with the Micro Bond Tester, some selected individual fibers are investigated by using the Zeiss Ultra 55 from the Institute of Electron Microscopy and Fine Structure Research in Graz. The big advantage of this scanning electron microscope is that it offers high resolution even at low electron energy values. The tests in this study are carried out at an energy value of 0.65 keV. When using this low-voltage mode the fibers do not need to be coated and the surface of single fibers, fiber crossings as well as the formerly bonded area can be analyzed directly without any pretreatment. Another advantage of this method is the strong interaction of the beam with the surface of the sample and so the resolution of small structures at the surface is much better with LVSEM. At higher electron energy values information about the surface is lost.

Fiber and joint fixation: Glue versus nail polish

For mechanical testing, the single fibers and fiber to fiber joints are fixed with glue to a sample holder. The adhesive used in this study formed a layer on the surface of the sample holder which is an indication for a reaction between the glue and the holder. In order to find out if there is a reaction between the glue and the fibers, the surface of the fibers as well as the formerly bonded area of fiber crossings were examined in the SEM. Cyanoacrylate glue (7 samples), a two-component glue (1 samples) as well as nail polish (7 samples) were investigated.

In the first instance the fibers and joints were fixed onto the sample holder by

using Loctite 454 (cyanoacrylate glue). Figure 4.2a shows a SEM image of a fiber which was fixed with this glue. The image shows that there is some kind of film on

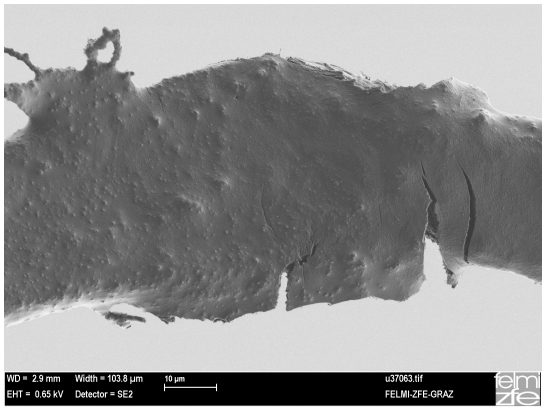

(a) fiber fixed with Loctite 454

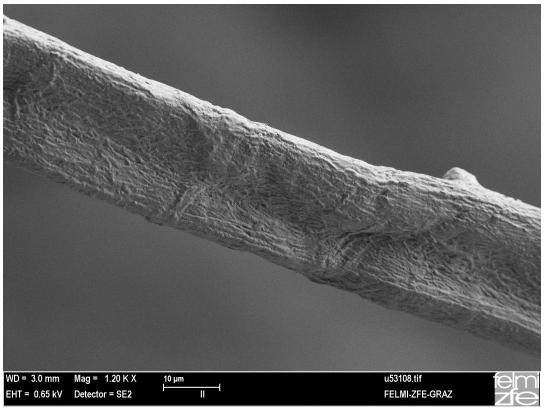

(b) fiber fixed with ergo 5012

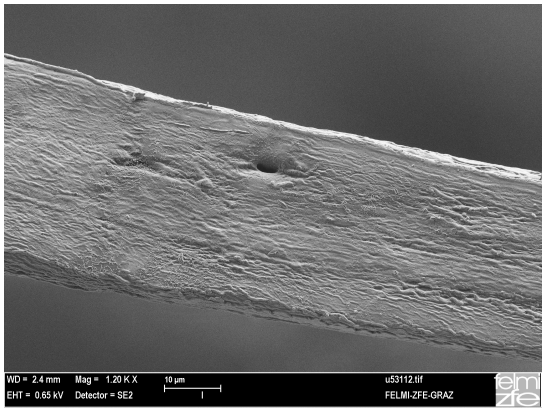

(c) fiber fixed with ergo 5039

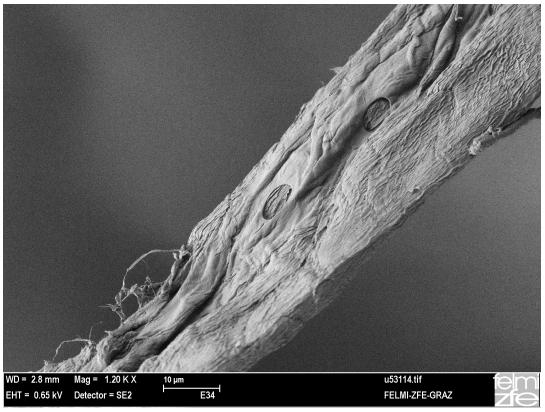

(d) fiber fixed with UHU PLUS Sofortfest

Figure 4.2 SEM images of fibers that were fixed with different glues

the fiber surface. It seems as if there is also a reaction between the fiber surface and the gaseous phase of the glue. In order to ensure that the formation of this adhesive layer is not only the result of LOCTITE 454, two other cyanoacrylate glues as well as a two-component glue (UHU PLUS Sofortfest) were tested by means of the scanning electron microscope. Figure 4.2b shows a fiber fixed with ergo 5012, figure 4.2c a fiber fixed with ergo 5039 and figure 4.2d a fiber that was fixed with UHU PLUS. From these images it is apparent that also in figure 4.2b, c and d a film is formed but this time the layer on the fiber surface is not as thick as with LOCTITE 454. Figure 4.4 shows fibers that were fixed with nail polish (NP). From the images it is apparent that in case of nail polish no film can be seen on the surface of the fibers as well as on the sample holder surface. On this account it has been decided to fix the individual fiber to fiber joints with NP. The film observed in the LVSEM images (see figure 4.2) could have a negative effect on the joint strength and this could lead

to wrong measurement results. Another explanation why nail polish is used is that Schmied [2011] also investigated the formerly bonded area of joints that were fixed with nail polish with the atomic force microscope (AFM). His tests also showed that there is no film on the fiber surface if NP is used. The only exception in that glue is still used (see section 3.4.1) are the micro tensile tests on single fibers. The reason for this is that the fibers are pulled out of the nail polish if a load of about 60 mN (much lower than the breaking load of kraft pulp fibers, see section 5.6) is reached in these tests. For single fiber tensile testing UHU PLUS Sofortfest was used because it is hardened after 2 minutes (much faster than cyanoacrylate glues) and offers the required adhesion force.

Another outcome of these investigations is that the formerly bonded area of fiber crossings that were fixed with cyanoacrylate glue (LOCTITE 454) look different compared to joints fixed with nail polish (see figure 4.3). The figures show that the for-

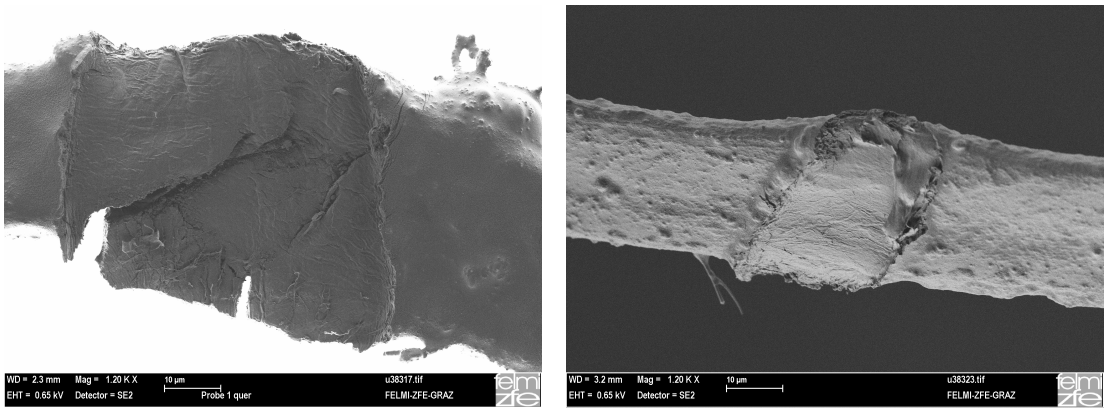

Figure 4.3 Formerly bonded area of fiber to fiber joints that were fixed with cyanoacrylate glue (LOCTITE 454)

merly bonded area is delimited by sharp edges if the glue is used. In case of nail polish, smooth transitions ranging from the boundary areas to the inner bonding region are visible (see figure 4.4). So a lot of information about this border area is lost when the individual fiber crossings are fixed with glue. Furthermore, it is apparent that the formerly bonded area of fiber crossings that were fixed with adhesive show much more damage than those of joints fixed with nail polish (compare figure 4.3 and figure 4.4). This effect could be observed for all formerly boned areas of joints that were fixed with glue. This leads to the assumption that glue particles are also transported into the bonding region. Due to this, parts of the fibers inside the bonded area may be glued together which in turn leads to more damage of the contact area. To clarify this, further investigation are needed. Nevertheless, it can be said that this result is another reason to use nail polish instead of glue for mechanical testing of single fiber crossings.

Formerly bonded area

After the decision to replace the glue by nail polish, additional tests with the SEM were made. Figure 4.4 shows fibers that were fixed with nail polish. The formerly

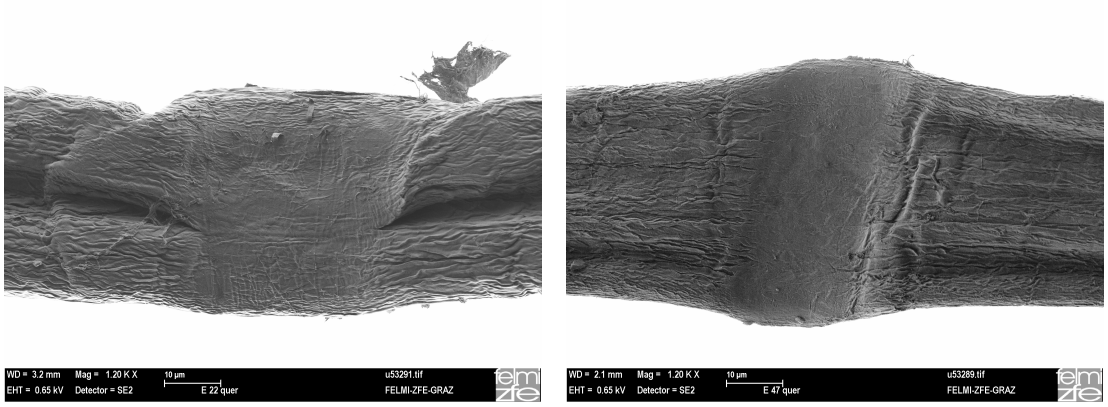

Figure 4.4 SEM images of the formerly bonded area of two cross fibers tested in mode II

bonded area of both fibers shown in figure 4.4 is easy to see and compared to the rest of the fiber surface it is much smoother. Differences in the shrinkage processes of the contact zone compared to the unbonded fiber regions during drying might have caused this. Another explanation for this is that the fibers are pressed into each other during the sample preparation process (see section 3.4). From the images it is also apparent that the width of the fiber in the region of the formerly bonded area is increased. This might be an indication that the fibers were not or not completely collapsed which in turn leads to the compression of the lumen and this is the explanation for the greater width of the fiber. Another explanation could be the effect of restrained drying. In some cases the delamination of the fiber wall as well as pits are also clearly visible (see figure 4.5b). The images in figure 4.4 as well as those of figure 4.5 show no indication for mechanical interlocking within the FBA (no fibrils visible). Schmied [2011] also found no fibrils inside the bonding region of unbeaten pulp fibers. In his study fibrils could only be found in the border zone of the FBA. However, in the case of beaten pulp Schmied et al. [2013] could find fibrils inside the contact zone. The results of this study and those obtained by Schmied could lead to the assumption that mechanical interlocking only occurs in the boundary area of the formerly bonded area of refined pulp fibers.

Furthermore, the formerly bonded area of fiber to fiber joints tested at different loading rates (1 and $5\mu m/s$) were examined. Also a comparison between the FBA of a joint which was loaded to failure in a conventional shear strength test (see section 3.5.1) as well as the one of a crossing broken in cyclic testing (see section 3.5.2) was carried out. The results of these scanning electron microscope investigations are shown in figure 4.5. The figures 4.5a and b show the formerly bonded area of the

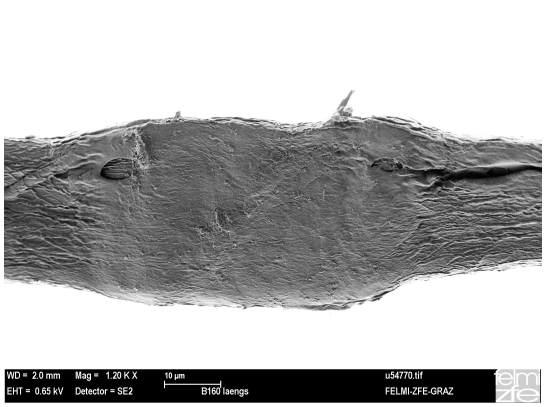

(a) joint tested in mode II at 1 $\mu m/s$

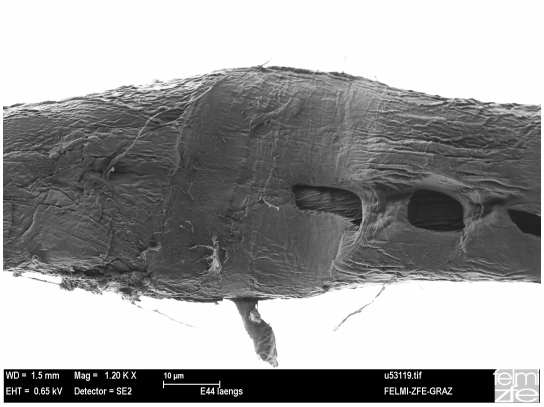

(b) joint tested in mode II at 5 $\mu m/s$

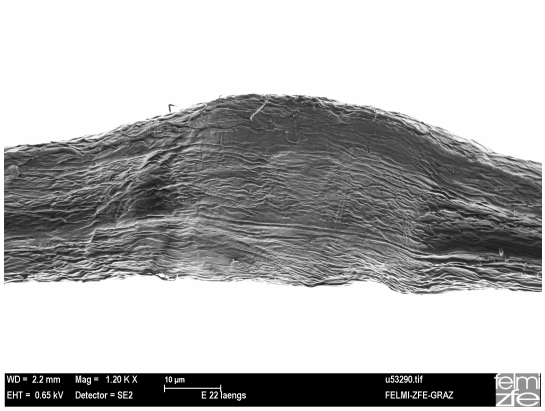

(c) joint tested in cyclic loading at 5 $\mu m/s$

Figure 4.5 SEM investigations of the FBA of joints tested at different testing conditions

longitudinal fiber of joints which were loaded to failure in mode II testing at loading rates of 1 $\mu m/s$ and 5 $\mu m/s$ and figure 4.5c the longitudinal fiber of a crossing broken during cyclic loading at a loading rate of 5 $\mu m/s$. No significant differences in the appearance of the formerly bonded area are visible. It seems as if there is no influence of the testing procedure or the rate of loading on the appearance of the formerly bonded area. Due to the small number of tested samples, further investigations of the formerly bonded area after mechanical testing in the scanning electron microscope are needed.

Low voltage electron microscopy offers the possibility of high resolution images of the formerly bonded area. The results obtained in the scanning electron microscopy investigations show that there is a film on the fiber surface if glue is used. If nail polish is used no glue layer is visible. Furthermore, the appearance of the formerly bonded area of joints that were fixed with glue look different from those of a crossing that were fixed with nail polish. On this account it has been decided to use nail polish instead of glue. The results of the LVSEM investigations also show that the type of

loading (cyclic loading or mode II loading) has no influence on the appearance of the FBA and that there are no fibrils inside the contact zone of unbeaten pulp fibers.

4.3 In-situ ultramicrotome investigation of fiber-fiber joints

Part of the research work of the Institute for Paper, Pulp and Fiber Technology (IPZ) within the CD-Laboratory concentrated on the determination of the size of the contact region between two single fibers. The methods used for this are the polarized light microscopy which has been introduced by Page [1960] and a 3D serial sectioning technique which has been developed at the IPZ in Graz (see Wiltsche [2006]). In order to determine the bonded area by means of the microtome method, the individual fiber to fiber joints were glued onto a strip of paper across a hole (diameter 1 mm), embedded in resin and finally cut with the microtome. The results obtained in these tests were used to calculate the size of the contact region between to fibers (Kappel et al. [2009]). Figure 4.6 shows the cross section of a fiber to fiber joint after cutting with the microtome. A problem in using this kind of method is, that it is not known whether

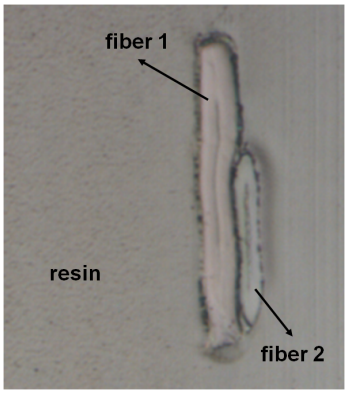

Figure 4.6 Microtome cross section of a fiber to fiber joint

one sees the true contact area of the joint or whether the resin penetrates between the interface. Penetration of the resin into the contact zone leads to a wrong impression of the size of the contact zone (overestimation of bonded area). For that reason, investigations with an in-situ ultramicrotome (3View^{TM} from Gatan Inc.), at the Institute of Electron Microscopy and Fine Structure Research in Graz, were performed. This microtome is directly integrated in an environmental scanning electron microscope. With this microtome slices with a thickness of 50 nm are cut off the embedded sample and the cutting area is imaged after every cut. First results showed that it was not possible to detected the interface between the two fibers within the contact region (see figure 4.7). Thus, a statement regarding the resin penetration could not be made. A possible explanation why there is no visible interface between the fibers is damage of the fibers due to the electron beam i.e. beam damage of the fibers.

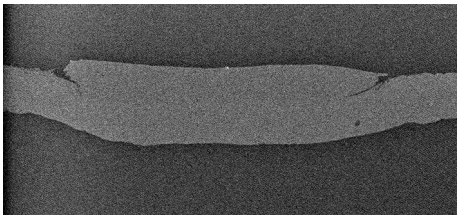

Figure 4.7 ESEM image of the cross sectional area of a fiber-fiber bond

In another experiment, an attempt has been made to stain the fiber wall by using a sulfur-based dye before preparation and embedding of the joints. After cutting of the samples with the microtome, the cross sections were imaged in a SEM. The reason for dyeing the fibers is that both, the fibers as well as the resin are based on carbon and due to this it is difficult to distinguish the resin from the fiber in the electron microscope images. The dye is used to enhance the contrast between the resin and the fibers. In this case, the problem was that the sulfur staining, used for this investigations, formed deposits on the surface as well as at the interface of the bonded fibers (see figure 4.8). Another problem is that this crust may also have an

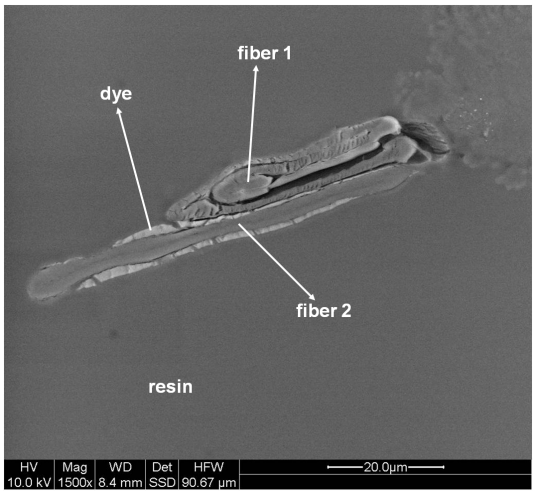

Figure 4.8 SEM image of a fiber crossing (fiber dyed with sulfur-based dye)

influence on the bonding behavior of the fibers. Based on the results of this test it was not possible to find out whether the resin enters into the bonding region or not.

So no reliable method has been found so far to clarify the question whether the resin penetrates into the contact region of two bonded fibers. Possible next steps would be dyeing of the resin by means of sulfur containing dyes. Such dyes are for example Eriochrome T or Toluidine blue. Another possible solution maybe Raman spectroscopy.

Chapter 5

Results and Discussion

In order to get a deeper understanding regarding the strength of paper it is of fundamental importance to learn more about the mechanical properties of single fibers and fiber to fiber joints. With the micro bond tester developed within the framework of this thesis it is possible to determine:

- the mode II strength of a single fiber crossing with and without preloading the cross fiber (see section 3.5.1)
- the energy needed to break a joint (see section 3.5.2)
- the bending stiffness of a single fiber (see section 3.5.3)
- the mode III strength of single fiber to fiber joints (see section 3.5.4)
- the tensile strength of single fibers (see section 3.5.5)

In this section the results of these measurement methods are discussed in detail and compared to those of other studies. All tests were performed using unrefined, unbleached softwood kraft pulp (mixture of spruce and pine).

5.1 Mode II joint strength

As is to be expected, the results show that there is an influence of preloading on mode II joint strength. The mean joint strength without preloading the cross fiber is 6.58 mN (median 4.56 mN) and with preloading it is 2.72 mN (median 2.84 mN). So, if the cross fiber is preloaded with 20 mN, the strength of a fiber joint is reduced by 58%. A possible outlier (10.48 mN) was initially included in the results for the preloaded cross fiber. It has been removed after a Dixon outlier test according to DIN 53804 turned out to be significant on the 99% confidence level. The results of

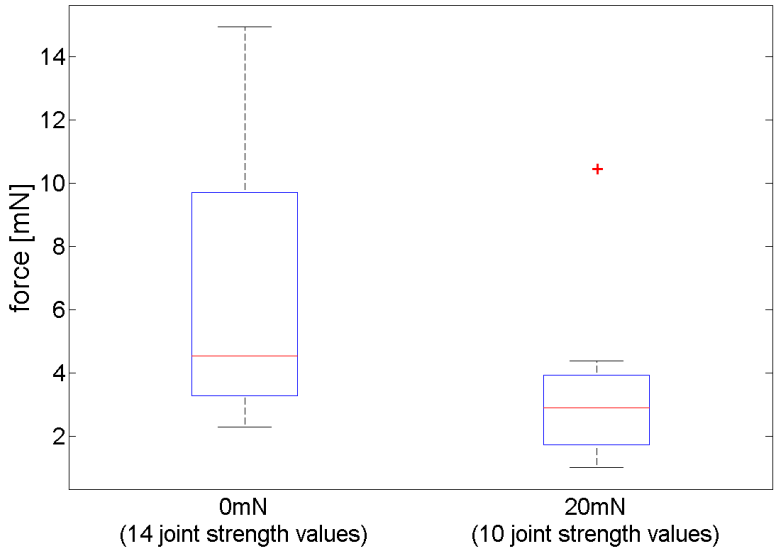

Figure 5.1 Joint strength values without preloading the cross fiber (left) and with preloading the cross fiber (right)

these tests are shown in figure 5.1. In order to see if the difference is statistically significant a t-test with a confidence level $\alpha = 0.01$ was performed. The obtained p-value of 0.0036 confirms a difference of mean joint strength on the 99% confidence level. An explanation for the difference is mainly additional mode II loading of the joint. When the cross fiber is preloaded, there is already mode II loading of the joint due to deformation of the bonding region. So, it is important to say that it is not really preloading of the cross fiber but rather of the joint itself. Furthermore there is also some mode III loading due to deflection of the longitudinal fiber. The larger the deflection of the longitudinal fiber the higher the mode III load. As already mentioned in section 2.2.1, the crossing angle plays an important role in mode III loading.

The mean strength values of fiber crossings obtained in the tests without preloading the cross fiber corresponds to values obtained in other studies (see figure 5.2). Mayhood et al. [1962] measured a mean strength value of about 6.102 mN for unbleached, unbeaten kraft pulp (mixture of spruce and pine) and Saketi and Kallio [2011a] 4.98 mN for joints of untreated softwood. Stratton and Colson [1990] obtained 4.61 mN for loblolly pine springwood and 8.53 mN for loblolly pine summerwood joints. Only the breaking loads measured by Button [1979] are significantly higher. The strength values of lap joints made of loblolly pine holocellulose tracheids ranged from 28.3 mN up to 142.8 mN for summerwood and from 28.3 mN to 78 mN for springwood. An explanation for this is that the behavior of a lap joint during loading is different due the fact that torsional loading (mode III, see section 2.2.1) of the fiber crossing is excluded. Furthermore, the principal strain direction is the same for both

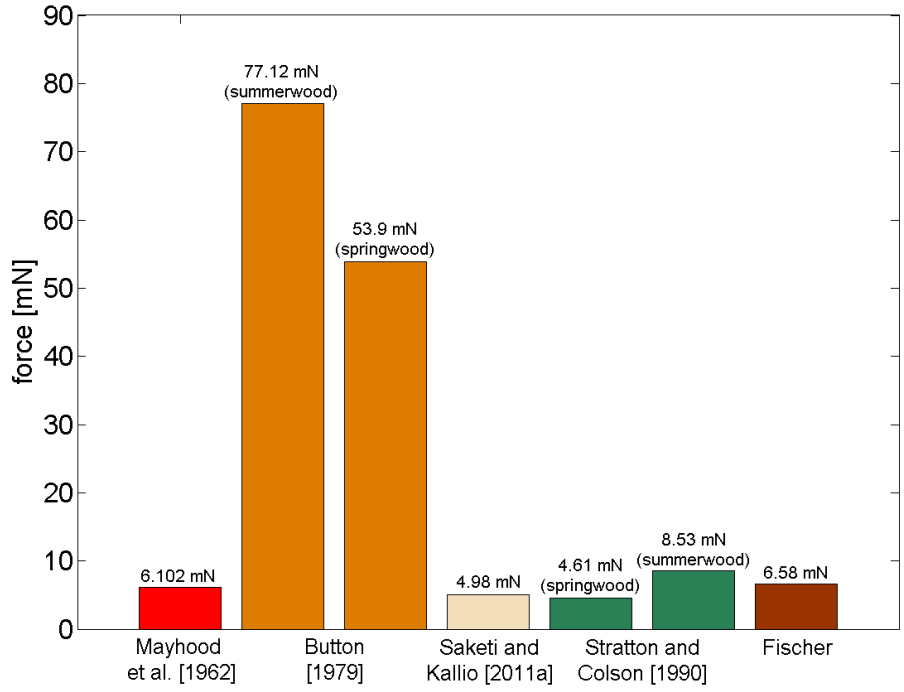

Figure 5.2 Comparison between mean joint strength values of softwood pulp obtained in different studies

fibers which means that one can assume that also the elongation is the same. Due to this, no further stresses that reduce the breaking load of the joint are introduced. In case of a fiber to fiber joint with a crossing angle of or close to 90°, the principal strain directions of the fibers do not match. During mechanical testing additional stresses are generated which in turn lead to a reduction of the breaking load of single fiber crossings.

5.1.1 Specific bonding strength (SBS)

In addition, the optical bonded area (OBA) of 8 fiber to fiber joints was also determined. For this the method (polarized light microscopy) described in the work of Kappel [2010] was used, but in this case the fibers were not dyed because dyeing would change the chemistry of the fiber and this in turn will lead to a falsification of the measured strength values. After mechanical testing of these joints, the specific bonding strength (force per unit area) was calculated. A comparison between the values obtained in this study and those of others is shown in figure 5.3. An important remark is that the specific bond strength values calculated in this thesis as well as those of Saketi and Kallio [2011a], Mayhood et al. [1962] and Mohlin [1974] are the result of all possible fiber to fiber combinations (summerwood to summerwood,

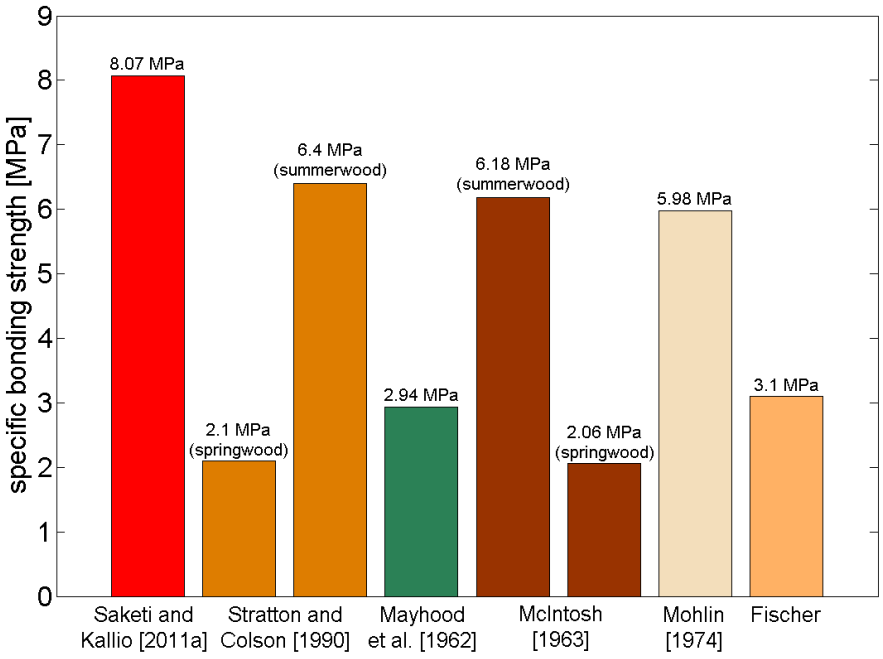

Figure 5.3 Comparison between specific bond strength values obtained in different studies (unbeaten, unbleached softwood pulp)

springwood to springwood or springwood to summerwood joint). For a more accurate comparison between the SBS values of this and other studies, the type of joint should be considered. But nevertheless, all results range between 2 to 8.1 MPa.

Another factor that is of utmost importance for the specific bonding strength of a fiber to fiber joint is the size of the bonded area. The development of the joint strength over the size of optical bonded area (OBA) is shown figure 5.4. From this figure it is apparent that there is no relationship between the force that is needed to break a single fiber crossing and the size of the optical bonded area. Here, the joint which has the largest contact area has one of the lowest breaking loads. This is in accordance with other studies. Stratton and Colson [1990] for example measured a higher breaking load between joints of summerwood to summerwood fibers as springwood to springwood joints although the bonded area for the summerwood joints was smaller. A similar result was found by McIntosh [1963]. The problem when using the optical bonded area is that no information regarding the area in molecular contact is known. So the true contact area is often much smaller than the OBA and for that reason it is difficult to detect a relationship between between breaking load and contact zone.

Basically all kinds of fiber and joint parameters - such as the fiber width, the fiber wall thickness, the fiber diameter, the crossing angle, the area in molecular contact ... - influence the force that is needed to break a single fiber crossing as well as the

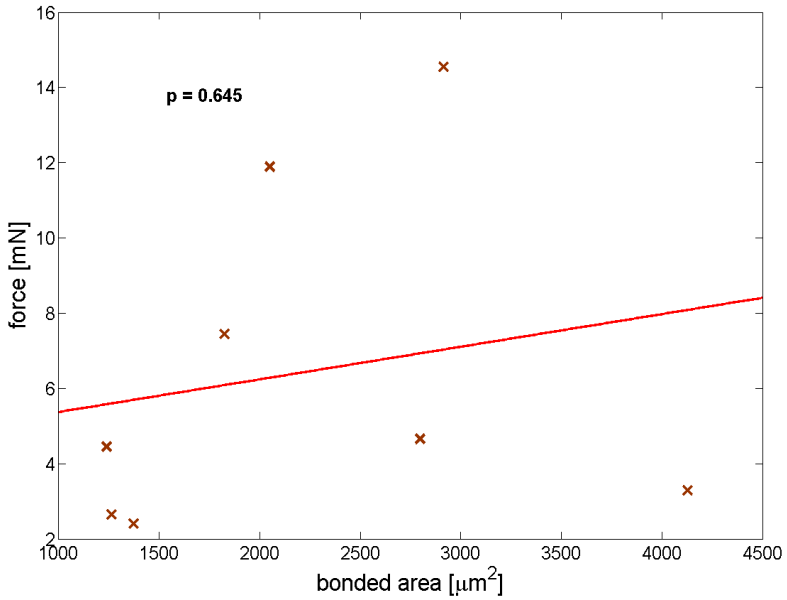

Figure 5.4 Breaking load versus bonded area

specific bonding strength. A combination of these parameters leads to peak stresses in or at the edge of the contact zone. These stresses that finally cause failure of the joint seem to be even higher than the force divided by unit area (see section 5.4). In other words, in these regions the specific bonding strength is higher than the force per unit area. On this account it is of utmost importance to look at the overall system because it controls the breaking load of fiber to fiber joints. This also explains why a direct relationship between breaking load and bonded area could not be found.

5.1.2 Influence of handling

Another outcome is that these kinds of tests are difficult to handle. In this thesis a total number of 112 fiber joints have been tested (mode II with and without preloading). 21% of the joints could be successfully tested, 70% broke during handling (melting of bridges and preloading), 9% were already broken before the sample holder could be fixed to the bond tester (see figure 5.5a). The statistics of mode II testing without preloading the cross fiber is shown in figure 5.5b and the statistics of mode II testing with preloading in figure 5.5c. Both figures show that a large proportion of the joints broke due to melting of the bridges. This is especially a problem in the tests in which the cross fiber is preloaded. In these tests the individual parts of the sample holder are only connected via the joint (see section 3.5.1), and therefore, even low vibrations (generated by the soldering rod) lead to weakening or even breaking of the joint. This may lead to a systematic overestimation of the true joint strength because all of the weak crossings already fail prior to testing. On the other hand also a systematic

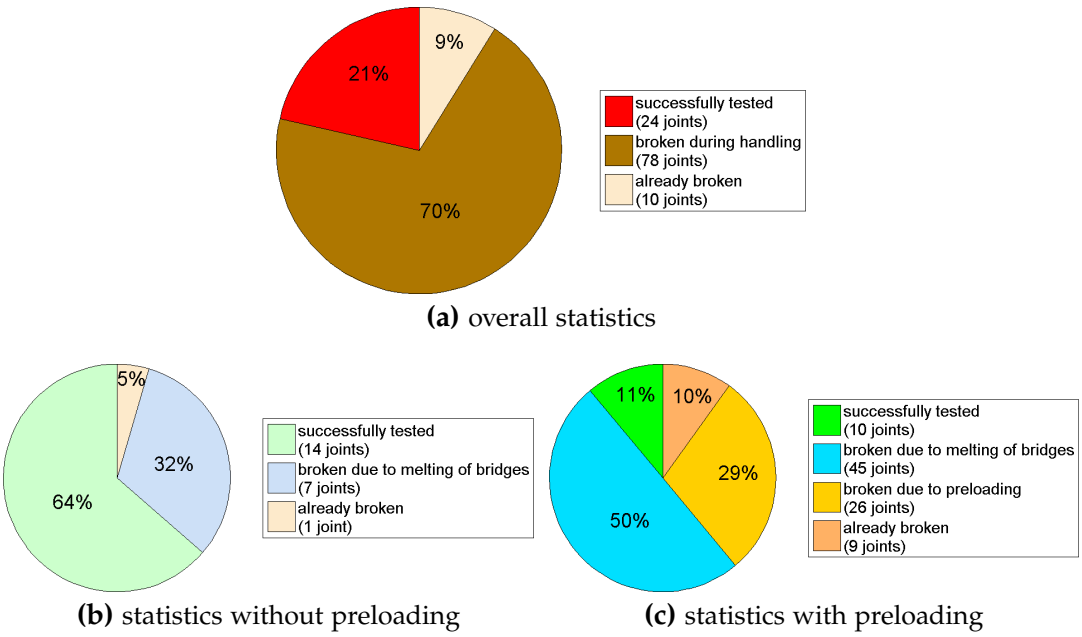

(a) overall statistics

(b) statistics without preloading

(c) statistics with preloading

Figure 5.5 Statistics of mode II testing

underestimation of the strength of single fiber to fiber joints is possible because all joints are weakened. The vibrations could be reduced by replacing the soldering rod by a hot-wire since the resistance during melting is much lower than the one of the soldering rod because of the much higher melting temperature as well as the smaller diameter of the wire compared to the soldering rod.

A comparison between the total number of joints that were preloaded (36 joints) and those that survived preloading (10 joints) show, that only 28% of these joints could be tested. 72% already broke due to preloading. So the major part of the joints that were preloaded broke due to the initial loading of the cross fiber without reaching a defined force of 20 mN. This means that these joints are already weakened to such an extent that no further load is needed. In this study only an average strength value of the joints that survived preloading is presented. The results demonstrate the large effect of multiaxial loading of fiber-fiber joints. However, because of the additional mode III loading due to deflection of the longitudinal fiber - as discussed above - the effect of exclusively preloading the cross fiber is somewhat lower than the measurement results.

From the results obtained in this thesis it is apparent that there are several factors that influence the breaking load of single fiber crossings. All of these factors (crossing angle, preloading of joint, handling of the joints, loading mode and others) have to be taken into account in order to get a deeper understanding regarding the mechanical behavior of fiber to fiber joints during testing as well as the strength of paper.

5.2 Bonding energy

Figure 5.6 shows the results of the bonding energy measurements. The estimated energy values determined in this study range from 3.82 x 10^{-10} to 1.83 x 10^{-11} kJ per joint. The results of these tests can be interpreted as an upper limit of the bonding en-

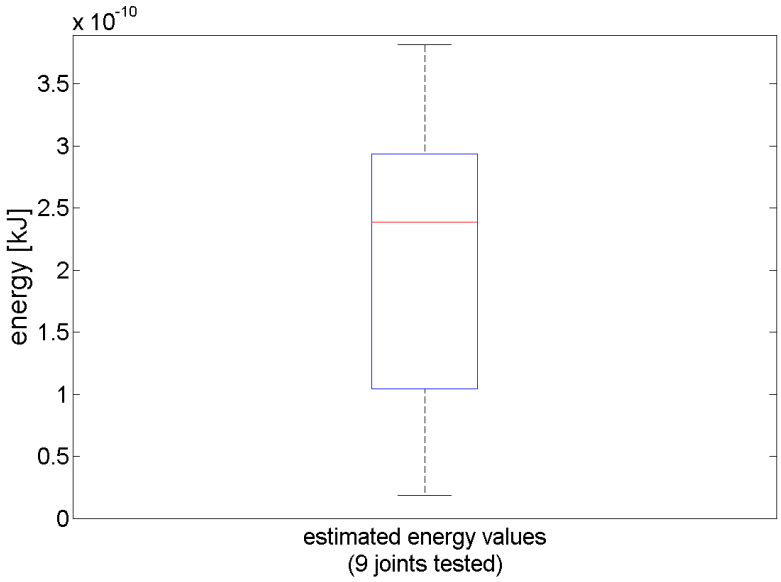

Figure 5.6 Results of the energy values

ergy because the dissipated energy is measured, i.e. the sum of the energy needed to break the single fiber crossing plus the energy consumed due to plastic deformations. Considering the large fraction of plastic energy it is very likely that the bonding energy - the difference between the measured dissipated energy and the plastic energy - is one or two orders of magnitude below the dissipated energy.

Considering a bonded area of 1130 μm^2 (Kappel et al. [2009] investigated the same pulp) for the joints used in these investigations, a mean dissipated energy of about 1.78 x 10^{-5} kJ per cm^2 with a σ value of 1.12 x 10^{-5} kJ per cm^2 is calculated. For 3 of the joints the size of the optical bonded area (OBA) was determined using polarized light microscopy. A comparison between the energy values related to the optical bonded area as well as to 1130 μm^2 is shown in table 5.1. Nordman et al.

estimated energy [kJ]	OBA [μm^2]	energy per optical area [kJ/cm^2]	energy per 1130μm^2 [kJ/cm^2]
$1.83 \cdot 10^{-11}$	1193.9	$1.53 \cdot 10^{-6}$	$1.62 \cdot 10^{-6}$
$2.71 \cdot 10^{-10}$	1857.7	$1.46 \cdot 10^{-5}$	$2.40 \cdot 10^{-5}$
$1.29 \cdot 10^{-10}$	1521.7	$8.51 \cdot 10^{-6}$	$1.45 \cdot 10^{-5}$

Table 5.1 Estimated energy per unit area for 3 fiber to fiber joints under cyclic mode II loading

[1952, 1958] for example determined a so-called "Nordman bond strength" value of 4 x 10^{-5} kJ/cm^2 for paper strips made of unbleached kraft pulp and 2 x 10^{-5} kJ/cm^2 for strips made of bleached aspen pulp. Stone [1963] obtained energy values for different types of pulps with different xylan contents ranging from 1.4 x 10^{-6} to 8.0 x 10^{-7} kJ/cm^2 measured with the nitrogen adsorption method and 7.8 x 10^{-5} to 3.2 x 10^{-5} kJ/cm^2 measured with the light scattering method. Schmied [2011] determined a mean energy value of 9.5 x 10^{-12} kJ per joint. Relating this value to 1130 μm^2 results in 8.41 x 10^{-7} kJ/cm^2. A comparison of the results obtained for softwood kraft pulp in the different studies show that the energy values are close to each other (see figure 5.7). This supports the idea that all of these methods (except the one of

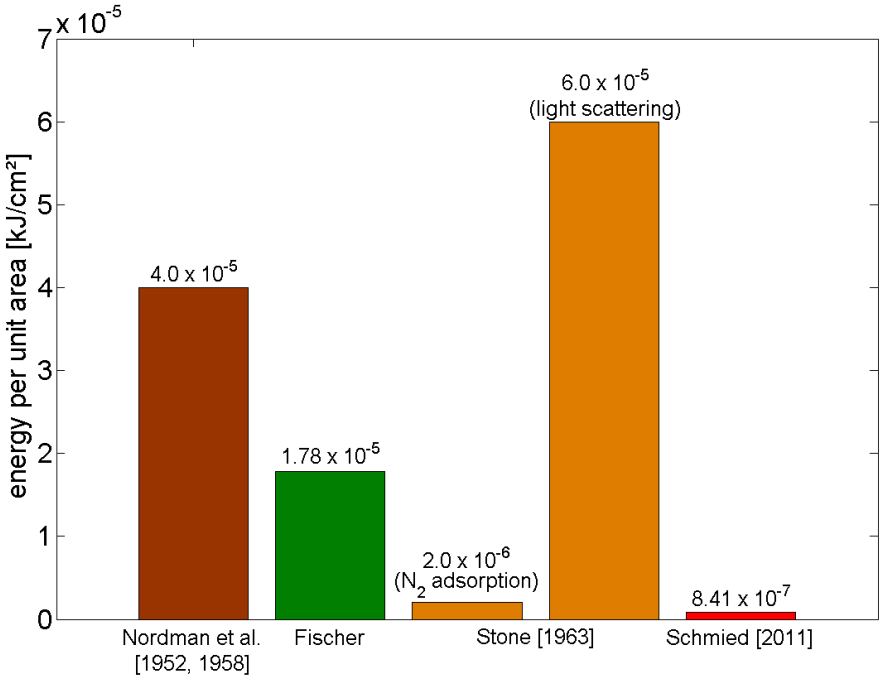

Figure 5.7 Comparison between energy values obtained in different studies

Schmied) are measuring the total energy consumed during breaking of fiber to fiber joints and this means that they give an upper boundary for bonding energy. The value of Schmied is about one percent of the one obtained in this study. This can be explained by the different loading mode (mode I loading of a fiber to fiber joint, see section 2.2.1). Due to this, the energy take-up of the system as well as the maximum breaking load is much lower than in the method described in section 3.5.2. Furthermore, the test of Schmied is much faster and there is also less plastic deformation. This means that the energy value measured by Schmied [2011] is closer to the actual bonding energy.

Figure 5.8 shows the portions of elastic and dissipated energy of one cycle. It

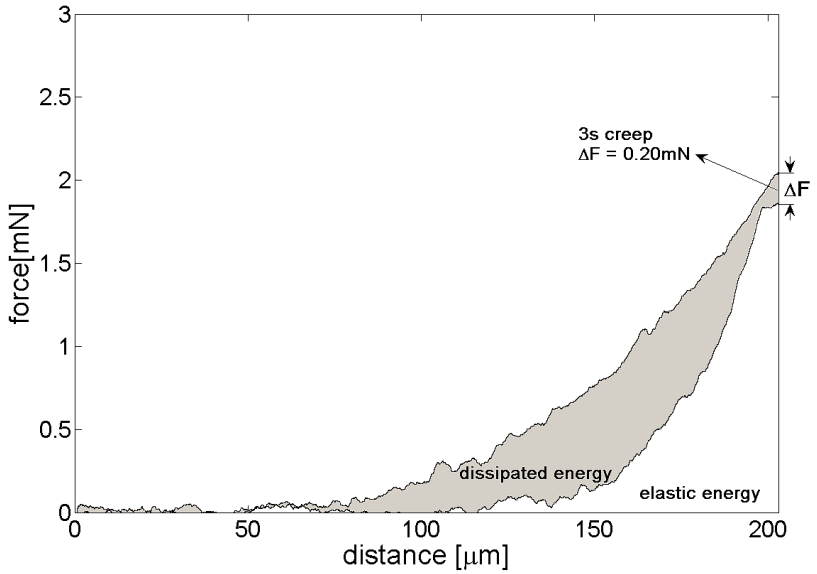

Figure 5.8 Proportions of elastic energy and dissipated energy in one loading-unloading cycle

shows that there is a pause of about 3 seconds between loading and unloading. Within this time there is a reduction in force of 0.20 mN, most likely due to creep in the fibers. Considering this relatively large force drop within 3 seconds it must be assumed that a substantial amount of creep is taking place during testing. Thus a large part of the dissipated energy apparently consists of plastic energy. In order to overcome the influence of creep a modification of the control software was carried out. The modification concerned the reduction of the pause between the loading and unloading cycle. When this time period is reduced it is possible to reduce the influence of creep which in turn is one step closer to determine the true bonding energy. Initial trials with the new software showed that the interval between the cycles is now less than one second.

Summing up it can be said that the investigation of the energy needed to break single fiber to fiber joints will lead to a better understanding of the different bonding mechanisms. Furthermore, the results of this study may also contribute to clarify the question how important each of these mechanisms is.

5.3 Fiber bending stiffness

The bending stiffness values obtained at the end of the beam were measured at maximum load, just before breaking. They range from 1.1724 x 10^{-9} to 5.333 x 10^{-11} Nm^2 (see figure 5.9). From these results it is apparent that there is a strong variation within these values. An explanation is the natural strong variation in fiber wall thickness (e.g.

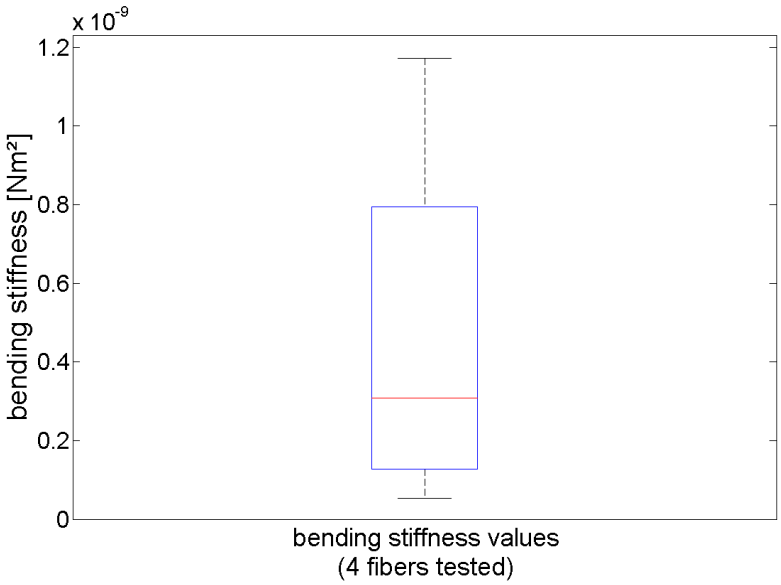

Figure 5.9 Results of the bending stiffness tests

springwood versus summerwood), cross sectional dimensions as well as changes in the degree of fiber collapse. All these variations, occurring naturally in fiber cross sectional morphology lead to highly different moments of inertia I. Additionally the longitudinal fiber elastic modulus E (Page et al. [1977]) is known to vary strongly for fibers of the same pulp, resulting from different fibril angles in different fibers. All these variations in fiber properties lead to the large variations in fiber bending stiffness. Also microcompressions which are the reason for locally pronounced low local bending stiffness, increase the variation in this measurement. In order to demonstrate that the variations are not caused by the measurement method we checked the repeatability by measuring the bending stiffness of the same fiber but with different deflections (bending forces) and at different positions along the fiber, see table 5.2 and 5.3. Here w_1 and w_2 denote different deflections due to different bending forces

$E \cdot I$ at $x_1 = 195\ \mu m$	$1.2724 \cdot 10^{-10}$
$E \cdot I$ at $x_2 = 311\ \mu m$	$1.7103 \cdot 10^{-10}$
$E \cdot I$ at $x = l = 382\ \mu m$	$2.0024 \cdot 10^{-10}$

Table 5.2 Bending stiffness values at different positions

$E \cdot I$ at $w_1 = 9.8\ \mu m$	$1.9637 \cdot 10^{-10}$
$E \cdot I$ at $w_2 = 29.3\ \mu m$	$1.9083 \cdot 10^{-10}$
$E \cdot I$ at $w_{max} = 58.4\ \mu m$	$2.0024 \cdot 10^{-10}$

Table 5.3 Bending stiffness values at different forces

and x_1, x_2 denote different positions along the fiber (see figure 5.10). These results and also those of other fibers show that the values measured for one fiber are well repeatable. It has to be mentioned that if the joint is twisting or if there is movement in the z-direction during testing, an accurate analysis is not possible. Twisting or z-directional movement of the joint makes it impossible to determine the deflection w

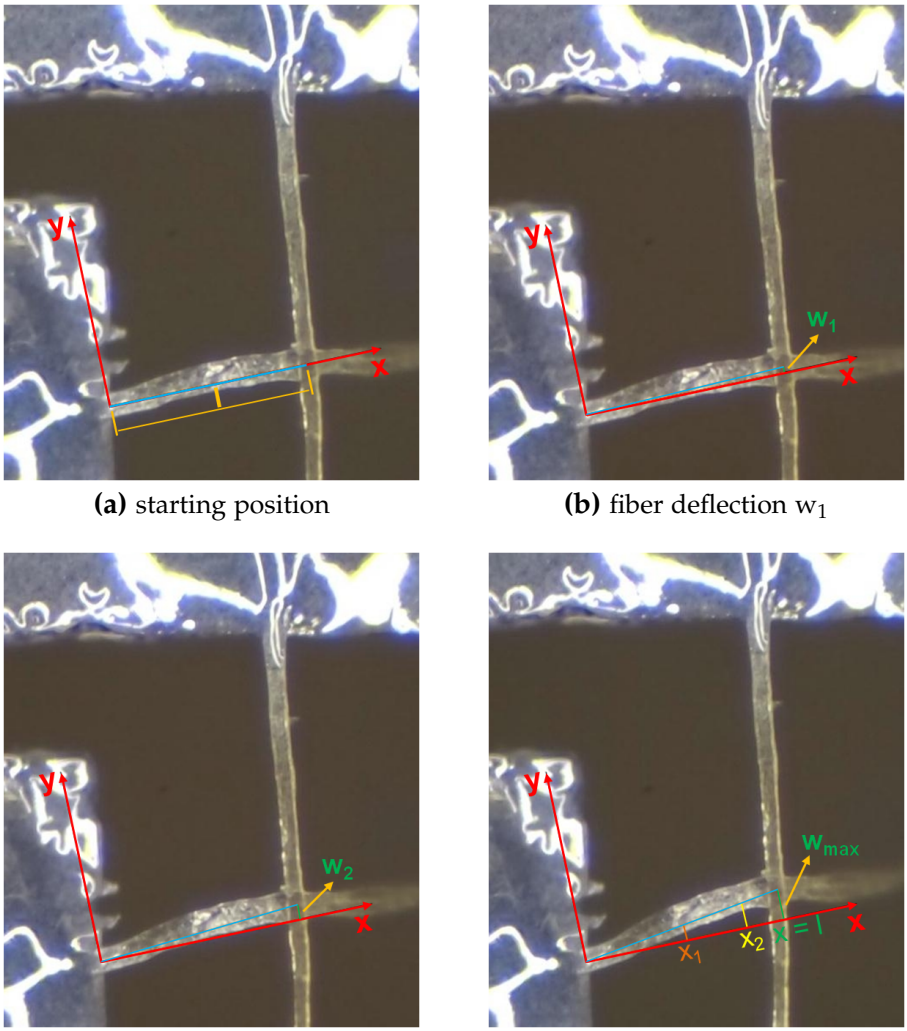

(a) starting position

(b) fiber deflection w_1

(c) fiber deflection w_2

(d) maximum deflection w_{max} as well as position x_1 and x_1

Figure 5.10 Measurement of fiber bending stiffness

correctly because the movement of the fiber out of the image plane produces a skewed image of the fiber. The results of such measurements have to be discarded.

Table 5.4 shows a comparison between the bending stiffness values of this study and those obtained by others. The method developed in this thesis uses the principle of a cantilever beam (dry fiber) that is fixed on one side and free on the other one. The system of Schniewind et al. [1966] is based on the same principle. The main difference compared to the method developed in this thesis is that in this case it was possible to determine the bending stiffness in the wet and dry state (see section 2.4). In this study, they also investigated the difference between springwood and summerwood fibers. Saketi and Kallio [2011b] (section 2.4) for example measured the deflection of

		bending stiffness [Nm^2]	
Fischer		$4.61 \cdot 10^{-10}$	dry
Schniewind et al. [1966]			
	summerwood	$1.45 \cdot 10^{-10}$	dry
	springwood	$2.90 \cdot 10^{-11}$	dry
Saketi and Kallio [2011b]		$1.20 \cdot 10^{-10}$	wet

Table 5.4 Bending stiffness values for softwood pulps obtained in different studies

wet fibers (prior to testing fibers were soaked in water for 5 min) supported at two points. Nevertheless, from the results shown in table 5.4 it is apparent that the values of the bending stiffness are within the same range although different measurement setups have been used.

A method having the capability to determine the bending stiffness in dry as well as in the wet state would be preferable as a direct comparison between dry and wet bending stiffness of the same fiber can be carried out. This in turn will lead to a better understanding of the mechanical behavior of single fibers.

5.4 Mode III joint strength

The results of the mode III joint strength measurements show that the breaking load of a single fiber crossing is significantly lower than that obtained from a conventional mode II shear joint strength test (without loading the cross fiber, see figure 5.11). The mean joint strength obtained from mode II testing is about 6.58 mN and the one obtained from mode III testing is about 1.057 mN. In mode III the strength value is about 84% smaller than in mode II. The strong difference in breaking force can only be explained by the additional mode III loading of the joint. Based on these results, it is apparent that the mode of loading has a significant influence on the strength of individual fiber-fiber joints. The main difference of a mode III strength test compared to a conventional shear strength test is the torsional loading of the joint, see section 2.2.1 and 3.5.4. As a consequence one has to avoid torsional loading of the joints during mode II testing. Torsional load is introduced into fiber crossings that are not exactly perpendicular.

An important remark is that with the developed micro bond tester it is only possible to determine the force that leads to breaking of the joint in mode III loading. But in case of mode III testing, the moment that is acting on the joint is more important because torsional loading leads to joint failure in these tests. Knowledge of this moment permits the determination of the mode III joint strength, i.e. the torsion strength of single fiber to fiber crossings. In order to learn more about the resultant forces and moments that are acting on the joint, simulations with the data of three

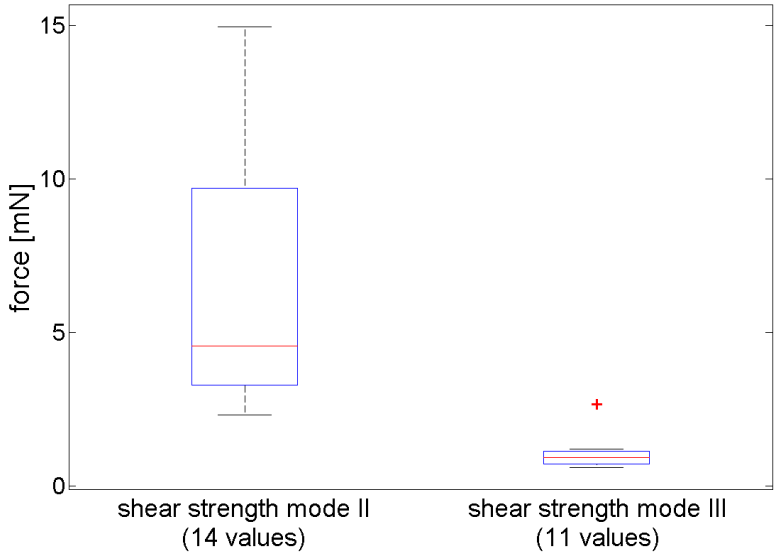

Figure 5.11 Comparison of breaking force in mode II (left, 14 joint strength values) and mode III (right, 11 joint strength values) shear load.

crossings were performed at KTH, Royal Institute of Technology, in Stockholm. For these investigations the images of the initial state as well as directly before breaking of the fiber joints were used and analyzed by using a finite element method developed by Magnusson [2013]. Figure 5.12 shows the undeformed and deformed fiber to fiber crossing with the geometry of the model. This model is used to calculate the state

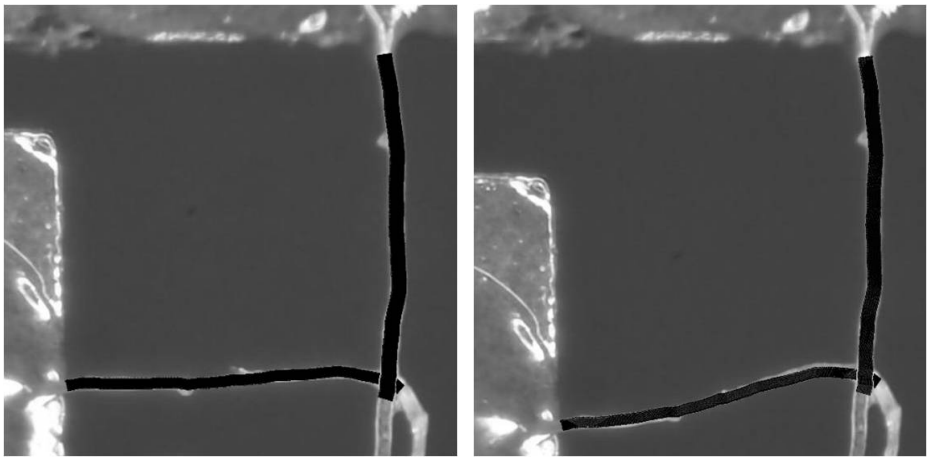

(a) undeformed state **(b)** deformed state

Figure 5.12 Fiber to fiber joint with the model geometry (Magnusson, M.S., personal communication, October 4^{th}, 2012)

of loading in terms of resultant forces and moments that are transferred by the joint

(whole overlap considered to be in contact). By means of the force distribution within the contact zone, the resultant forces and moments at the centroid of the overlap area were obtained. These are:

F_n ..... force normal to interface
F_s ..... shear force in major shear direction
M_n ..... twisting moment about the normal to the bond interface
M_{st} ..... resultant of the peeling moments about the first shear direction (M_s) and about the transverse shear direction (M_t)

The results of these simulations are shown in table 5.5. Especially from sample 1 it

	F_n [mN]	F_s [mN]	M_n [μNm]	M_{st} [μNm]
sample 1	0.06	-0.74	-0.17	0.02
sample 2	0.18	-0.53	-0.06	0.02
sample 3	0.41	-0.59	-0.04	0.03

Table 5.5 Results of the FEM simulations (Magnusson, M.S., personal communication, October 4^{th}, 2012)

is apparent that in this case the failure is predominantly caused by the shear force F_s as well as the twisting moment M_n ($F_s \gg F_n$ and $M_n \gg M_{st}$). In the two other cases F_n and F_s are predominating but also in this case the twisting moment is involved (Magnusson, M.S., personal communication, October 4^{th}, 2012). From the results shown in table 5.5 it is apparent that the variation of F_s is much lower than the one of M_n. Therefore, F_s seems to be the limiting factor that leads to failure of the joint in mode III testing. The images illustrated in the figures 5.13, 5.14 and 5.15 show the normal stress as well as the shear stress distributions in the contact region of the joint shown in figure 5.12. There are high stress peaks in the bonding region. They also show that the highest stress concentrations are located at the edges (see highlighted areas in figure 5.13, 5.14 and 5.15) of the contact zone which is a good explanation for the low breaking force obtained in mode III testing. The stress concentrations in these regions indicate that breaking of the fiber to fiber joint originates from the edges of the joint. Apparently, the specific bonding strength seems to be higher than the force per unit area of bonded area (F_{break}/A_{bond}) and in these areas the present stress σ is higher than the force divided by the bonded area.

In a next step the model developed by Magnusson [2013] will be further modified. Here, the naturally occurring twists in the fibers will also be considered. This will lead to a more precise approximation of the bending as well as the twisting behavior of the fibers. Due to the fact that the contact zone is not completely bonded, a circular contact area (biggest circle that fits into overlap) will be assumed. The introduction of a circular contact area will avoid stress concentrations at the edge of the bonding

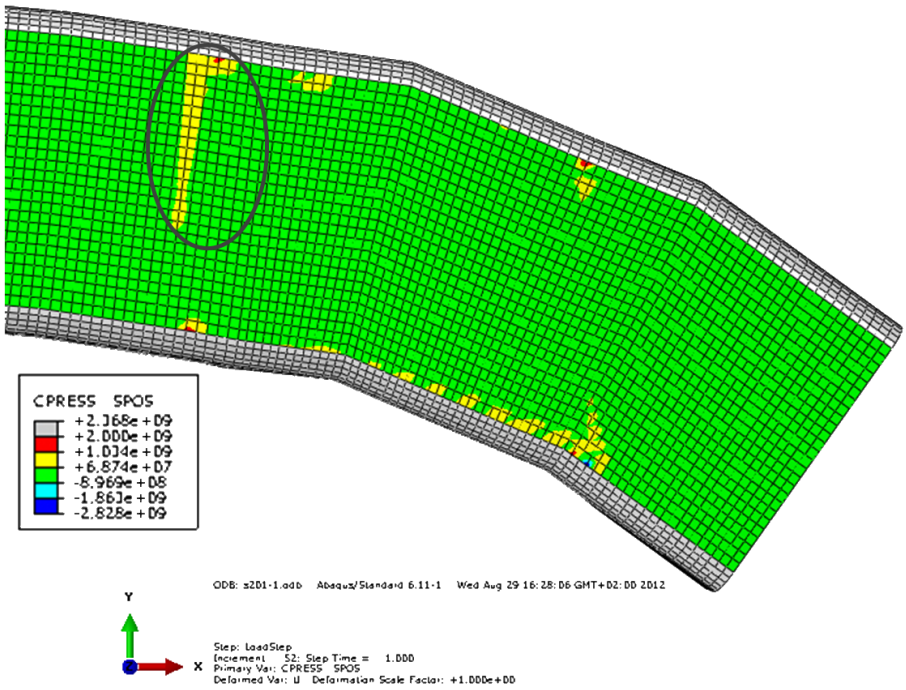

Figure 5.13 Stress distribution normal to the interface surface (Magnusson, M.S., personal communication, January 24th, 2013)

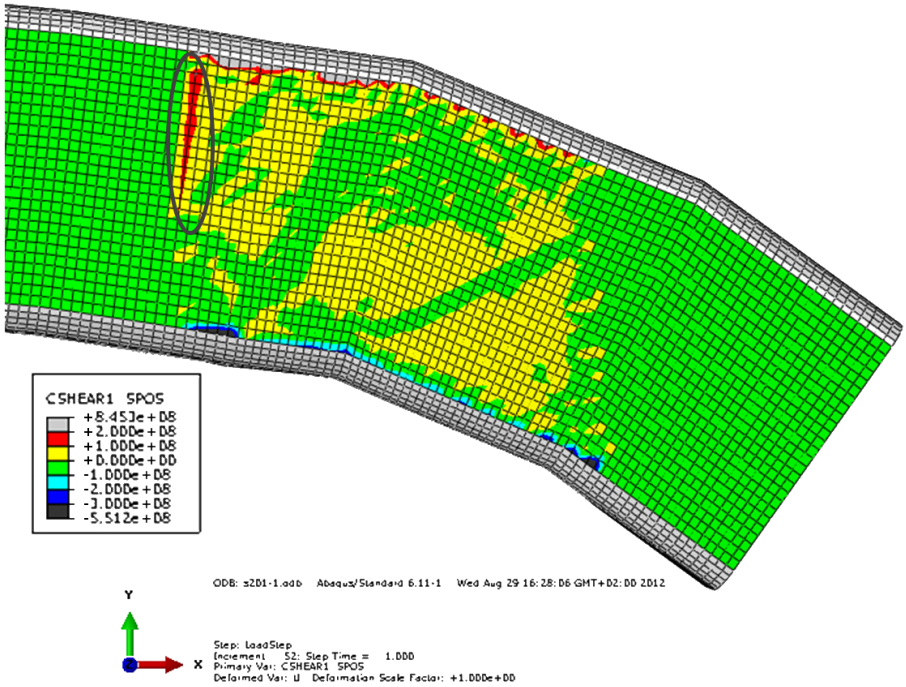

Figure 5.14 Shear stress (shear 1) in the direction of the largest shear direction (Magnusson, M.S., personal communication, January 24th, 2013)

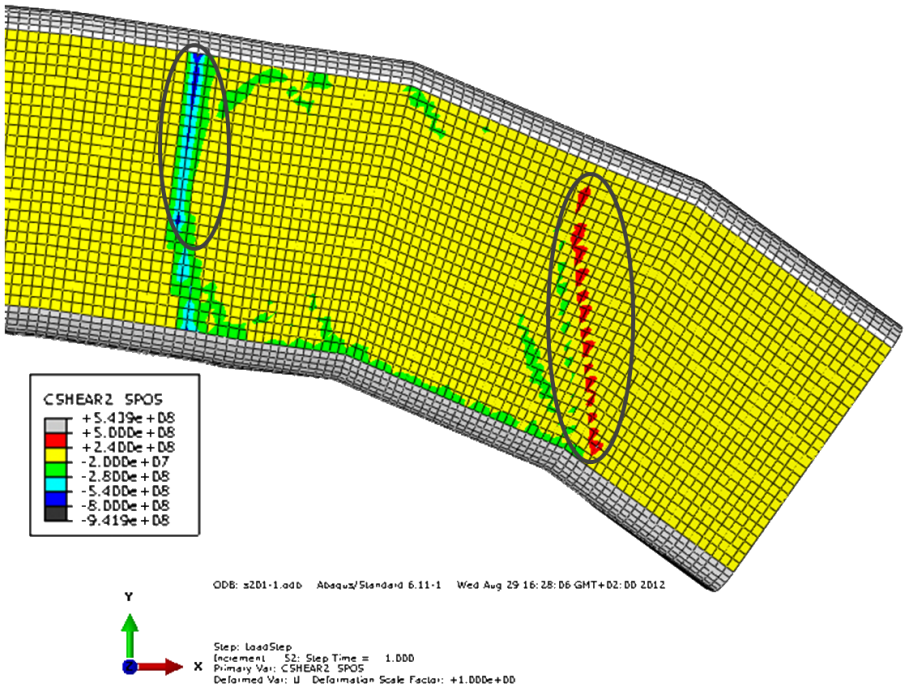

Figure 5.15 Shear stress (shear 2) in direction perpendicular to shear 1 (Magnusson, M.S., personal communication, January 24th, 2013)

region in the simulations. Results of these simulations are presented in Magnusson et al. [2013].

The results obtained in the mode III tests as well as in the FEM simulations demonstrate that the twisting moment significantly influences the fracture behavior of single fiber crossings. Furthermore, they show that there is an interplay between the different modes of loading during mechanical testing of fiber to fiber joints (mode II + III loading). The only exception are joints with a crossing angle of or close to 90°. The angle between the fibers thus has a major impact on mode III loading in a conventional shear strength test. For a better understanding of the behavior of a joint during loading as well as the force needed to break the crossing, the influence of the various modes of loading should be considered as a whole. Whether and how the concept of mode III loading can be applied to a paper network remains to be clarified. The results of the FEM simulations provide a basis for network modeling and this may give an answer to this question.

5.5 Joint strength at different loading modes

Figure 5.16 shows a comparison between the mode I, mode II and mode III strength of individual fiber to fiber joints (all tests were performed with the same pulp). Schmied et al. [2012] developed a method to determine the mode I strength (z-directional

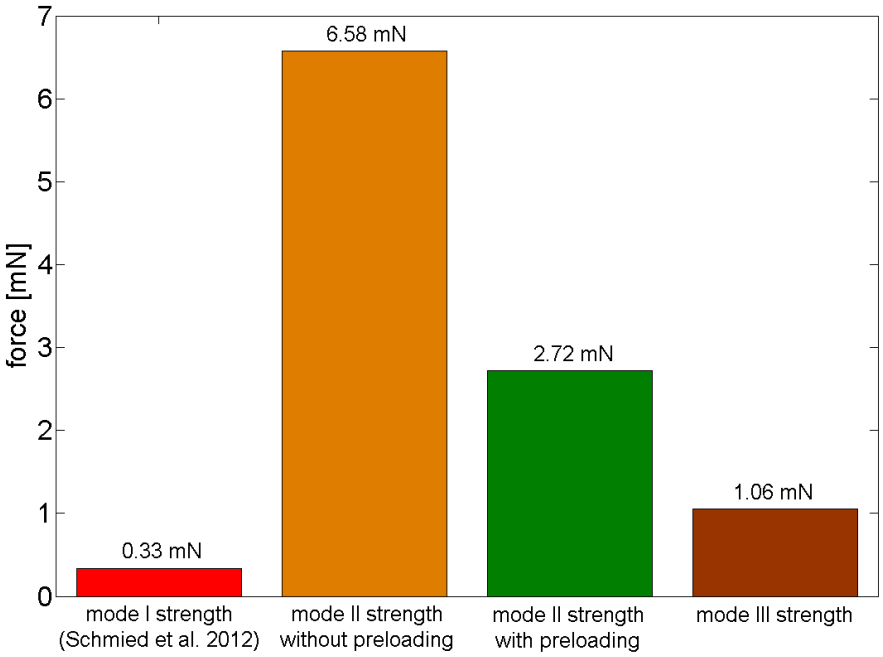

Figure 5.16 Joint strength values for softwood kraft pulp obtained at different loading modes

strength) of single fiber to fiber joints (principle is shown in section 2.2.1). In this study a mean breaking load of about 330 μN was obtained. This value is about 20 times lower than the mean joint strength without preloading (6.58 mN) and about 8 times lower than the strength of crossings with preloading (2.72 mN) the cross fiber. The difference between mode II and mode III loading is not that large. In this case the mode III strength (1.06 mN) is about 6 times smaller than the one of a conventional shear strength test (without preloading) and 2.5 times than mode II testing with preloading.

From the results shown in figure 5.16 it is apparent that the loading mode significantly influences the breaking load of single fiber crossings. This result is of utmost importance in mechanical testing of single fiber to fiber joints because care must be taken which loading mode leads to breaking of the fiber crossing.

5.6 Tensile strength of single fibers

The mean strength value obtained in the single fiber tensile tests is about 160.17 mN for unbleached, unrefined kraft pulp fibers (mixture of spruce and pine) with a free span of 1 mm. In addition, individual viscose fibers (circular shape, dtex = 1.7) were also analyzed. In this case a mean breaking load of 38.34 mN (test span = 2 mm) was measured. Figure 5.17 shows the results of these tests. The tensile strength

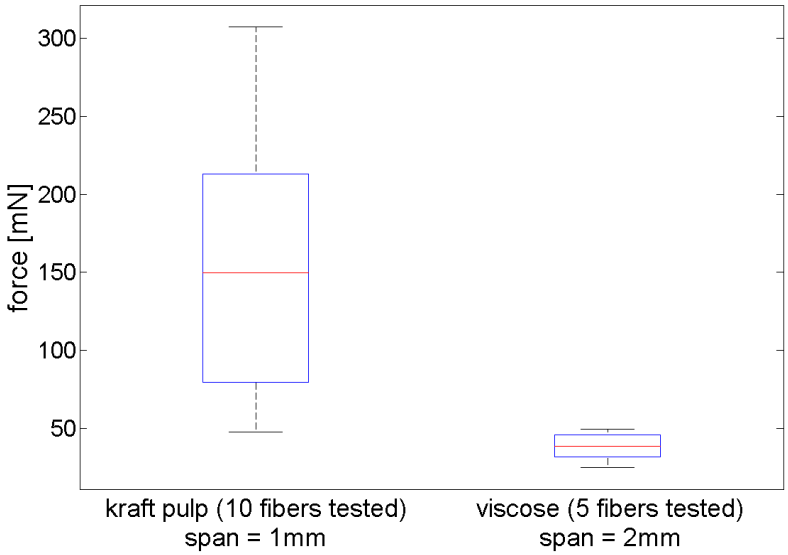

Figure 5.17 Result of tensile strength measurements

values of the kraft pulp fibers show that there is a strong scatter within the measured data whereas the values obtained for the viscose fibers do not show this behavior. Explanations for this are the differences in the fibril angle of the kraft pulp fibers, the presence or absence of dislocations as well as twist in the free length of the fiber. Especially twists are a considerable problem because if a fiber is strained to failure the breaking load is reduced due to stress concentrations in regions of twists (see table 5.7). In some cases the fiber broke at one of the two fixation points. This was also observed by Van Den Akker et al. [1958] who found out that there are stress concentrations in this areas due to hardening of the glue. The stress concentrations cause failure of the fibers which means that the test is no longer a pure tensile test. Therefore, the strength values of fibers that fail at the fixations points as well as those of fibers with a twist in the free fiber length should be excluded. Another problem by using two-component glue (UHU PLUS Sofortfest) is the mixing ratio between the binder and the hardener. If the ratio is not exactly 1:1 the fiber is pulled out of the glue. The reason for this is that the glue could not completely cure if a wrong mixing ratio is used.

Besides the force that is needed to break a single pulp fiber, the elongation ε of the fibers was determined by image analysis (see section 3.5.5). In the future the cross section of the individual fibers after mechanical testing will be analyzed by means of the 3 dimensional serial sectioning method developed by Wiltsche [2006]. Presently only information about the mean size of the cross sectional area of the investigated kraft pulp fibers is available. Lorbach et al. [2012] investigated small paper pieces made of the same pulp as used in this thesis with the microtome method. An example

of a paper cross section after microtome cutting is shown in figure 5.18. Based on the

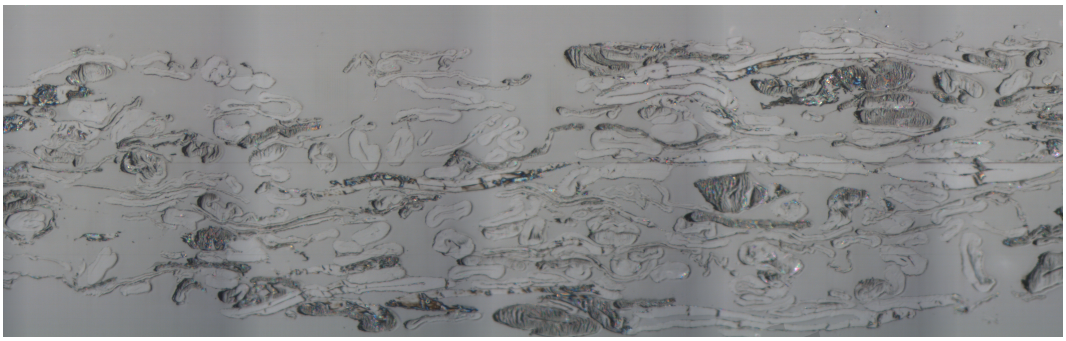

Figure 5.18 Paper cross section after microtome cutting (Lorbach, C., personal communication, January 23^{th}, 2013)

results obtained in the study of Lorbach a mean cross sectional area A of 154 μm^2 (internal report) was determined. This value is used in conjunction with the measured breaking force F for calculation of the breaking stress (σ) acting on the fiber. The strain to break ε together with σ is used to calculate the modulus of elasticity. Initial results of these calculations are summarized in table 5.6. In the work of Groom et al. [2002]

	F_{break} [mN]	E [GPa]	σ [MPa]	ε [-]	span [mm]	n
kraft pulp	160.17	13.91	1040.10	0.0869	1	10
viscose	38.34	-	-	0.0558	2	5

Table 5.6 Mechanical properties of softwood kraft pulp and viscose fibers

the tensile behavior of loblolly pine latewood fibers were investigated. The modulus of elasticity values obtained in this study range from 6.55 to about 27.5 GPa. Page et al. [1977] measured values ranging from 20 to 80 GPa for spruce. Again it is apparent that the E-modulus values are varying within a large range. The differences can be explained by the different testing and fixation methods, dislocations as well as the fibril angle. Another explanation is that the results of the fibers that were twisted are also included in this thesis. Table 5.7 shows a comparison between the mean breaking load and the mean E-modulus of straight and twisted fibers. From the result shown

	F_{break} [mN]	E [GPa]	n
straight fibers	232.78	20.23	5
twisted fibers	87.57	7.59	5

Table 5.7 Mechanical properties of straight and twisted softwood kraft pulp fibers

in table 5.7 it is apparent that the mean breaking load of twisted fibers is about 2.7 times lower than the one of straight fibers. Due to this fact, the E-modulus values of twisted fibers should be excluded. Another factor of interest is the fibril angle. In

order to get a better understanding of the mechanical properties of single fibers, the fibril angle of each fiber should also be determined prior to testing.

As the E-modulus values obtained in this study are based on a mean cross sectional area of 154 μm^2, the next step is the determination of the cross sectional area of each tested fiber. This will enable the determination of the modulus of elasticity as well as the moment of inertia I for each fiber. The modulus of elasticity together with the moment of inertia can be used to calculated the theoretical bending stiffness.

The strength of the fiber network is significantly influenced by the strength of single fibers which in turn is influenced by several other factors. The breaking load of a single fiber is strongly influenced by dislocations in the fiber and the fibril angle which changes from fiber to fiber. Stress concentrations are another factor reducing the tensile strength of fibers. They arise at the fixation points due to hardening of the glue or in regions of twists in the free fiber length. Fibers which are twisted (see table 5.7) or that fail at the fixation point should be excluded from further analysis due to their reduced breaking load. A wrong tensile strength will lead to wrong mechanical parameters such as the E-modulus and the stress σ.

Chapter 6

Conclusion and Outlook

The strength of paper is one of the most important properties of this material. For a better understanding of paper strength it is necessary to understand the fracture behavior as well as the mechanical properties of individual fibers and fiber to fiber joints. In this thesis a novel direct method for mechanical testing of single fibers and joints is presented, allowing the analysis of the geometry and the deformation of joints and fibers during testing. Furthermore, it offers the possibility of biaxial loading i.e. loading of both fibers. The additional information regarding loading geometry, fiber deformation and behavior under biaxial load will help to clarify the specific loading situation of the tested joints and thus provide a step towards obtaining information about specific bonding strength. Another feature of this measurement technique is its wide applicability.

From the results obtained in the bond strength measurements it is apparent that preloading of the cross fiber significantly influences the strength of single softwood fiber crossings. The mean breaking load without preloading the cross fiber is about 6.58 mN compared to 2.72 mN with preloading. An explanation for this is additional loading of the joint with mode II and mode III load. One of the most important results of these tests is that the strength of a fiber to fiber joint is significantly influenced by the interplay of the different modes of loading.

With the device developed in this thesis it is also possible to provide an estimate for an upper boundary for the bonding energy (bonding energy as well as plastic energy is measured) of softwood fiber to fiber joints. The values obtained in this thesis range from about 3.82 x 10^{-10} to 1.83 x 10^{-11} kJ per joint. A comparison of these values and those of Nordman et al. [1952, 1958] and Stone [1963] show that the energy values are close to each other. This supports the idea that all of these methods are measuring the total energy consumed during breaking of fiber to fiber joints.

Another application of the micro bond tester is the determination of the dry bend-

ing stiffness of single softwood fibers. The values measured in this study range from 1.1724 x 10^{-9} to 3.8798 x 10^{-11} Nm^2. The reason for the high variation in the data is that the bending stiffness is significantly influenced by the fiber cross section (shape, fiber wall thickness, degree of collapse and others), the longitudinal E-modulus of the fibers as well as defects along the fiber.

The breaking loads obtained in the bending stiffness tests demonstrate that the joint configuration used in these tests leads to a situation that is close to mode III loading. The mean mode III joint strength of 1.057 mN is about 84% lower compared to the results obtained in a conventional shear strength test (mode II test without preloading the cross fiber). The mode of loading thus significantly influences the strength of individual fiber to fiber joints. Initial results of simulations presented by Magnusson et al. [2013] show that the low breaking loads can be explained by the resultant twisting moment as well as the high stress concentrations at the edges of the bonding region.

Tensile tests of softwood kraft pulp fibers, using a free span length of 1 mm, resulted in a mean strength of about 160.17 mN. The strength values as well as initial estimates of the modulus of elasticity (3.46 to 33.30 GPa) of the softwood kraft fibers show strong scatter. Possible explanations are differences in the fibril angle, twists within the free fiber length as well as dislocations in the fiber. Especially the twist leads to stress concentrations which in turn decreases the breaking load.

Investigations using low-voltage scanning electron microscopy show the formation of a layer that covers the surface of the fibers if cyanoacrylate glue is used for joint fixation. The use of nail polish, which does not show this behavior, eliminates the possible influence of this glue layer on the strength of single fiber crossings. Furthermore, it seems that strong damage within the bonding region can be avoided if the glue is replaced by nail polish. This damage is an indication that glue is transported into the contact zone. Images of the formerly bonded area of joints fixed with nail polish and tested at different test conditions also show that there is almost no difference in the appearance of the contact zone. The smooth surfaces of the formerly bonded area show no breaking of fibrils.

Future applications

In order to obtain a more precise description of the fracture behavior of single fiber crossings tested in mode II, additional tests at different velocities are needed (distinction between brittle and ductile behavior). If there is no change in the mechanical properties at different speeds one can conclude that the joint shows a ductile behavior and if there are big differences the joint exhibits a brittle behavior. In addition, the images of these tests should be analyzed using digital image correlation. This will provide a better understanding of the deformation behavior of joints and fibers during mechanical testing. Another topic of interest is the fibril angle within the con-

tact zone in order to find out whether the fibril angle influences the joint strength. Furthermore, the contribution of refining on the strength of individual fiber to fiber joints should be investigated. The tests will contribute to clarify if beating influences the fiber to fiber joint strength.

Additional bonding energy measurements carried out at higher testing velocities will lead to a more precise description of the bonding energy due to the fact that the influence of viscoelastic effects is reduced. Further work in this field will be undertaken.

Further development of the existing method used to determine the bending stiffness of single fibers will help to eliminate the problem of blurred images that result from twisting of the fiber as well as movement of the joint in z-direction. Another interesting aspect is the combination of the bending stiffness tests with measurement of the cross sectional morphology using the microtome method. This will enable to calculate the area moment of inertia I. The bending stiffness values together with I can be used to calculate the theoretical modulus of elasticity.

Additional FEM simulations of mode III tests with different testing conditions will provide a better insight about the influence of torsional loading on the strength of fiber to fiber joints.

To learn more about the influence of fiber defects more tensile tests with different test spans could be performed. Furthermore, the cross section of each tested fiber should be analyzed with the microtome. This will enable to calculate the stresses acting on the fiber, the modulus of elasticity as well as the area moment of inertia for each fiber. The E-modulus together with the area moment of inertia can be used to calculate the theoretical bending stiffness. Furthermore, the determination of the fibril angle as well as the evaluation of its influence on the breaking load will provide a more precise description of the mechanical properties of single fibers.

Last but not least it should be mentioned that for each of the measurement methods presented in this thesis a large sample size is needed in order to get better statistics.

Appendix A

Fibers fixed with cyanoacrylate glue

SEM images of the formerly bonded area.

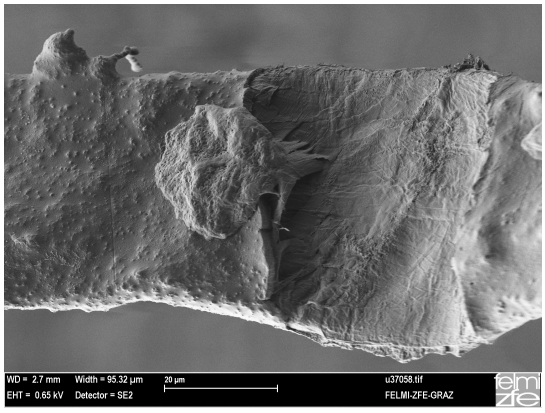

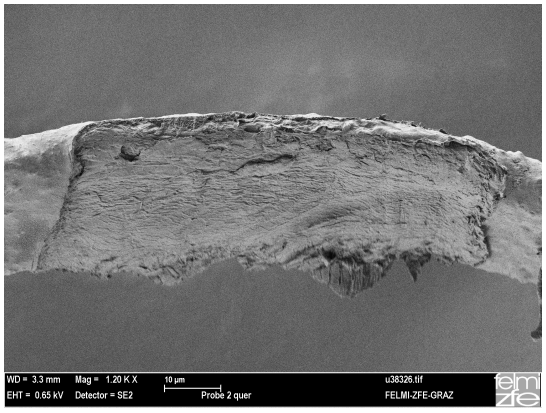

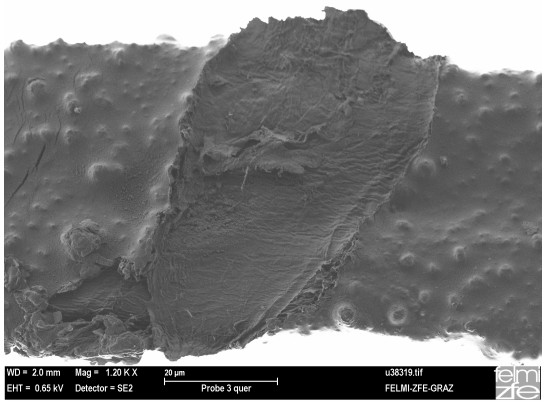

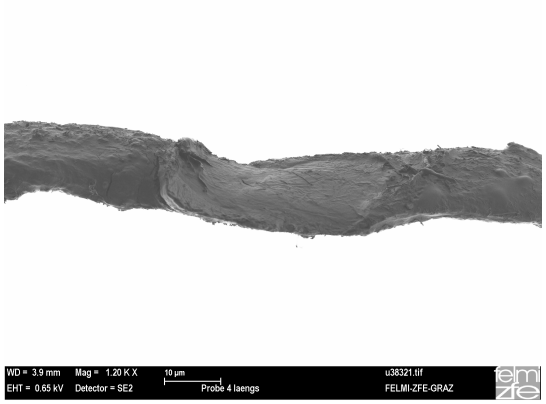

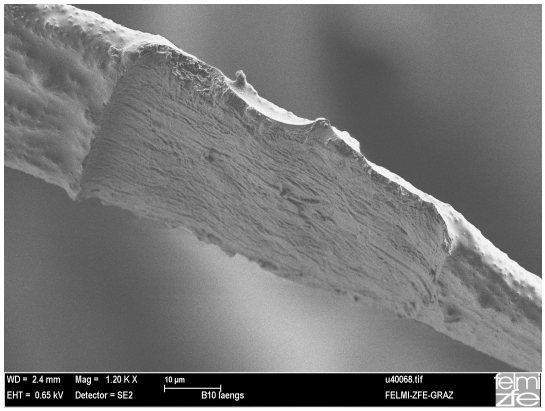

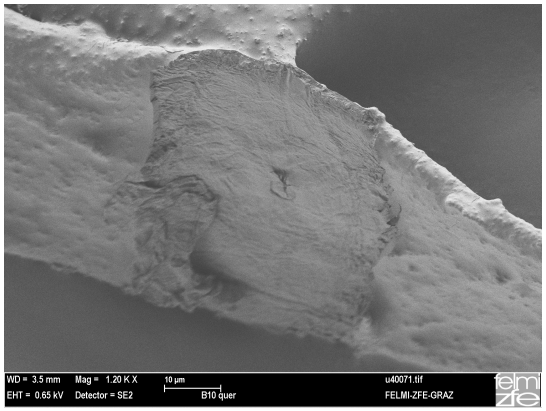

SEM images of the fiber surface.

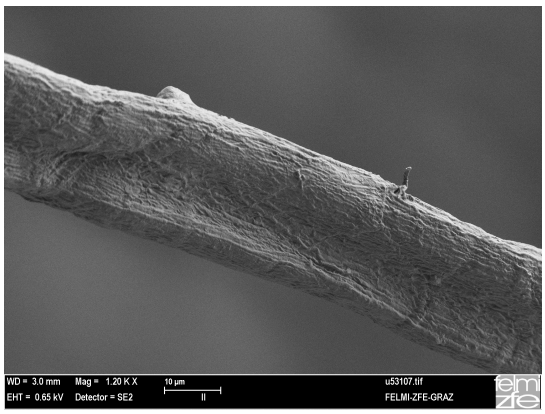

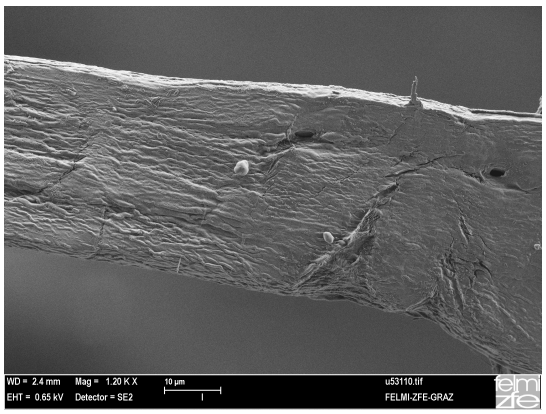

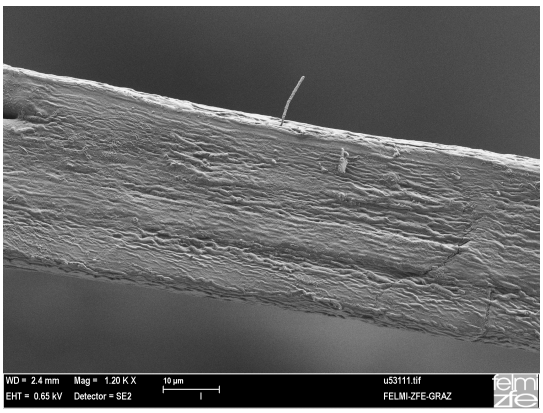

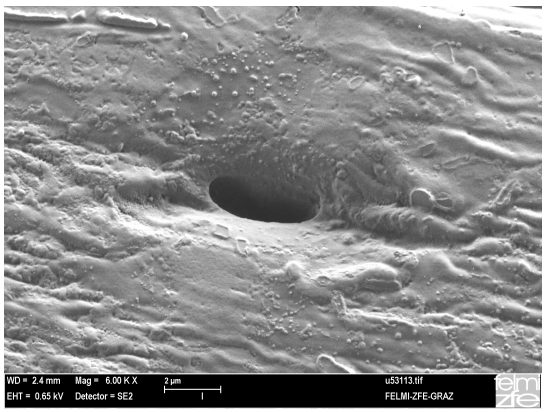

Fibers fixed with UHU Plus Sofortfest

SEM images of the fiber surface.

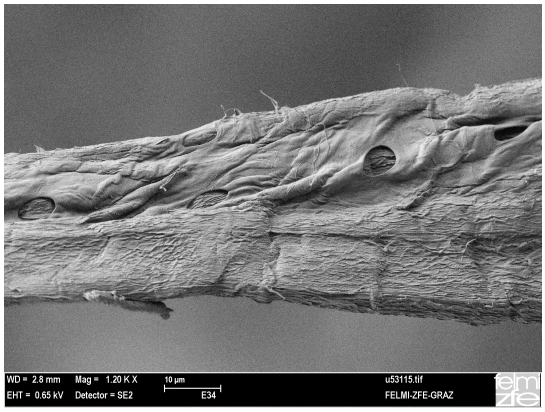

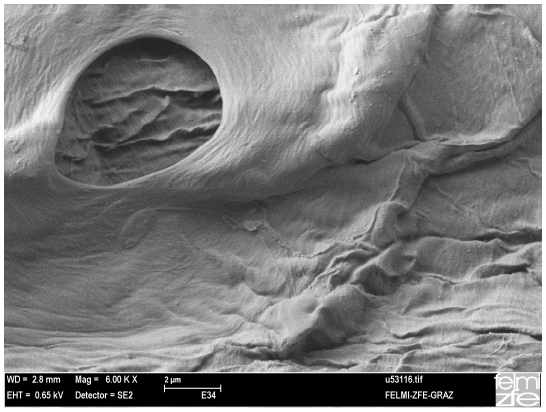

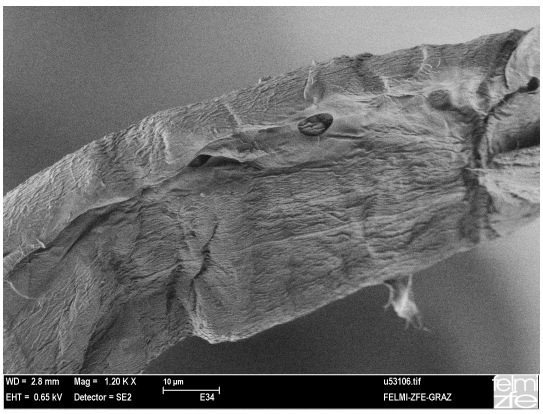

Fibers fixed with nail polish

SEM images of the formerly bonded area.

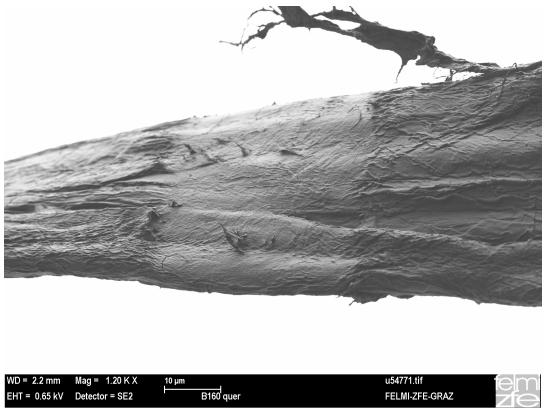

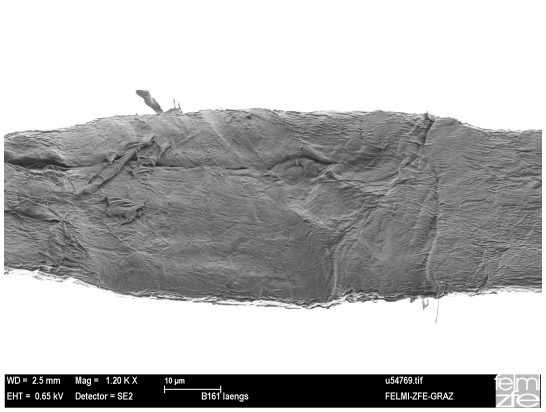

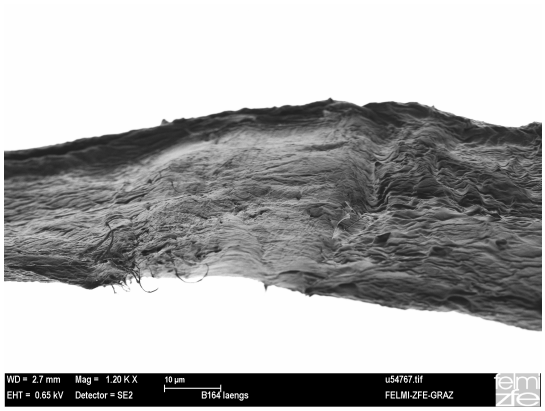

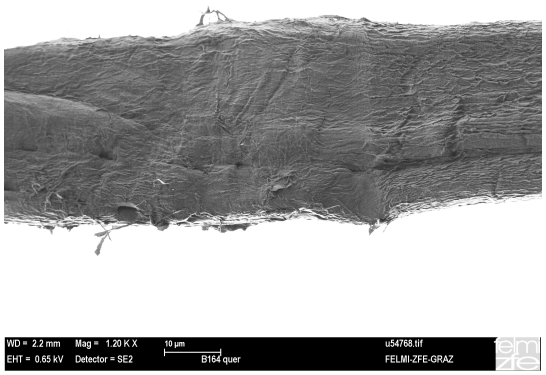

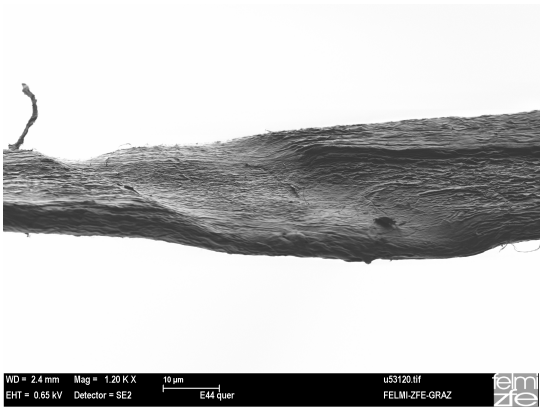

SEM images of the fiber surface.

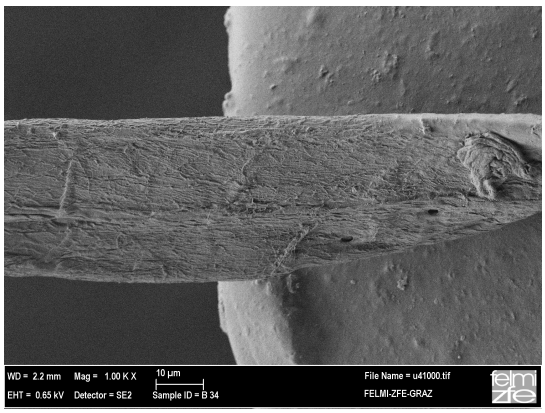

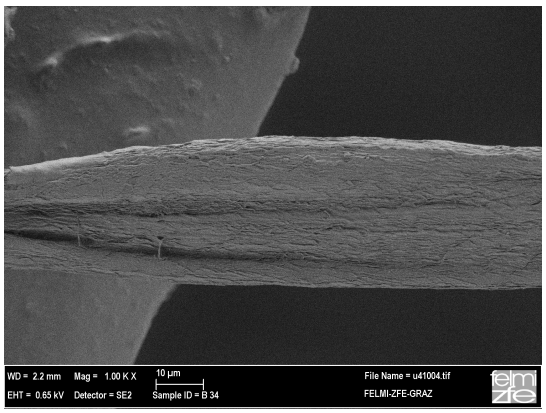

Bibliography

Adusumalli, R. B., Müller, U., Weber, H., Roeder, T., Sixta, H., and Gindl, W. (2006). Tensile Testing of Single Rgenerated Cellulose Fibres. *Macromolecular Symposia*, 244(1):83–88.

Alén, R. (2000). Structure and chemical composition of wood. In Stenius, P., editor, *Forest Products Chemistry*, Book 3 of Papermaking Science and Technology, chapter 1, pages 11–57. Fapet Oy.

Andersson, N., Germgård, U., Johansson, K., Ljungqvist, C. H., and Thuvander, F. (2002). Determining the strain to failure for constrained pulp fibres by means of single-fibre fragmentation. *Appita*, 55(3):224–229.

Askeland, D. R., Fulay, P. P., and Wright, W. J. (2011). *The Science and Engineering of Materials*. Cengage Learning, 6th edition.

Borodulina, S., Kulachenko, A., Galland, S., and Nygårds, M. (2012). Stress-strain curve of paper revisited. *Nordic Pulp and Paper Research Journal*, 27(2):318–328.

Boucai, E. (1971). Zero-Span Tensile Test and Fibre Strength. *Pulp and Paper Magazine of Canada*, 72(10):73–76.

Burgert, I., Frühmann, K., Keckes, J., Fratzl, P., and Stanzl-Tschegg, S. E. (2003). Microtensile Testing of Wood Fibers Combined with Video Extensometry for Efficient Strain Detection. *Holzforschung*, 57:661–664.

Button, A. F. (1979). *Fiber-fiber bond strength: A study on the linear elastic model structure*. PhD thesis, Institute of Paper Chemisry, Appleton, Wisconsin.

Clark, J. d'A. (1985). *Pulp Technology and Treatment for Paper*. Miller Freeman Publications, 2nd edition. ISBN 0-87930-164-3.

Conn, A. B. and Batchelor, W. J. (1999). Conversion of an Instron to mechaical testing of single fibres. *Appita*, 52(4):290–294.

Dunford, J. and Wild, P. (2002). Cyclic Transverse Compression of Single Wood-Pulp Fibres. *Journal of Pulp and Paper Science*, 28(4):136–141.

Eder, M., Terziev, N., Daniel, G., and Burgert, I. (2008). The effect of (induced) dislocations on the tensile properties of individual Norway spruce fibres. *Holzforschung*, 62(1):77–81.

Elwenspoek, M. and Wiegerink, R. (2001). *Mechanical Microsensors*. Springer. ISBN 3-540-67582-5.

Feih, S., Wonsyld, K., Minzari, D., Westermann, P., and Lilholt, H. (2004). Testing procedure for the single fiberfragmentation test. Technical report, Risø National

Laboratory.

Fengel, D. and Wegener, G. (2003). *WOOD - Chemistry, Ultrastructure, Reactions*. Kessel Verlag, Remagen.

Fenner, R. T. and Reddy, J. N. (2012). *Mechanics of Solids and Structures*. CRC Press, 2nd edition.

Forsström, J., Torgnysdotter, A., and Wågberg, L. (2005). Influence of fibre/fibre joint strength and fibre flexibility on the strength of papers from unbleached kraft fibres. *Nordic Pulp and Paper Research Journal*, 20(2):186–191.

Fraden, J. (2011). *Handbook of Modern Sensors: Physics, Designs, and Applications*. Springer, 4th edition. ISBN 978-1-4419-6465-6.

Ghosh, A. K. (2009). *Introduction To Measurements And Instrumentation*. PHI Learning, 3rd edition. ISBN 9788120338586.

Groom, L., Mott, L., and Shaler, S. (2002). Mechanical properties of individual southern pine fibers. Part I. Determination and variability of stress-strain curves with respect to tree height and juvenility. *Wood and Fiber Science*, 34(1):14–27.

Gurnagul, N., Ju, S., and Page, D. H. (2001). Fibre-Fibre Bond Strength of Once-Dried Pulps. *Journal of Pulp and Paper Science*, 27(3):88.

Hardacker, K. W. (1962). The Automatic Recording of the Load-Elongation Characteristic of Single Papermaking Fibers. *Tappi*, 45(3):237–246.

Hägglund, R., Gradin, P. A., and Tarakameh, D. (2004). Some aspects on the zero-span tensile test. *Experimental Mechanics*, 44(4):365–374.

Hu, W., Ton-That, M.-T., Perrin-Sarazin, F., and Denault, J. (2010). An improved method for single fiber tensile test of natural fibers. *Polymer Engineering and Science*, 50(4):819–825.

Jayme, G. and Hunger, G. (2003). Electron Microscopy 2- and 3-Dimensional Classification of Fibre Bonding. In Bolam, F., editor, *Formation and Structure of Paper*, Transaction of the IIth Fundamental Research Symposium Oxford 1961, pages 135–170. The Pulp and Paper Fundamental Research Society.

Jayne, B. A. (1959). Mechanical Properties of Wood Fibers. *Tappi*, 42(6):461–467.

Jones, A. R. (1972). Strength Evaluationof Unbleached Kraft Pulps. *Tappi*, 55(10):1522–1527.

Joshi, K., Batchelor, W., and A., R. K. (2011). Investigation of the effect of drying and refining on the fiber-fiber shear bond strength measured using tensile fracture line analysis of sheets weakened by acid gas exposure. *Cellulose*, 18(6):1407.

Joy, D.C. & Joy, C. (1996). Low Voltage Scanning Electron Microscopy. *Micron*, 27(3-4):247–263.

Kang, T., Paulapuro, H., and Hiltunen, E. (2004). Fracture mechanism in interfibre bond failure - microscopic observations. *Appita*, 57(3):199.

Kappel, L. (2010). *Development and Application of a Method for Fiber-Fiber Bonded Area*

Measurement. PhD thesis, Institute for Paper, Pulp and Fiber Technology, Graz University of Technology, Austria.

Kappel, L., Hirn, U., Bauer, W., and Schennach, R. (2009). A novel method for the determination of bonded area of individual fiber-fiber bonds. *Nordic Pulp and Paper Research Journal*, 24(2):199.

Kompella, M. K. and Lambros, J. (2002). Micromechanical characterization of cellulose fibers. *Polymer Testing*, 21:523.

Kulachenko, A. and Uesaka, T. (2012). Direct simulations of fiber network deformation and failure. *Mechanics of Materials*, 51:1–14.

Leopold, B. and McIntosh, D. C. (1961). Chemical Composition and Physical Properties of Wood Fibers III. Tensile Strength of Individual Fibers From Alkali Extracted Loblolly Pine Holocellulose. *Tappi*, 44(3):235–240.

Li, K., Lei, X., Lu, L., and Camm, C. (2010). Surface Characterization and Surface Modification of Mechanical Pulp Fibres. *Pulp & Paper Canada*, 111(1):T11–T16.

Lindström, T., Wågberg, L., and Larsson, T. (2005). On the nature of joint strength in paper - a review of dry and wet strength resins used in paper manufacturing. In I'Anson, S. J., editor, *Advances in Paper Science and Technology*, Transaction of the 13th Fundamental Research Symposium, pages 457–562. The Pulp and Paper Fundamental Research Society, Cambridge (UK).

Liu, J. (2000). High-Resolution and Low-Voltage FE-SEM Imaging and Microanalysis in Materials Characterization. *Material Characterization*, 44:353–363.

Lorbach, C., Hirn, U., Kritzinger, J., and Bauer, W. (2012). Automated 3D measurement of fiber cross section morphology in handsheets. *Nordic Pulp and Paper Research Journal*, 27(2):264–269.

Lossada, A. A. (1998). Reviewing the dependence of wet fiber flexibility : I and E. *Paperi ja Puu*, 80(3):257–259.

Magnusson, M. S. (2013). Testing and evaluation of interfibre joint strength under mixed-mode loading. Licentiate Thesis. KTH, Royal Institue of Technology, Stockholm.

Magnusson, M. S., Fischer, W. J., Östlund, S., and Hirn, U. (2013). Interfibre joint strength under peeling, shearing and tearing type of loading. In preparation for publication for the 15th Fundamental Research Symposium, Cambridge.

Magnusson, M. S. and Östlund, S. (2011). Inter-Fibre Bond Strength and Combined Normal and Shear Loading. In Hirn, U., editor, *Progress in Paper Physics Seminar*, pages 205–207. Verlag der Technischen Universität Graz.

Mayhood, C. H., Kallmes, O. J., and Cauley, M. M. (1962). The Mechanical Properties of Paper Part II. Measured Shear Strength of Individual Fiber to Fiber Contacts. *Tappi*, 45(1):69–73.

McIntosh, D. C. (1963). Tensile and Bonding Strengths of Loblolly Pine Kraft Fibers

Cooked to Different Yields. *Tappi*, 46(5):273.

Mohlin, U. B. (1974). Cellulose fibre bonding: Determination of interfibre bond strength. *Svensk Papperstidning*, 77(4):131–137.

Molin, U. and Daniel, G. (2004). Effects of refining on the fibre structure of kraft pulps as revealed by FE-SEM and TEM: Influence of alkaline degradation. *Holzforschung*, 58(3):226–232.

Mott, L., Shaler, S. M., Groom, L. H., and Liang, B. H. (1995). The tensile testing of individual wood fibers using envronmental scanning electron microscopy and video image analysis. *Tappi*, 78(5):143–148.

Navaranjan, N., Richardson, J. D., Dickson, A. R., Blaikie, R. J., and Prabhu, A. N. (2007). A New Method for the Measurement of Longitudinal Fibre Flexibility. In *61st Appita Annual Conference and Exhibition*, pages 267–273. Appita Inc.

Nordman, L., Gustafsson, C., and Olofsson, G. (1952). On the Strength of Bondings in Paper. *Paperi ja Puu*, 3:47.

Nordman, L., Gustafsson, C., and Olofsson, G. (1958). On the Strength of Bondings in Paper II. *Paperi ja Puu*, 8:315.

Okamoto, T. and Meshitsuka, G. (2012). The nanostructure of kraft pulp1: evaluation of various mild drying methods using field emission scanning electron microscopy. *Cellulose*, 17(6):1171–1182.

Paavilainen, L. (1993). Conformability - flexibility and collapsibility - of sulphate pulp fibres. *Paperi ja Puu - Paper and Timber*, 75(9):689–702.

Page, D. H. (1960). Fibre-to-fibre bonds Part 1 - A method for their direct observation. *Paper Technology*, 1(4):407–411.

Page, D. H. (1969). A Theory for the Tensile Strength of Paper. *Tappi*, 52(4):674.

Page, D. H., El-Hosseiny, F., Winkler, K., and Bain, R. (1972). The Mechanical Properties of Single Wood-Pulp Fibres. Part I: A New Approach. *Pulp*, 73(8):72–77.

Page, D. H., El-Hosseiny, F., Winkler, K., and Lancaster, A. P. S. (1977). Elastic modulus of single wood pulp fibers. *Tappi*, 60(4):114.

Perez, N. (2004). *Fracture mechanics.* Kluwer Academic Publisher, Boston.

Peters, F. J. (2010). Paper fibers: on the development and application of a tensile testing setup. Eindhoven University of Technolgy, Department of Mechanical Engineering, Mechanics of Materials.

Reimer, L. (1993). *Image Formation in Low-Voltage Scanning Electron Microscopy*, volume TT 12. SPIE-Press.

Robertson, A. A., Meindersma, E., and Mason, S. G. (1961). The Measurement of Fibre Flexibility. *Pulp and Paper Magazine of Canada*, 62(1):T3–T10.

Russell, J., Kallmes, O. J., and Mayhood, C. H. (1964). The inluence of two wet-strength resins on fibers and fiber-fiber contacts. *Tappi*, 47(1):22–25.

Saketi, P. and Kallio, P. (2011a). Measuring Bond Strength of Individual Paper Fibers using Microrobotics. In Hirn, U., editor, *Progress in Paper Physics Seminar*, pages 199–203. Verlag der Technischen Universität Graz.

Saketi, P. and Kallio, P. (2011b). Microrobotic Platform for Manipulation and Mechanical Characterization of Individual Paper Fibers. In Ander, P., editor, *Fine Structure of Papermaking Fibres. COST Action E54 "Characterization of the fine structure and properties of papermaking fibres using new technology"*, pages 133–146. COST Office. Brussels.

Schmied, F. (2011). *Atomic Force Microscopy investigations of fiber-fiber bonds in paper*. PhD thesis, Institute of Physics, University of Leoben, Austria.

Schmied, F., Teichert, C., Kappel, L., Hirn, U., and Schennach, R. (2012). Joint strength measurements of individual fiber-fiber bonds: An atomic force microscopy based method. *Review of Scientific Instruments*, 83(7).

Schmied, F. J., Teichert, C., Kappel, L., Hirn, U., Bauer, W., and Schennach, R. (2013). What holds paper together: Nanometre scale exploration of bonding between paper fibres. In preparation for publication in Scientific Reports.

Schnell, W., Gross, D., and Hauger, W. (1995). *Technische Mechanik 2 Elastostatik*. Springer, 5th edition.

Schniewind, A. P., Ifju, G., and Brink, D. L. (1966). Effect of Drying on the Fexural Rigidity of Single Fibres. In Bolam, F., editor, *Consolidation of the Paper Web*, volume 1 of *Transaction of the 3rd Fundamental Research Sympposium Cambridge*, pages 538–543. The Pulp and Paper Fundamental Research Society, Cambridge (UK).

Schniewind, A. P., Nemeth, L. J., and Brink, D. L. (1964). Fiber and Pulp Properties I. Shear Strength of Single Fiber Crossings. *Tappi*, 47(4):244.

Seborg, C. O. and Simmonds, F. A. (1941). Measurement of the Stiffness in Bending of Single Fibers. *Paper Trade Journal*, 113(17):49–50.

Seth, R. S. (2001). Zero-span tensile strength of papermaking fibres. *Paperi ja Puu - Paper and Timber*, 83(8):597–604.

Sirviö, J. (2008). Fibres and bonds. In Niskanen, K., editor, *Paper Physics*, Book 16 of Papermaking Science and Technology, chapter 2, pages 59–92. Finnish paper Engineers Association/Paperi ja Puu Oy, 2nd edition.

Sixta, H. (2006). *Handbook of Pulp*, volume 1. WILEY-VCH. ISBN 3-527-30997-7.

Smith, S. W. (2003). *Digital Signal Processing: A Practical Guide for Engineers and Scientists*. Newnes.

Stone, J. E. (1963). Bond Strength in Paper. *Pulp and Paper Magazine of Canada*, 64(12):T528–T532.

Stratton, R. A. and Colson, N. L. (1990). Dependence of Fiber/Fiber Bonding on some Papermaking Variables. Technical Report 357, Institute of Paper Science and Technology Atlanta, Georgia.

Torgnysdotter, A. and Wågberg, L. (2003). Study of the joint strength between regen-

erated cellulose fibres and its influence on the sheet strength. *Nordic Pulp and Paper Research Journal*, 18(4):455.

Uesaka, T. (1984). *Determiantion of fiber-fiber bond, In: Handbook of Physical and Mechanical Testing of Paper and Paperboard*, volume 2. Marcel Dekker Inc. New York.

Van Den Akker, J. A., Lathrop, A. L., Voelker, M. H., and Dearth, L. R. (1958). Importance of Fiber Strength to Sheet Strength. *Tappi*, 41(8):416–425.

Wathén, R. (2006). *Studies on fiber strength and its effect on paper properties*. PhD thesis, Helsinki University of Technology, Department of Forest Products Technology, Espoo, Finland.

Wiltsche, M. (2006). *Three Dimensional Analysis of Paper Structure Using Automated Microtomy*. PhD thesis, Institute for Paper, Pulp and Fiber Technology, Graz University of Technology, Austria.

Yu, Y., Jiang, Z., Fei, B., Wang, G., and Wang, H. (2011a). An improved microtensile technique for mechanical characterization of short plant fibers: a case study on bamboo fibers. *Journal of Material Science*, 46(3):739–746.

Yu, Y., Tian, G., Wang, H., Fei, B., and Wang, G. (2011b). Mechanical characterization of single bamboo fibers with nanoindentation and microtensile technique. *Holzforschung*, 65(1):113–119.

Zhao, H., Kwak, J., Zhang, Z. C., Brown, H., Arey, B., and Holladay, J. E. (2007). Studying cellulose fiber structure by SEM, XRD, NMR and acid hydrolysis. *Carbohydrate Polymers*, 68:235–241.